The role of translation in keratinocyte cell fate determination

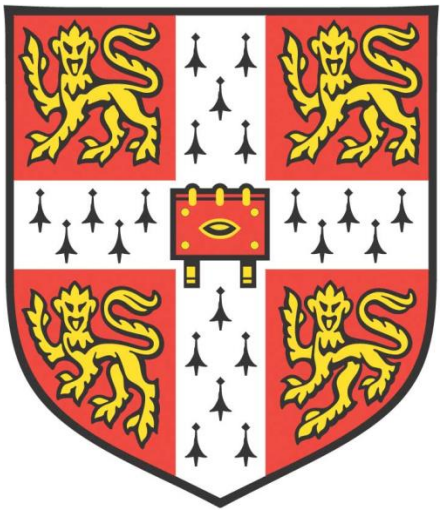

Aleksandra Jolanta Lewicka

Clare College

Wellcome Sanger Institute

Graduate School of Life Sciences

University of Cambridge

This dissertation is submitted for the degree of Doctor of Philosophy

September 2018

To my parents

Moim rodzicom

Summary

Mammalian epidermis is both maintained and repaired after injury by a population of proliferating progenitor cells localised in the basal layer of the tissue. While progenitor cells normally remain in the basal layer throughout their lifetime, differentiating cells move up the tissue and are eventually shed off, helping to maintain tissue homeostasis. Cultured human keratinocytes generate a range of colony sizes, but can be separated into two groups based on the ratio of outcomes after cell division. On average, 'balanced' colonies give rise to equal numbers of proliferative and differentiating cells, whereas 'expanding' colonies grow in an exponential manner, with the majority of divisions resulting in the generation of two proliferative daughter cells. Previous work has demonstrated that cells in the middle third of a growing 'expanding' colony spontaneously switch their behaviour towards the 'balanced' state. Cells are also able to switch back from 'balanced' to 'expanding' after a scratch injury. These results suggest the existence of a tuneable mechanism determining the fate of proliferative keratinocytes, but the molecular identity of this switch remains unknown. In this thesis I will discuss the potential role of protein translation levels in defining the division outcomes of cultured human keratinocytes. Using a combination of cell imaging and RNA sequencing technologies, I show that the two modes of proliferation produce distinct transcriptional and translational profiles. I am able to distinguish between the 'balanced' and 'expanding' colonies at a very early stage during colony growth using specific markers for translation and a global transcription marker suggesting a colony's fate is set early on. Finally, use of RNA interference allowed me to knock-down a specific Eukaryotic translation initiation factor, leading to an apparent switch in the colony's proliferative potential. This suggests that translation level may actually determine the cell fate of human keratinocytes and is not only a marker of keratinocyte differentiation. Overall, these findings bring us closer to understanding the molecular basis of progenitor fate determination, and may give us insight into how epidermal homeostasis is maintained and how it is modulated in tissue repair and cancer.

Declarations

This dissertation is the result of my own work and includes nothing, which is the outcome of work done in collaboration except where specifically indicated in the text.

It is not substantially the same as any that I have submitted, or, is being concurrently submitted for a degree or diploma or other qualification at the University of Cambridge or any other University or similar institution. I further state that no substantial part of my dissertation has already been submitted, or, is being concurrently submitted for any such degree, diploma or other qualification at the University of Cambridge or any other University or similar institution.

In accordance with the School of Biological Sciences guidelines, this thesis does not exceed the prescribed word limit of 60,000 words.

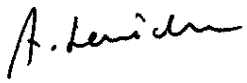

Aleksandra Jolanta Lewicka

September 2018

Cambridge

Acknowledgements

I would like to begin by thanking my supervisor, Professor Phil Jones, for allowing me to join his research laboratory and for the help and thoughtful advice he has offered me over the past four years.

I would also like to thank my advisors, Dr Christian Frezza and Dr Mathew Garnett, for their valuable suggestions and encouraging comments. I am indebted to both of them for the discussions that helped to shape this research thesis. My sincere thanks to Dr Annabel Smith, Dr Christina Hedberg-Delouka and Dr Carl Anderson who supervised the PhD programme and offered me great help both with my studies and with my transition to the Wellcome Sanger Institute.

The Medical Research Council and the Wellcome Trust have afforded me with funding, which has made the entire pursuit possible and for that I owe them a sincere debt of gratitude.

My research would have been impossible without the aid and support of all the members of the Jones team, past and current. I am particularly grateful for the time and patient guidance so generously given by Dr Jo Fowler. Dr Tibor Nagy and Dr Swee Hoe Ong gave me invaluable help with the analysis of sequencing data. My special thanks are also extended to Ms Esther Choolun, who has made me feel welcome from the moment I stepped into the front entrance at the MRC Cancer Unit on my very first day, and to Dr Emilie Abby, who is not only my colleague but also a dear friend.

On that note, I would like to thank my friends, who are spread through the world, yet are always present in my life. Thanks for the stimulating discussions and many fun times. And for sticking with me all these years.

Heartfelt thanks go to my partner and best friend, Jan Łyczakowski. Thank you for joining me on that journey, and may it continue to be a great one.

And finally, last but by no means least, I would like to thank my parents, Małgorzata and Ignacy Lewiccy, who sparked my fascination with the natural world, and all the rest of my family, without whom none of my success would be possible.

Table of contents

List of tables

List of figures

List of abbreviations

4′,6-Diamidine-2′-phenylindole dihydrochloride	DAPI
5- ethynyl uridine	EU
5-ethynyl-2'-deoxyuridine	EdU
Activating transcription factor 3	ATF3
Annexin A2	ANXA2
Basal cell carcinoma	BCC
Base pairs	bp
Bovine serum albumin	BSA
Clustered regularly interspaced short palindromic repeats	CRISPRs
Complementary DNA	cDNA
Complete FAD medium	C'FAD
CRISPR associated protein 9	Cas9
Cyclin D1	CCND1
Cyclin G1	CCNG1
Deoxynucleotide triphosphate	dNTP
Deoxyribonucleic acid	DNA
Dimethyl sulfoxide	DMSO
Dithiothreitol	DTT
Dulbecco's Modified Eagle Medium	DMEM
Elongation initiation factor	eIF
Embryonic stem cell	ESC
Epidermal growth factor	EGF

Ethylenediaminetetraacetic acid	EDTA
Eukaryotic Translation Initiation Factor 3, Subunit E	eIF3E
Eukaryotic Translation Initiation Factor 4 Gamma 2	eIF4G2
Fish skin gelatine	FSG
Glyceraldehyde 3-phosphate dehydrogenase	GAPDH
Green fluorescent protein	GFP
Hematoxylin and eosin staining	H&E staining
Histone 2b	H2B
HMG-CoA reductase	HMGCR
Human histone H2B	H2B
Human neonatal foreskin keratinocytes	NFSKs
Human type I hair keratin pseudogene phihHaA	KRTHAP1
Integrin alpha 2	ITGA2
Involucrin	IVL
Keratin 1, Type II	KRT1
Keratin 5	KRT5
Keratin 14	KRT14
Keratin 17	KRT17
Mammalian target of rapamycin	mTOR
Mitomycin C	MMC
mTOR Complex 1	mTORC1
mTOR Complex 2	mTORC2
N-acetyl-D-glucosamine kinase	NAGK
O-propargyl-puromycin	OP-puro
Optimal cutting temperature compound	OCT
Origin recognition complex	ORC

Paraformaldehyde	PFA
Pelota	Pelo
Phosphate buffered saline	PBS
Polymerase chain reaction	PCR
Principal Component Analysis	PCA
Protein kinase B	Akt
Real-time reverse-transcription PCR	RT-PCR
Relative centrifugal force	RCF
Reverse Phase Protein Array	RPPA
Reverse transcriptase	RT
Ribonucleic acid	RNA
Ribosome profiling	Ribo-seq
RNA interference	RNAi
RNA sequencing	RNA-seq
S100 calcium-binding protein A10	S100A10
S6 kinase	S6K
Small interfering RNA	siRNA
Squamous cell carcinoma	SCC
Standard error of the mean	SEM
Steroid receptor coactivator 3	SRC3
Sterol regulatory element-binding protein 1	SREBP1
Synthesis phase	S-phase
Transcription factor	TCF
Ubiquitin-conjugating enzyme E2L	UBE2L
Ultraviolet radiation	UV radiation

Chapter 1 Introduction

1.1. Reasons to study cell fate determination

Although virtually all healthy cells in the human body share the same DNA sequence, with only small variations in this sequence acquired through mutations, they can all differ significantly in their morphology and functions. The question how these uniquely specialised and distinct cell types, such as for example the multinucleated skeletal muscle fibres and oxygen-carrying red blood cells, can all originate from a single ancestral cell has intrigued and baffled developmental biologists for decades, if not centuries.

Today we know that how a particular cell develops into the final cell type, and essentially how its fate is determined, can depend on a number of factors. Any cell within a multicellular organism, both in a developing embryo and within an adult tissue, receives and gives cues to its neighbours, ultimately influencing each other's cell fate decisions (Artavanis-Tsakonas, Rand and Lake, 1999; Enver *et al.*, 2009; Furlong, 2010). Cells can also respond to endogenous developmental factors, as well as external signals, such as hormones, sugar and oxygen levels or injury (Cross *et al.*, 1995; Liu *et al.*, 2010; Klein *et al.*, 2010). However, since there are so many cell types and so many possible states they can be in, we are only beginning to understand the complexity of the regulatory networks involved in the control of cellular fate.

Study of stem cells, the progenitors which give rise to all the differentiated cell types in the body, gives a unique insight into the mechanisms behind the cell fate determination. As the progenitor cell commits to one lineage or state over another, or more likely it is pushed towards a given state by a combination of internal and external stimuli and often chance, it acquires a specific molecular profile, which can include changes to its transcriptome, proteome and its chromatin structure (Seery and Watt, 2000; Simons and Clevers, 2011). Studying these changes can have immense implications on our understating of human disease, including cancer. Human keratinocyte cultures are an excellent model for investigating the molecular basis of progenitor fate within a single lineage and, alongside adult skin samples from human donors, they will be used throughout this thesis.

1.2. Structure and function of human skin

Skin is the largest organ in the human body, accounting for about 12 to 15% of total body weight (Martini and Nath, 2009). Together with its appendages, skin forms part of the integumentary system, which acts to protect the body from damage, such as abrasion, infection and water loss (Proksch, Brandner and Jensen, 2008). Other functions of the integumentary system include regulating body temperature, excreting wastes and cushioning (Madison, 2003). Additionally, skin is the attachment site for multiple sensory receptors, which enable mammals to detect changes in temperature, pressure, touch and pain (Moqrich *et al.*, 2005; Bessou, Perl and Schmittr.La, 1969). In humans, as well as many other land vertebrates, skin is also the site of vitamin D synthesis (Hawker *et al.*, 2007). Human skin is similar in its structure to that of other mammals, including mice which are often used in the studies of skin regeneration and maintenance, however, it is probably the most similar to pig skin (Sullivan *et al.*, 2001; Liu *et al.*, 2009). It is composed of two major layers of tissue, epidermis and dermis, separated by a fibrous basement membrane, and is connected to the cushioning subcutaneous layer (Figure 1.1) (Shier, Butler and Lewis, 1999). Skin is also a rich and diverse habitat for bacteria and fungi, and there is an increasing interest in the role of the microbiome in skin health (Grice and Segre, 2011; Huttenhower *et al.*, 2012), As many as a 1000 species of bacteria from 19 bacterial phyla have been found to be present on the human skin, with different bacterial population preferentially occupying certain areas, further highlighting the diversity in human skin types (Grice *et al.*, 2009).

Though skin can often appear hairless, majority of human skin is covered in hair follicles, which themselves can play a role in skin maintenance, in particular in epidermal homeostasis (Kazantseva *et al.*, 2006; Taylor *et al.*, 2000). Genuinely hairless skin can be found on the soles of the feet and palms of hands, and is often referred to as glabrous skin or thick skin (Marks and Miller, 2006). Nevertheless, compared to other related species, majority of human body is essentially hairless. Humans are the only primate species that have undergone such a significant hair loss, which is thought to be a consequence of the loss of functionality in the pseudogene KRTHAP1 in the human lineage about 240 thousand years ago (Winter *et al.*, 2001). Since a thick fur helps to protect the skin of most mammals from the strong UV radiation, it is believed that the variations in human skin coloration evolved after humans lost their hair as an alternative way of protecting their skin (Jablonski and Chaplin, 2000; Brenner and Hearing, 2008).

Today, human skin colour varies significantly, although there is a correlation between the distribution of indigenous skin pigmentation and the geographic distribution of UV radiation, with darker skin tones observed in individuals populating areas receiving higher levels of UV radiation (Webb, 2006). Increased mobility of human populations over the past few hundred years has led to many people settling far away from their ancestral homelands (Muehlenbein, 2010). An unexpected consequence of such migrations, as well as changes in customs and dress styles, is the global increase in the incidence of UV-induced cancers, and in particular non-melanoma skin cancer (Pfeifer and Besaratinia, 2012; Armstrong and Kricker, 2001). In regions such as Australia, nowadays largely populated by pale-skinned individuals, yet still receiving very high levels of UV radiation, the problem is particularly pronounced, with as many as 1,466.6 cases of keratinocyte cancers diagnosed per 100 thousand individuals in South Australia between the years 2010 and 2014 (Czarnecki, 2018).

This project will investigate the formation of the epidermis layer of the skin. This part of the organ is made with keratinocytes which differentiate from progenitor cells located at basal layer, the junction between dermis and epidermis. Renewal of epidermis, which is critical for skin healing, relies on keratinocyte proliferation. This process can be also disrupted in disease conditions, such as the UV induced skin cancers discussed above.

Figure 1.1. The structure of human skin. The diagram shows the main two layers of mammalian skin, epidermis and dermis, as well as the subcutaneous layer and various appendages of the skin. Image adapted from Shier et al., 1999.

1.3. Cellular organisation of human epidermis

1.3.1. Structure of human epidermis

This thesis will focus around the study of human epidermis, which is the outermost layer of the skin. In particular, I shall focus on the interfollicular epidermis, which is a region of epidermis localised in-between the hair follicles (Doupe and Jones, 2012).

Epidermis is composed of multiple layers of cells called keratinocytes, which produce high levels of structural proteins called keratins (Madison, 2003). Other cell types, which can be found in the epidermis include melanocytes, Langerhans cells, Merkel cells and inflammatory cells (Shier, Butler and Lewis, 1999). Multiple layers of differentiated flattened keratinocytes overlie a layer of tightly packed columnar cells, called a basal layer or stratum basale (McGrath, Eady and Pope, 2004) (Figure 1.2). There are no blood vessels present in the epidermis, hence it is thought to be supplied exclusively by nutrients diffusing from dermal capillaries (Tohya *et al.*, 1998) and the diffused oxygen taken up from the surrounding air (Stucker *et al.*, 2002).

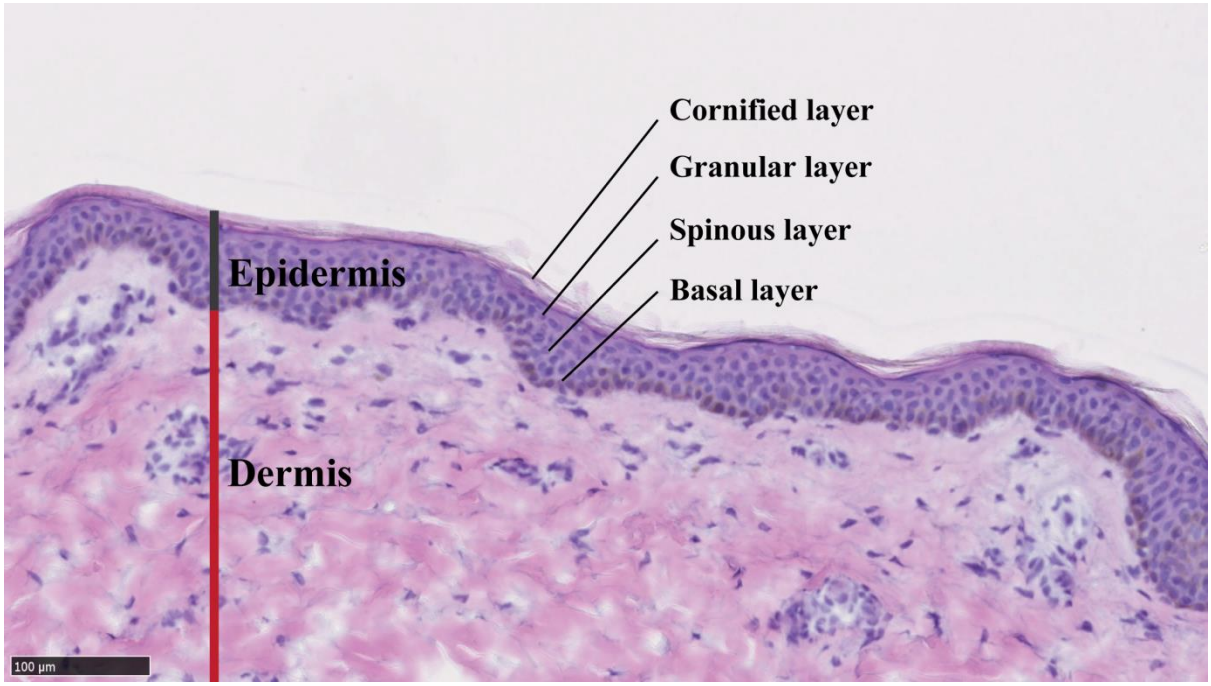

Figure 1.2. Structure of human epidermis. A microscopic image of a haematoxylin and eosin stained section of human abdominal skin, showing the localisation of the four main epidermal layers (my own image).

Histologically, epidermis is composed of four distinct layers, which can vary in thickness, organised into vertical zones by stages of differentiation (Figure 1.2). Each layer is made up of keratinocytes which are held together by the components of the extracellular matrix and specific cell-cell interactions (Marks and Miller, 2006). From the outermost to innermost, the layers are: cornified layer, granular layer, spinous layer and basal layer.

The outermost cornified layer, or the stratum corneum, is the first point of contact with the outside environment and can vary significantly in thickness depending on the location on the body (Ma and Ozers, 1996). In humans, it can contain up to 20 layers of denucleated keratinocytes. These effectively dead cells contain very high levels of keratins and are surrounded by a hydrophobic phospholipid matrix excreted by the underlying granular cells. In the most superficial layers, desmosomal attachments between flattened keratinocytes are sparse, which aids shedding (Madison, 2003).

Directly beneath the cornified layer sits the granular layer, or stratum granulosum, which however is not always apparent (Madison, 2003). The granular layer reinforces the barrier function of the skin by excreting a water resistant lipid-rich product, which helps to ensure skin's partial impermeability (Sata, 1900). Sphingolipids are one of the main constituents of this impermeable layer. Recent evidence suggests that mutations in transcription factors controlling sphingolipid biosynthesis lead to changes in granular layer lipid composition and loss of its biological function in the mouse model (Li *et al.*, 2017).

Spinous layer, or stratum spinosum, is localised just below the granular layer and directly above the basal layer. Keratinocytes within the spinous layer form very strong intercellular junctions, which help to maintain epidermal integrity (McGrath, Eady and Pope, 2004). The thickness of this layer can vary even more dramatically than the thickness of the cornified layer, and can depend on the factors such as sex, age, ethnicity and anatomical localisation on the body (Marks and Miller, 2006).

Finally, the basal layer or stratum basale, which is of key importance to my work, is localised in the deepest layer of human epidermis. It is composed of a single layer of proliferating cells and is attached directly to the basement membrane and hence dermis (McGrath, Eady and Pope, 2004). In health, it contains the only mitotically active keratinocytes in the epidermis and its main responsibility is to generate the cells required to maintain and repair the epidermis (Doupe and Jones, 2012).

1.3.2. Epidermal homeostasis

Healthy mammalian interfollicular epidermis is maintained by a population of epidermal progenitor cells localised at the basal layer of the tissue (Clayton *et al.*, 2007; Doupe *et al.*, 2012). Proliferative keratinocytes divide to give rise to new progenitor cells, as well as differentiating keratinocytes (Mascre *et al.*, 2012). While progenitor cells would normally remain in the basal layer throughout their lifetime, differentiating cells move up the tissue. As they are pushed up, they become more and more differentiated (Fuchs, 2007). Eventually, they become fully stratified and are shed off (Sotiropoulou and Blanpain, 2012). This delicate balance, which is crucial for skin maintenance, relies on producing just enough proliferating cells to sustain the population without overgrowth and loss of tissue integrity (Blanpain and Fuchs, 2009). If not enough new cells are produced, wounds will not be able to heal and skin ulcers will develop (Singer and Clark, 1999). If too many cells are produced, multiple pathologies can arise, including cancer formation (Gloster and Neal, 2006; Saladi and Persaud, 2005; Jemal *et al.*, 2011). In this thesis, I will attempt to describe some of the molecular processes behind the establishment and maintenance of homeostasis in human epidermis. While investigating keratinocyte differentiation it is important to consider the contribution from fibroblasts. Recent evidence suggests that fibroblast cultures sourced from differently aged donors have variable performance in skin regeneration assays (Hausmann *et al.*, 2019). It is possible this may be caused by changes in extracellular matrix made by fibroblasts which is affected by their metabolic activity (Zhao *et al.*, 2019).

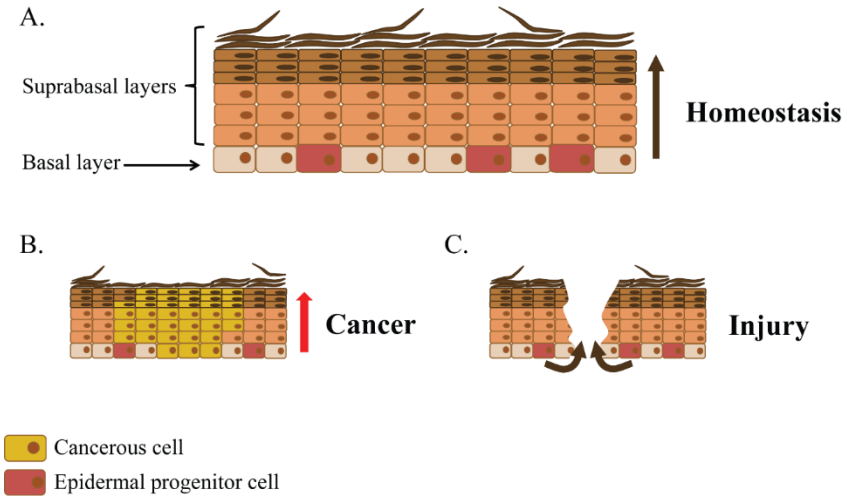

Figure 1.3. Epidermal homeostasis. **A**: Schematic representation of a homeostatic epidermis, with epidermal progenitor cells localised in the basal layer of the tissue. **B**: Cancer formation due to imbalance in proliferation. **C**: Tissue repair upon injury, facilitated by progenitors derived from the basal layer.

1.3.3. Keratinocyte differentiation

As discussed so far, in a homeostatic epidermis, on average half of the cells produced in the basal layer will commit to differentiation (Doupe *et al.*, 2012). Once committed, differentiating keratinocytes undergo a series of changes, involving enucleation and accumulation of cytokeratins, which ultimately lead to their stratification and shedding (Eckert and Rorke, 1989). As the differentiating keratinocytes move up the tissue, their gene expression profiles change and one of the consequences of these stepwise changes is the stacking of epidermal layers, namely basal layer, spinous layer, granular layer and cornified layer (Denecker *et al.*, 2008) (Figure 1.4).

Keratinocytes originate in the basal layer and initially express basal cell associated marker proteins, such as Keratin 5 and Keratin 14 (Eckert *et al.*, 2002). During the process of differentiation, keratinocytes will not only move up the tissue, but also change their morphology by becoming increasingly flat and large (Eckert, Crish and Robinson, 1997). Similar changes can be also observed during differentiation of cultured keratinocytes (Gandarillas, 2000; Borowiec *et al.*, 2013).

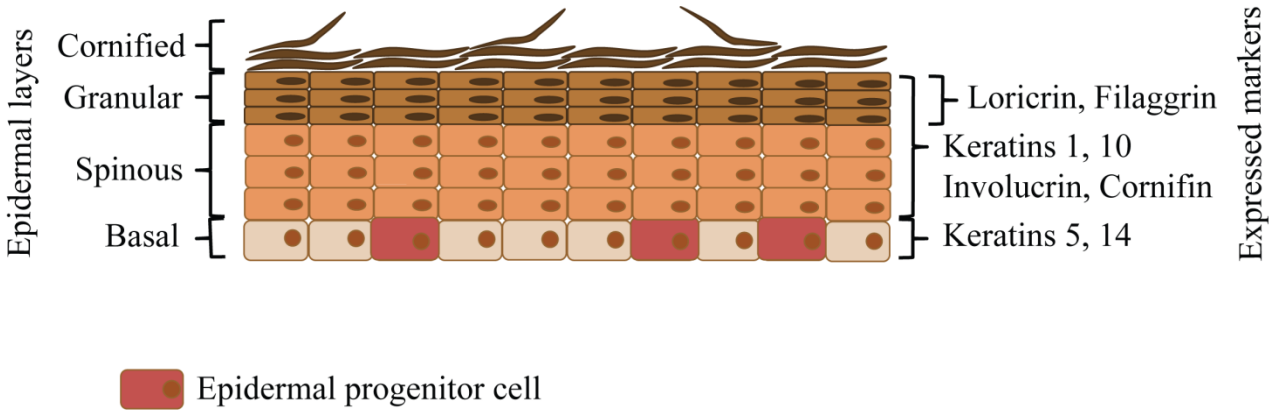

Figure 1.4. Epidermal differentiation markers. A schematic representation of mammalian epidermis composed of keratinocytes at various stages of differentiation is shown. Specific cytokeratins and other proteins expressed in different layers of the epidermis are indicated.

Once keratinocytes move into the spinous layer, they normally exit the cell cycle and are no longer able to divide (Denecker *et al.*, 2008). They start expressing early differentiation markers such as Keratin 1 and Keratin 10, as well as Involucrin and Cornifin. Reinforcement of the cytoskeleton and formation of tight intercellular junctions are the key features of keratinocyte differentiation at this stage (D'Orazio *et al.*, 2013). Eventually, keratinocytes are pushed into the granular layer and start the enucleation process. Enucleation occurs over several hours in keratinocytes localised at the top layer of *stratum granulosum* but the mechanism for this process is not fully understood (Rogerson, Bergamaschi and O'Shaughnessy, 2018). It is proposed of nuclear DNA degradation is mediated by TREX2 exonuclease and DNase1L2 and 2 (Fischer *et al.*, 2017; Manils *et al.*, 2017). Moreover, the process of enucleation involves degradation of lamin A/C which is an AKT1-mediated process (Naeem *et al.*, 2015). At this stage, the keratinocytes normally express high levels of late differentiation markers, such as Loricrin and Filaggrin (Denecker *et al.*, 2008). They also acquire additional excretory functions, which aim to reinforce the barrier function of the epithelium (Ma and Ozers, 1996). The final stages in the keratinocyte differentiation are the formation of the cornified envelopes and finally shedding of dead corneocytes, which is facilitated by the progressive loss of intercellular junctions (Denecker *et al.*, 2008; Madison, 2003). Any disturbance the described sequence of events can results is serious pathologies of the skin, therefore understanding the processes which underlie keratinocyte differentiation is of key importance.

Over the past few decades, a lot of emphasis was placed on trying to understand the pathways which regulate keratinocyte differentiation. To achieve a better understanding of this complex decision making process, intricate cell culture methods have been developed, which try to mimic the processes observed *in vivo* (Barrandon *et al.*, 2012; Borowiec *et al.*, 2013). Several regulatory cascades were identified to play an important role in keratinocyte differentiation, including mitogen-activated protein kinase (MAPK) cascades (Eckert *et al.*, 2002). Changes in lipid synthesis in keratinocytes were also suggested to play a role in committing to differentiation (Ponec *et al.*, 1987), alongside the involvement of the mTOR signalling pathway (Laplante and Sabatini, 2009; Sampath *et al.*, 2008). The role of the latter two processes in keratinocyte differentiation will be further investigated in this thesis.

1.3.4. Epidermal pathologies and clinical significance

Given the importance of the epidermis is maintaining the barrier function of the skin it is not surprising that any disturbances to its homeostasis and integrity can have serious consequences for the human health. There are many medical conditions which affect the skin and the epidermis in particular. Diseases of the skin which are directly linked to the function of the epidermis include epidermal neoplasms and lesions, a number of autoimmune conditions, chronic blistering and many more (Marks and Miller, 2006).

Skin cancer is probably the most relevant to the study of tissue homeostasis, since its most apparent characteristics are an abnormal growth of the tissue and development of cells that have the ability to divide indefinitely and spread to other tissues and parts of the body (Cakir, Adamson and Cingi, 2012). Skin cancer accounts for at least 40% of all cancer cases, making it by far the most common form of the disease (Jemal *et al.*, 2011; Cakir, Adamson and Cingi, 2012). The three main types of skin cancer are basal cell carcinoma (BCC), squamous cell carcinoma (SCC) and melanoma (Saladi and Persaud, 2005). The first two types, together with other less common types of skin cancer, are collectively classified as nonmelanoma skin cancers, and are the most common type of cancer in Caucasians, with at least 2 to 3 million new cases diagnosed around the world every year (Lomas, Leonardi-Bee and Bath-Hextall, 2012). It is believed that more than 90% of all skin cancers are caused by exposure to excessive ultraviolet radiation and decreasing exposure to the sun and the use of sunscreen has been shown to reduce the risk of developing melanoma and nonmelanoma skin cancer significantly (Armstrong and Kricker, 2001; Grant, 2008; Jou, Feldman and Tomecki, 2012).

Both, basal-cell carcinomas and squamous-cell carcinomas are most often found on sun-exposed areas of the skin (Pfeifer and Besaratinia, 2012). They often carry mutations which are characteristic of DNA damage caused directly by UVB radiation (Brash, 2015), however, there is a growing body of evidence suggesting the involvement of indirect DNA damage caused by oxygen free radicals (Murugesan *et al.*, 2005; Cooke *et al.*, 2007; Pfeifer and Besaratinia, 2012). Interestingly, the maintenance of the physiological function of the epidermis is a robust process. Biopsies from non-cancerous UVB exposed human skin contain up to 140 mutations, normally linked to cancer development, on each square cm of the tissue (Martincorena *et al.*, 2015). While BCCs are very rarely metastatic, SCCs metastasise more frequently, especially when present in people who are immunosuppressed (Lomas, Leonardi-Bee and Bath-Hextall, 2012). Cutaneous squamous-cell carcinomas (cSCC) are the most relevant to this thesis, as they arise from the squamous epithelium.

Amongst the autoimmune conditions of the skin, one with a particular relevance to the epidermal homeostasis is psoriasis. Psoriasis is characterised by patches of abnormal skin, which are red, dry and scaly, and is thought to be a genetic disease triggered by environmental stimuli (Menter *et al.*, 2008). Factors such as infections, psychological stress, medications, changes in climate and seasons have all been shown to aggravate the condition, however, genetic factors can clearly predispose to psoriasis with identical twins being three times more likely to develop a condition if a sibling is affected than non-identical twins (Lebwohl, 2003). Patches of skin affected by psoriasis are characterised by abnormal production of keratinocytes resulting in the excessive growth of the epidermal layer (Lowes, Bowcock and Krueger, 2007). In psoriasis, the turnover of keratinocytes can be up to six times faster than in normal epidermis, which is thought to be due to disruptions to keratinocyte differentiation and premature shedding (Broome, Ryan and Eckert, 2003; Griffiths and Barker, 2007). These changes are most likely induced by an inflammatory cascade in the dermis (Lowes, Suarez-Farinas and Krueger, 2014), but several mutations in proteins responsible for ensuring the barrier function of epidermis have been also shown to predispose to psoriasis (Roberson and Bowcock, 2010).

An effective barrier function of the epidermis is ensured not only by maintaining tissue homeostasis, but also by ensuring that epidermis is securely attached to the underlying dermis (Proksch, Brandner and Jensen, 2008). A number of genodermatoses, that is genetic diseases of the skin, are caused by the mutations in the proteins acting as anchors attaching the basal layer of epidermis to the basement membrane and underlying dermis (McGrath, Eady and Pope, 2004). Epidermolysis bullosa is a group of such genetic diseases, which result in painful blistering of the skin and mucous membranes and can lead to formation of highly aggressive SCCs in the affected children. (Tabor *et al.*, 2017). The severity of the condition can vary from mild to even lethal; largely depending on the type of genetic mutation that is causing the disease in the particular case (Kim *et al.*, 2017; Diociaiuti *et al.*, 2018). Until recently there was no cure for the condition, but the recent advances in gene editing and tissue engineering provide a great hope for the effective treatments of certain types of epidermolysis bullosa (Kocher *et al.*, 2017; Hirsch *et al.*, 2017).

1.4. Human epidermal keratinocyte culture

1.4.1. History of skin grafting and tissue engineering

Loss of protective layers of tissue due to trauma, infection, burns or medical procedures can be life threatening to the individuals affected, and it is not surprising that for centuries physicians have been looking for ways of replacing lost skin (Hauben, Baruchin and Mahler, 1982). Skin grafting involves transplanting pieces of skin, usually from one part of the body to another, and it is the oldest known form of tissue reconstruction. Texts reporting the use of skin grafting for nose reconstruction date back 2500 years, the oldest one being a medical compendium written by an Indian surgeon, Sushruta (Weathers *et al.*, 2013). *Sushruta Samhita*, which can be translated to Sushruta's Compendium, contains detailed descriptions of more than a thousand human diseases, as well as instructions for the use of medicinal plants, and for performing multiple surgical procedures. Amongst these procedures, there are descriptions of three types of skin grafts and reconstruction of the nose (Hauben, Baruchin and Mahler, 1982) (Figure 1.5A).

Despite the long history of the use of skin grafting, first attempts at maintaining fragments of human skin *in vitro* were only described towards the end of XIXth century. In a revolutionary paper published in 1898, Ljungrenn reports culturing skin from a child in ascitic liquid before transplanting it back to a donor (Ljunggren 1898). Following that, other scientists have later shown that skin fragments cultured in a saline-based medium can produce outgrowths of epithelial cells and connective tissues (Carrel and Montrose, 1910; Kreibich, 1914). Over the next decades, it became apparent that although epidermis needed for transplantation could be cultured using whole fragments of skin, known as explants, the quantity of cells produced using such approach is unlikely to be sufficient (Pinkus, 1932; Medawar, 1948; Parshley and Simms, 1950) (Figure 1.5B).

First successful attempts at culturing keratinocytes from dissociated tissue were undertaken in the mid-1970s and opened a new chapter in epithelial transplants (Rheinwald and Green, 1975; Rheinwald and Green, 1977). Rheiwald and Green developed culture methods which allowed for serial cultivation of human keratinocytes (Figure 1.5C). The use of inactivated feeders to support the growth of keratinocytes is still a go to method up to this day; however, a lot effort is invested into developing robust feeder-free approaches (Coolen *et al.*, 2007; Radtke *et al.*, 2009).

Figure 1.5. History of epidermal grafts. **A**: Image from the *Sushruta Samhita*, detailing the procedure for nose reconstruction surgery. Reproduction made in 1794 for the Gentleman's Magazine of London. **B**: Early example of skin explant showing migratory overgrowth of the epithelium (Medawar, 1948). **C**: First clonal human keratinocyte cultures (Rheinwald and Green, 1975). **D**: Epithelial sheet obtained from cultured keratinocytes ready for transplantation. Image credit to Ruhr-Universität Bochum. **E**: Fully regenerated epithelium generated from autologous transgenic keratinocyte grafts, exhibiting normal skin functionality and flexibility (Hirsch *et al.*, 2017).

Transplants of cultured epithelium are now routinely used to treat patients with substantial skin damage, including burn patients, and following surgical procedures, for instance after skin cancer removal, if it is not possible to obtain enough tissue from healthy donor sites on other parts of the body (Hunziker and Limat, 1999; Smirnov *et al.*, 2003) (Figure 1.5D).

The newest development in the applications of epithelial transplants is the use of genetic engineering to correct faulty genes in cultured keratinocytes, which are then transplanted back to the patient to treat genetic diseases of the skin. A truly incredible example of such application was achieved through the collaborative efforts of surgeons and scientists who were able to replace virtually the entire epithelium of a boy affected by a severe type of junctional epidermolysis bullosa with autologous grafts of cultured keratinocytes with a corrected version of a mutated gene, which was responsible for his symptoms (Hirsch *et al.*, 2017) (Figure 1.5E).

1.4.2. Clonal types of keratinocytes

Soon after the methods for culturing keratinocytes as individual cells were developed, scientists began to question the mechanisms behind the keratinocyte behaviour in culture terms of proliferation and differentiation. It soon became apparent that keratinocytes are not homogenous in their proliferative capacities, and while some keratinocytes keep on dividing in culture, some proceed to differentiate or produce daughters with mixed proliferative capacities (Barrandon and Green, 1987). This is when the notion of clonal types of keratinocytes was first proposed. It was suggested that colony forming human keratinocytes can be divided into three classes based on their growth potential *in vitro* (Barrandon and Green, 1987) (Figure 1.6). According to this theory, holoclones have the highest proliferative capacity and colonies formed by them rarely follow the route towards terminal differentiation. On the other side of the spectrum are the paraclones, which have a very limited life span in culture and never continue to divide beyond 15 cell generations. The final class characterised by Barrandon and Green are the meroclones, which in culture form middle sized colonies composed of cells with different proliferative potentials. Since the colonies classified as holoclones were later found to be the leading contributors to grafts in human patients (Pellegrini *et al.*, 1999), it was thought that the holoclones correspond to the basal stem cells, while the other two clonal types are the transit-amplifying cells and differentiated cells respectively.

Such classification was supported by other researchers in the field, who concluded that homeostatic epithelium is maintained by both, a small population of stem cells and a much larger population of transit-amplifying cells, which can occupy different niches in the epidermis, hair follicles and sebaceous glands (Jensen and Watt, 2006).

Figure 1.6. Historical classification of keratinocyte clonal types in culture. Three clonal types of keratinocytes with different proliferative capacities initially suggested by Barrandon and Green, 1987.

1.5. Human keratinocyte proliferation modes

1.5.1. Live imaging of keratinocytes

The initial studies of keratinocyte proliferative potential were based on subsequent plating of clones, but did not focus on following the division history of individual cells. For years researchers were trying to develop techniques, which would allow them to track the behaviour of keratinocytes in live cells. The first live tracing experiments were performed in the 1980s using time-lapse video recordings (Kitano *et al.*, 1983; Dover and Potten, 1988). These studies provided an interesting insight into the cell fate control of epidermal stem cells, revealing high heterogeneity in their proliferative potentials. While some keratinocytes were proliferating extensively, others produced daughter cells, which would go on to differentiate (Dover and Potten, 1988). Nevertheless, it was hard to draw any hard conclusions about how the epidermal homeostasis is maintained due to the technical difficulties faced by the researchers in both studies, which meant that only a very small number of cells were tracked, and also because the studies were done *in vitro*. More recent studies attempted cell tracking in live mice, but it is impossible to use a similar approach in humans (Rompolas *et al.*, 2012).

1.5.2. Two modes of division observed *in vitro*

A former member of our laboratory, Amit Roshan, was able to combine the advances in live cell tracking and imaging to bring us closer to understanding the cell fate determination in cultured human keratinocytes (Roshan *et al.*, 2016). His work was building on previous studies of epithelial homeostasis performed in mice, and was taking the lessons learnt there towards understanding the processes underlying progenitor fate decisions in human. At this stage, it was already understood that when a mammalian keratinocyte divides there can be three possible outcomes: two new progenitor cells, two differentiating cells or one of each kind can arise (Doupe *et al.*, 2012; Clayton *et al.*, 2007). In homeostatic tissue these different division outcomes would average out to produce equal numbers of differentiating and dividing cells in a fundamentally stochastic manner (Doupe *et al.*, 2012).

Roshan believed that the same division outcomes, with different probabilities of each of them occurring, could explain the great heterogeneity in the proliferative capacities of cultured human keratinocytes. Using an imaging instrument called an IncuCyte he has tracked thousands of keratinocyte divisions over many cell generations, and noted down outcomes of each of them. Firstly, he was able to conclude that the same three division outcomes observed *in vivo* in mice, can be also observed *in vitro* in human keratinocyte cultures (Roshan *et al.*, 2016). Secondly, it became apparent that the colonies of cultured keratinocytes can be divided into two groups based on the likelihood of each of the division outcomes happening in them, opposing the model previously proposed by Barrandon and Green, which suggested existence of three types of clonal keratinocytes (Barrandon and Green, 1987).

In Roshan's model, the two modes of proliferation observed *in vitro* are 'balanced' and 'expanding' (Roshan *et al.*, 2016) (Figure 1.7). Cells in the expanding mode divide in an exponential manner, with majority of resulting daughters going on to divide, which is most similar to the behaviour of epithelial progenitors during wound repair (Doupe *et al.*, 2012). This exponential manner of growth leads to a formation of very large colonies *in vitro* over several cell generations (Figure 1.8A). In balanced mode colonies, dividing keratinocytes produce on average equal numbers of differentiating and dividing daughters. This is similar to the division outcomes observed in a homeostatic epithelium (Doupe *et al.*, 2012; Clayton *et al.*, 2007) and leads to formation of much smaller colonies, with many of them going on to terminally differentiate (Figure 1.8B).

The observed two modes of proliferation strongly support the stochastic model of cell fate decisions in keratinocytes and can explain the variability observed in the colony sizes of keratinocytes grown *in vitro* and hence heterogeneity in their proliferative potential (Roshan *et al.*, 2016).

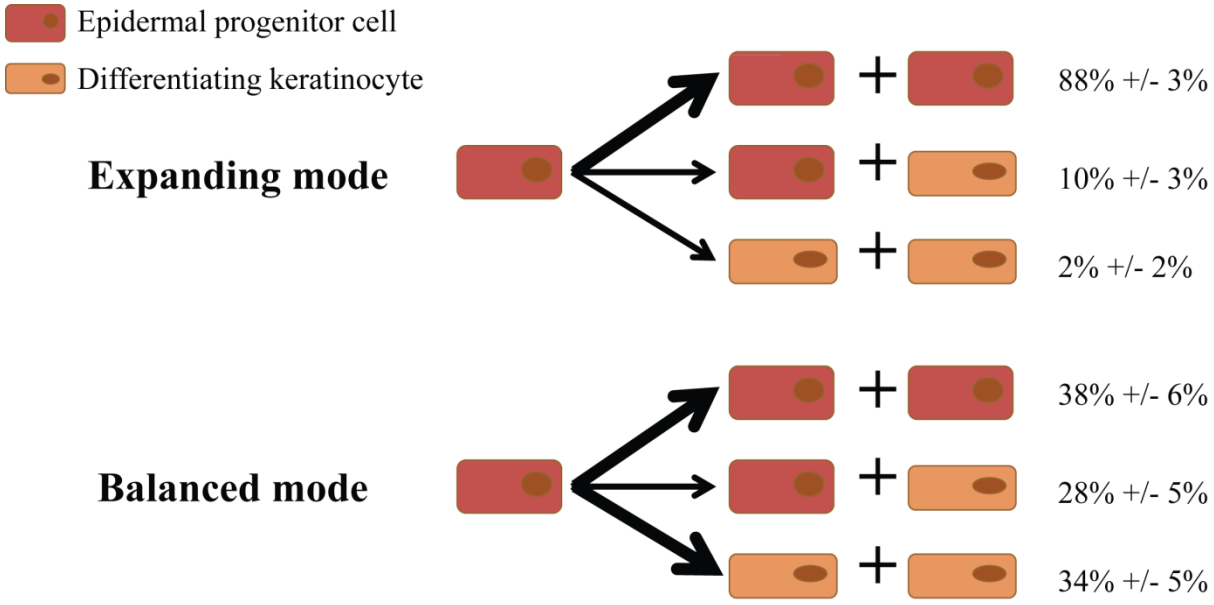

Figure 1.7. Expanding and balanced modes of proliferation. Average outcomes of cellular divisions of keratinocyte progenitor cells with different proliferative potential (Roshan *et al.*, 2016).

Another very interesting observation made by Roshan was that the modes of division are not fixed but are interchangeable (Figure 1.9). When a large expanding colony goes on dividing for several days, cells in the middle third of such colony actually switch their behaviour towards balanced mode in a density-dependent manner (Figure 1.9A). Interestingly, a similar switch in the proliferative mode can be observed when two large colonies merge together (Figure 1.9B). Also, keratinocytes seem to be able to revert back from balanced to expanding mode of division upon scratch injury (Roshan *et al.*, 2016).

The model proposed by Roshan seem to explain how the two interchangeable modes of division could be behind tissue maintenance and repair in human epidermis, however, as such, it does not explain any of the molecular processes, which would underlie fate determination in human keratinocytes. Therefore, after joining the laboratory, my efforts have focused on trying to understand these processes.

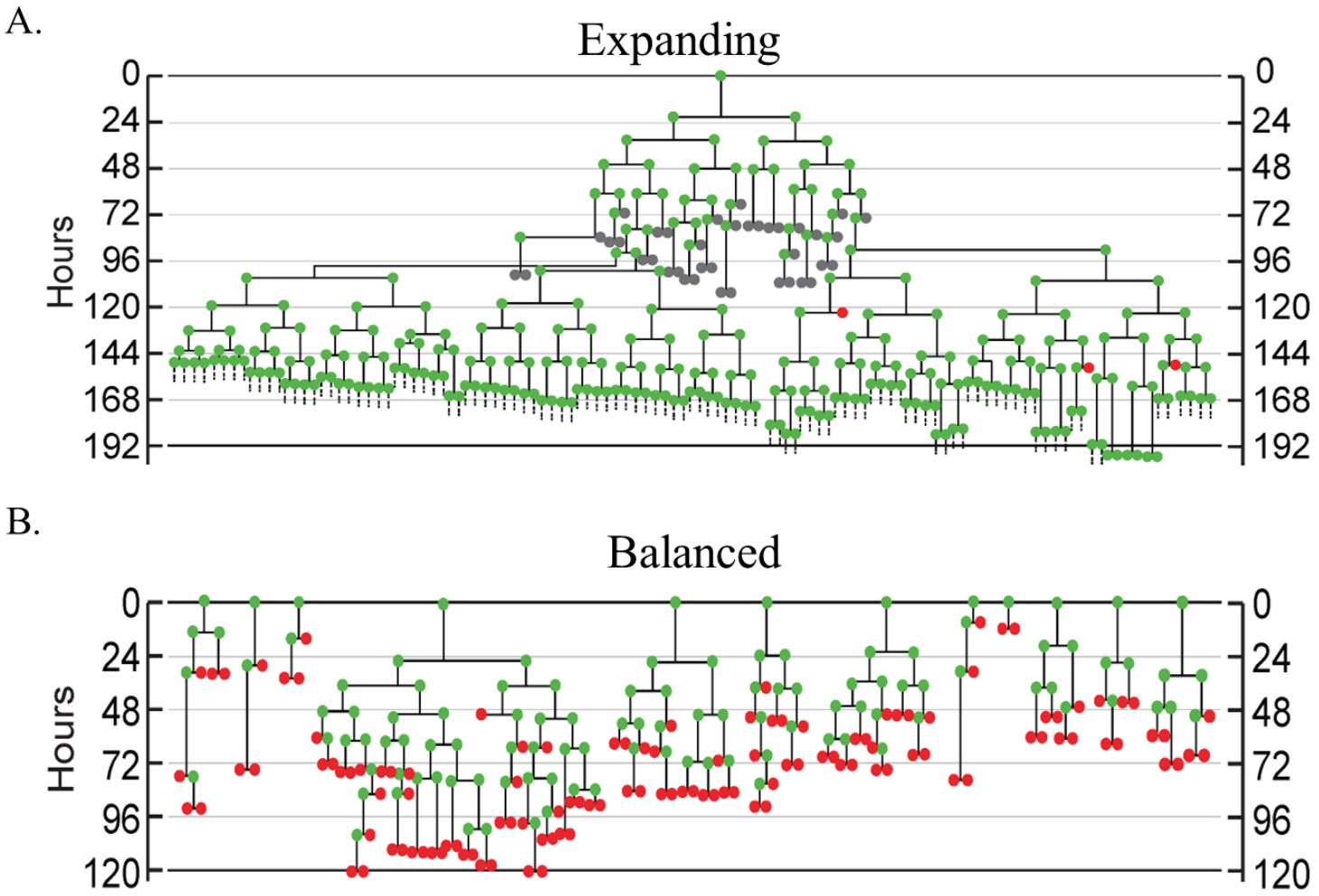

Figure 1.8. Family trees of cells with different proliferative potentials. Differentiating keratinocytes are marked in red, progenitors are marked in green (Roshan *et al.*, 2016).

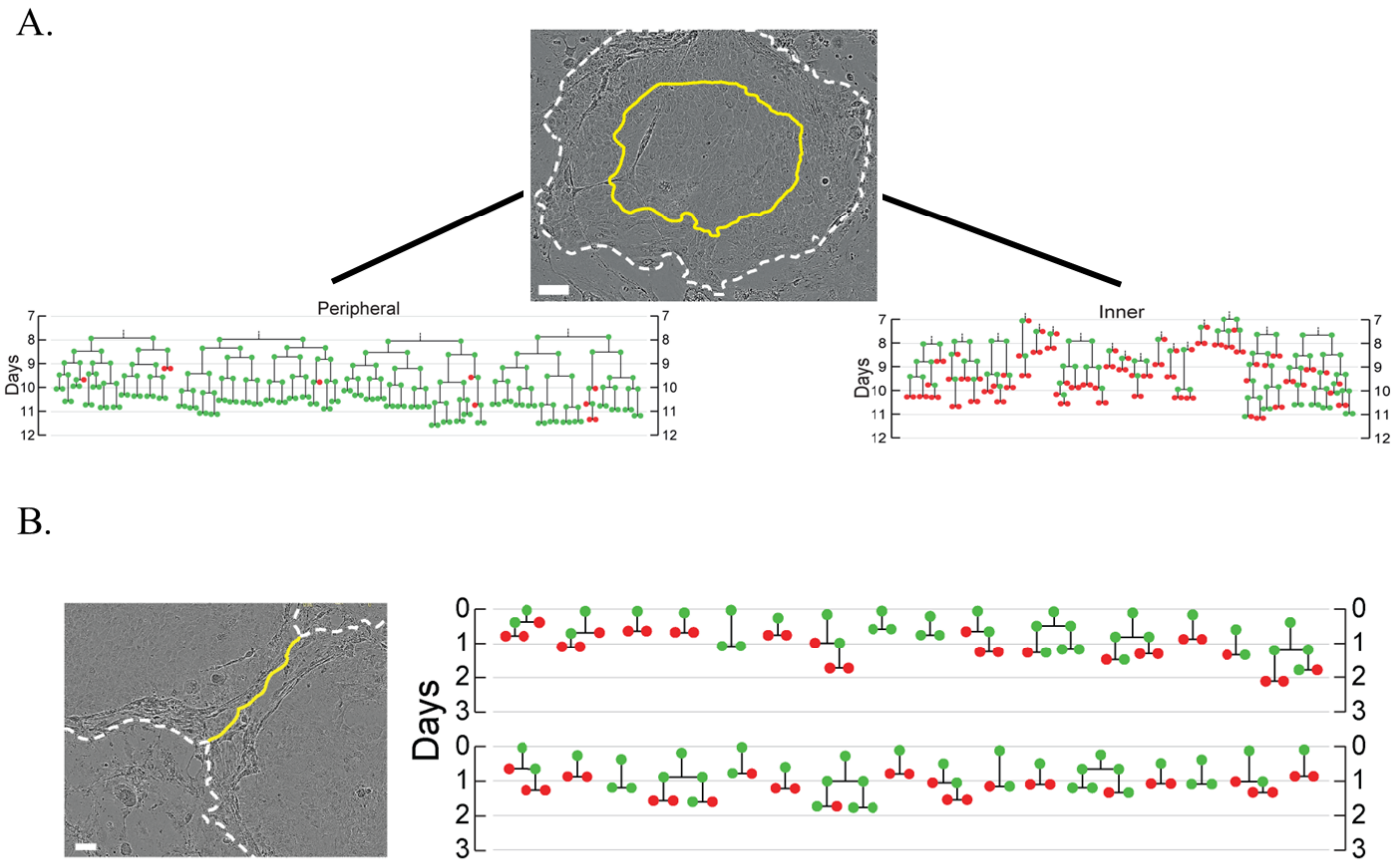

Figure 1.9. Confluence dependent switch in proliferation mode. Upon reaching local confluence, cells in the middles of large colonies (**A**), and at the interface with other colonies (**B**) switch their proliferative mode towards balanced (Roshan *et al.*, 2016).

1.6. Lipid biosynthesis and epidermal differentiation

Skin development and the formation of the skin permeability barrier are largely dependent on keratinocyte differentiation. Amongst the many changes which are happening during epidermal differentiation is an orchestrated remodelling of lipids (Radner *et al.*, 2011) in the extracellular matrix (ECM). ECM is a network of extracellular molecules which provides support and signalling cues to cells and can range from polysaccharide rich structure found in plants and fungi to largely protein-based structure found around animal cells. Interestingly, enzymatic conversion of glycerophospholipids, sphingomyelins, glucosylceramide and cholesterol sulfate, secreted by lamellar bodies from keratinocytes in the granular layer, leads to formation of the lipid-rich extracellular matrix, which surrounds the corneocytes in the cornified layer of the epidermis (Wertz, 1992; Wertz *et al.*, 1984; Schmitz and Muller, 1991). The main components of the resulting extracellular matrix are cholesterol, non-esterified fatty acids and ceramides (Freinkel and Traczyk, 1985; Feingold, 2009). Triacylglycerols are present in the extracellular matrix at lower quantities, but there is an increasing interest in the role of triacylglycerols metabolism in the formation of permeability barrier, due to its involvement in neutral lipid storage disease, such as the already mentioned ichthyosis (Freinkel and Traczyk, 1985; Schweiger *et al.*, 2009). It is believed that defective triacylglycerols metabolism causes disruption to the formation of the corneocyte lipid envelopes and hence impaired skin permeability barrier (Radner *et al.*, 2011).

Early on during the development of human keratinocyte culture methods, scientists observed changes in lipid synthesis happening during *in vitro* keratinocyte differentiation (Ponec *et al.*, 1987; Ponec *et al.*, 1988; Williams *et al.*, 1988). It was shown that cholesterol depletion, caused by specific inhibition of cholesterol synthesis, can affect differentiation capacity of cultured keratinocytes (Ponec *et al.*, 1987). Importantly, the lipid composition of keratinocytes was also shown to change depending on culture conditions (Williams *et al.*, 1988), with culture models which promote keratinocyte stratification displaying lipid profiles most similar to what is found in adult mammalian epidermis (Ponec *et al.*, 1988). On top of that, there were differences in lipid profiles between normal and immortalised human keratinocyte lines (Schurer *et al.*, 1993). More recent studies have also highlighted the role of lipids in wound healing and maintenance of healthy epidermal barrier (Amen *et al.*, 2013; Chon *et al.*, 2015), therefore, I was interested to see if changes in lipid biosynthesis are important solely for keratinocyte differentiation, or if they are also involved in progenitor fate determination.

1.7. Eukaryotic translation and cell fate

Part of the work which formed basis for my doctoral studies was an analysis of transcriptional profiles of balanced and expanding mode colonies performed at my laboratory before the start of my project (Roshan *et al.*, 2016). Single cells were seeded per well and allowed to grow up into 8-cell colonies. At 8-cell stage, the differences between the two proliferation modes should be already established and detectable. Entire colonies were then lysed *in situ*, as previous attempts to enzymatically isolate single cells have resulted in transcriptional profiles being erased. Resultant RNA was analysed on a human transcriptome micro-array. Two groups of colonies were identified through hierarchical clustering. Since the clustering was most strongly influenced by the levels of keratinocyte differentiation associated transcripts, it was concluded that the two observed groups correspond to colonies with the balanced and expanding modes of proliferation. One of the most pronounced differences in the transcriptional profiles of the two proliferation modes, apart from the levels of known differentiation markers, was that the putative balanced colonies had much higher levels of mRNA associated with translation, as compared to the expanding group. Increase in global translation in the balanced colonies was later confirmed in a fluorescence based O-propargyl-puromycin global translation assay (Roshan *et al.*, 2016), which further convinced me to focus my investigation on the role of translation in keratinocyte progenitor fate determination.

After joining the laboratory, I first wanted to identify the molecular markers of the colony's proliferation mode, building on data obtained from the micro-array analysis and my own RNA-seq analysis, which is described in Chapter 3 of this thesis. Eukaryotic translation initiation factors 3E (eIF3E) and 4G2 (eIF4G2) were amongst the genes identified to be differentially expressed by both analyses. These eIFs are both involved in translation, yet each of them plays a specific role in the initiation of this process, with each acting independently of the other factor studied (Figure 1.10) (Klann and Dever, 2004). During translation, eIF3 (orange arrow in Figure 1.10) positions mRNA near the exit site of the 40S ribosome subunit, thus promoting the assembly of the pre-initiation complex. At the same time, eIF4G (blue arrow in Figure 1.10) mediates circularisation and activation of mRNA by binding the poly(A) tail via an accessory protein. Significantly higher levels of eIF3E and eIF4G2 coding transcripts were detected in balanced mode cells than in expanding ones. Therefore, a big portion of my work has focused on the role of these two factors in the establishment and maintenance of balanced and expanding modes of division (Chapter 4).

Figure 1.10. Main steps in eukaryotic translation initiation. All featured translation initiation factors act as part of larger protein complexes, including eIF4G2 (a subunit of eIF4G, blue arrow) and eIF3E (subunit of eIF3E, orange arrow). Figure adapted from Klann and Dever, 2004.

Other studies have also highlighted the involvement of translation in keratinocyte differentiation and cell fate determination. While changes in cytoskeleton and especially changes in the intermediate filament components of it are known to be an important factor in multiple tissues repair processes (DePianto and Coulombe, 2004), research performed by Seyun Kim et al. investigated cytoskeletal remodelling specifically in keratinocyte regeneration (Kim, Wong and Coulombe, 2006). Researchers identified Keratin17 (KRT17) as one of intermediate filaments upregulated in the keratinocyte repair process. Interestingly, keratinocytes from *Krt17*$^{-/-}$ mouse model showed not only impaired wound closure but they also exhibit a reduction in global translation levels. Further work identified a novel and unexpected pathway in which KRT17 may specifically activates the mTOR pathway via a Stratifin intermediate. Importantly, this activation of mTOR signalling is resulting in changes in global translation levels which were observed to coincide with upregulation of specific translation initiation factors, including members of the eIF4E complex. Therefore, this work demonstrated that mTOR mediated increase in translation is a core part of tissue regeneration which is likely to result in a change of cell fate in affected keratinocytes.

A recently published study has also indicated a possible relationship between global translation levels and cell fate (Liakath-Ali *et al.*, 2018). The work focuses on the role of mouse protein Pelota (Pelo) in the control of epidermal homeostasis. Pelo is a homologue of yeast protein Dom34 which is involved in the rescue of stalled ribosomes (Guydosh and Green, 2014). Interestingly, loss of Pelo function resulted in upregulation of the global translation levels in the mouse model. This was observed to coincide with abnormal differentiation in certain keratinocytes. These abnormal differentiation events resulted in severe epidermal phenotypes in mice which prevented them from surviving beyond the 5th month *postpartum*. Interestingly, administration of Rapamycin resulted largely in the rescue of epidermal phenotypes associated with the loss of Pelo function in the mouse model. Further investigation indicated that the Rapamycin treatment did lead to expected inhibition of mTOR signalling which prevented translational upregulation associated with loss of Pelo. Although the specific role of Pelo in the maintenance of keratinocyte homeostasis remains unknown, this work presents a clear correlation between translational upregulation and abnormal keratinocyte differentiation. The fact that inhibition of mTOR signalling leads to the maintenance of normal epidermal development in mutant mice provides further evidence that keratinocyte differentiation and cell fate may be somehow linked with the global translation levels.

1.8. Research objectives

Taking into consideration the state of knowledge at the beginning of my doctoral studies, the main aim of my project was to try to identify the molecular basis of human keratinocyte cell fate determination and to find out what makes one colony balanced and another expanding. My hypothesis was that specific translational and transcriptional features define the identity of colonies and that by altering these characteristics the colony fate can be changed. In order to investigate his hypothesis, I decided to focus my investigation on achieving the following aims:

My first aim was to identify the molecular signatures of balanced and expanding modes of proliferation. In order to achieve that, I developed bulk culture models of the two modes and performed an RNA-seq analysis, the results of which are presented in Chapter 3.

Next, I aimed to analyse the specific mechanisms by which proliferation mode is maintained and controlled. To do that, I performed a series of immunochemistry and RNA interference experiments aimed to assess the role of translation initiation in balanced and expanding mode colonies, which are described in Chapter 4.

Finally, I aimed to investigate other pathways which could influence the progenitor fate in culture. Specifically, I looked at the role of lipid biosynthesis in keratinocyte differentiation and cell proliferation. The performed microscopic analysis, RNA interference experiments and drug treatments are described in Chapter 5, which is the last results chapter of this thesis.

.

Chapter 2 Materials and methods

2.1. Cell culture

In all experiments cells were cultured at 37°C in 5% CO_2. Cells were monitored and passaged as required using trypsin-EDTA (Sigma-Aldrich M4287). Medium was changed and new feeders added every 3 or 4 days, unless otherwise stated. All cultures were carried out in Nunc coated flasks or plates (Thermo Fisher Scientific).

2.1.1. J2 fibroblast culture

J2 fibroblasts (Jones laboratory stock, originally obtained from J. Rheinwald, Harvard University, USA (Rheinwald and Green, 1975) were maintained in low glucose DMEM (Thermo Fisher Scientific 21885-025) supplemented with 10% donor bovine serum (Thermo Fisher Scientific 16030-074). Cells were passaged at a 1 in 5 dilution every 3-4 days. Cells were not used beyond passage 16.

Before being used as feeders, cells were inactivated by incubating them for 3 hours with 4 µg/mL mitomycin C (Sigma-Aldrich M4287), washed 3 times with 1 x PBS and lifted using trypsin-EDTA. J2 suspension was then added to NFSK cultures, as detailed in Table 2.1.

Table 2.1. Cell plating densities for the J2 fibroblast feeder layers.

Target	No. of feeders
15 cm dish (140 cm^2)	$5x10^6$
10 cm dish (60 cm^2)	$2x10^6$
75 cm^2 flask	$2x10^6$
6-well plate (10 cm^2 per well)	$2.5x10^5$
12-well plate (3.8 cm^2 per well)	$1x10^5$
24-well plate (1.8 cm^2 per well)	$5x10^4$
96-well plate (0.3 cm^2 per well)	$2.5x10^4$

2.1.2. Human keratinocyte culture

Neonatal Foreskin Epidermal Keratinocytes (NFSKs, ATCC, PCS-200-010) were maintained in complete FAD medium (C'FAD), prepared by mixing 1:1 high glucose DMEM (Thermo Fisher Scientific 11971-025) and DMEM F12 (Thermo Fisher Scientific 31330-038), supplemented with 0.5 µg/mL hydrocortisone (Calbiochem 386698), 10 ng/mL EGF (PeproTech EC Ltd 100-15), 0.1 nM cholera toxin (Sigma-Aldrich C8052), 0.18 mM adenine (Sigma-Aldrich A3159), 5 µg/mL insulin (Sigma-Aldrich I5500) and 5% foetal bovine serum (Thermo Fisher Scientific 26140-079) (Rheinwald and Green, 1975).

Keratinocytes were grown on a layer of MMC- treated J2 fibroblast feeders, as described in Table 2.1 and were used for experiments between passage 3 and 8. Unless otherwise stated, all experiments were carried out at clonal plating densities, as summarised in table Table 2.2.

Table 2.2. Keratinocyte plating densities.

Target	No. of NFSKs
15 cm dish (140 cm^2)	$1x10^6$
10 cm dish (60 cm^2)	$5x10^5$
75 cm^2 flask	$6x10^5$
6-well plate (10 cm^2 per well)	$2x10^4$
12-well plate (3.8 cm^2 per well)	$1x10^4$
24-well plate (1.8 cm^2 per well)	$5x10^3$
96-well plate (0.3 cm^2 per well)	$1x10^3$

2.1.3. Cell transduction with viral vectors

2.1.3.1. H2B-GFP tracking experiments

A retrovirus encoding mouse histone 2b (H2B, UniProtKB: Q64475) fused to GFP (UniProtKB: P42212) under the control of the P_{TRE3GS} doxycycline-inducible promoter was generated using the Retro-X Tet-One Inducible Expression System (Clontech Laboratories 634307). Choosing a selectively inducible promoter ensured that no more H2B-GFP was produced after the withdrawal of doxycycline. Because parental histones are equally distributed between daughter cells with each cell division (Krude and Keller, 2001), one can expect the level of fluorescence to halve appropriately as the cells divide (Kanda, Sullivan and Wahl, 1998). Data presented in Figure 2.1 shows that monitoring the H2B-GFP dilution can indeed be used to determine whether a given cell has undergone division.

In order to produce a retrovirus for transduction of keratinocyte cultures, the GP2-293 Packaging Cell Line was grown to about 50% confluence, meaning that roughly half of the surface of the culture dish was covered and there was still room for cells to grow, before being transfected with an envelope vector and a retroviral expression vector, using the Xfect Transfection Reagent (Clontech Laboratories 631317). Culture conditions for the GP2-293 Packaging Cell Line were the same as for the J2 fibroblasts; however, extra precautions were taken due to increased biosafety risk. Retroviral supernatants were harvested 48 h after transfection and stored at -80°C if not used immediately.

NFSKs were infected with the H2B-GFP retrovirus 72 h before the start of the experiment. The feeder layer was removed for the duration of the overnight retrovirus incubation by washing vigorously with 1 x PBS. Incubation was terminated by washing the infected cells 3 times with 1 x PBS and replacing culture media with fresh C'FAD. 24 h post infection 0.2 µg/mL doxycycline was added to the cells for 48 h. After 48 h, cells were checked for expression of GFP and then seeded at $0.1x10^4$ cells per well of a 12-well plate with a standard number of feeders, as specified in Figure 2.1. Plates were placed in an IncuCyte imaging system (Essen Bioscience), which allowed colonies to be tracked throughout the experiment. Images were analysed when colonies reached 8 cells in size, and again after 7 days.

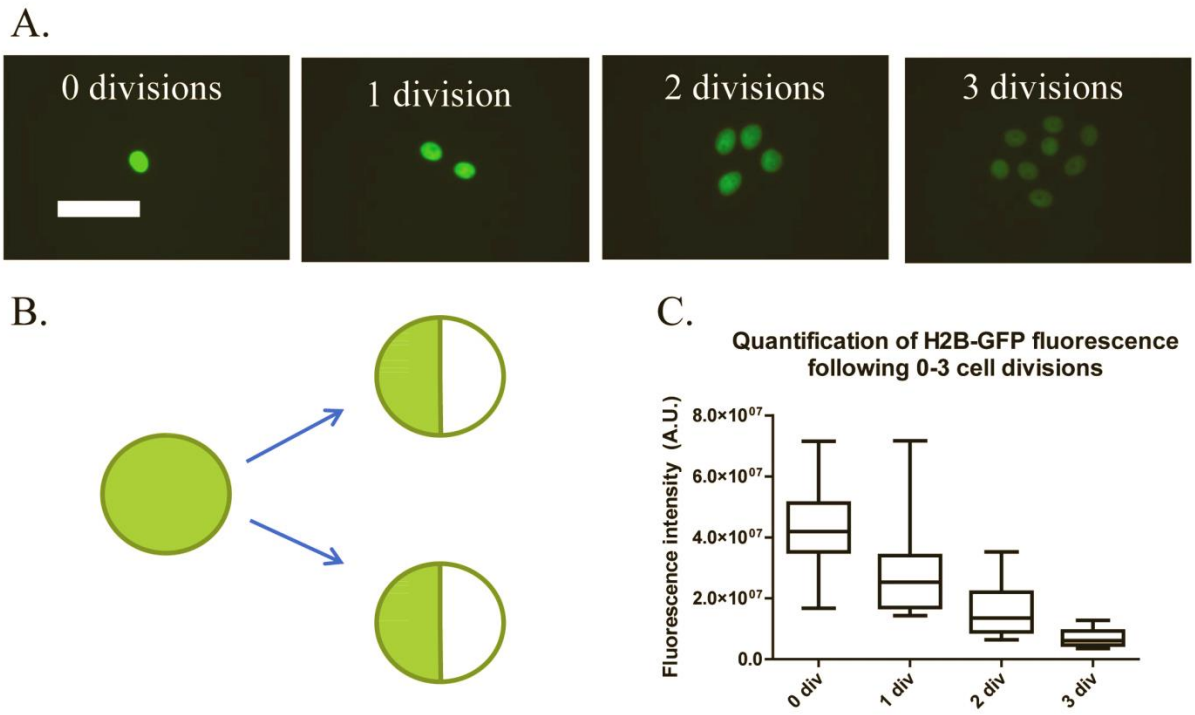

Figure 2.1. Measurements of H2B-GFP fluorescence after cell division. Following withdrawal of doxycycline, H2B-GFP fluorescence halves with each cell division as expected (**A, B**). Measurements performed by Emma Woolcock, shown in panel **B** prove that monitoring H2B-GFP dilutions can be used to estimate whether a given cell has divided or not. Scale bar in panel A represents the length of 40 µm and the images were obtained at 40 x magnification. For data in panel **C**, data distribution and medians are shown.

2.1.3.2. Flow sorting of H2B-GFP positive cells.

For the staining and EU-incorporation experiments, H2B-GFP expressing cells were flow-sorted into 96-well plates using a Mo-Flo XDP machine at Sanger's Cytometry Core Facility with kind help of the facility's staff. The sheath pressure was set to 60 psi and a 150 µm cytonozzle tip was used. Cells were resuspended in 1 x PBS supplemented with 2% foetal bovine serum. A 488 nm pinhole laser and a FL1 detector were used to sort for H2B-GFP positive cells. Three cells were sorted per well of a 96-well plate pre-seeded with MMC-treated J2s to maximise the chances of having one viable, dividing colony per well.

2.1.4. Non-viral transfection methods

2.1.4.1. Initial optimisation

Lipofectamine 3000 (Thermo Fisher Scientific L3000008) and Accell siRNAs (Dharmacon D-001940-01) were tested as potential means for performing Small interfering RNA (siRNA) mediated gene knock-downs in NFSKs (see Figure 2.2). While both reagents ensured delivery of a non-targetting GFP-tagged siRNA control (Thermo Fisher Scientific AM4626) into virtually all treated keratinocytes, Lipofectamine 3000 was preferable thanks to a shorter incubation time needed for effective transfection.

2.1.4.2. Delivery of siRNAs

Lipofectamine 3000 (Thermo Fisher Scientific L3000008) was used to transfect keratinocytes in the knock-down experiments. Manufacturer's instructions were followed throughout. The p3000 compound was not used, as advised in the protocol for RNA transfections. 160 pmol of siRNA and 3 µL of Lipofectamine 3000 diluted in 100 µL Opti-MEM (Thermo Fisher Scientific 31985062) were used per well of a 12-well plate. The amounts of reagents were scaled linearly depending on the size of the culture plate used. Transfections were carried out without the feeder layer, which was removed for the duration of the overnight siRNA incubation by washing vigorously with 1 x PBS. Cells were maintained in C'FAD thoughtout transfection. The details of the siRNAs used are shown in Table 2.3. When two siRNAs against a single target were used, an internal reference number was given to each of them.

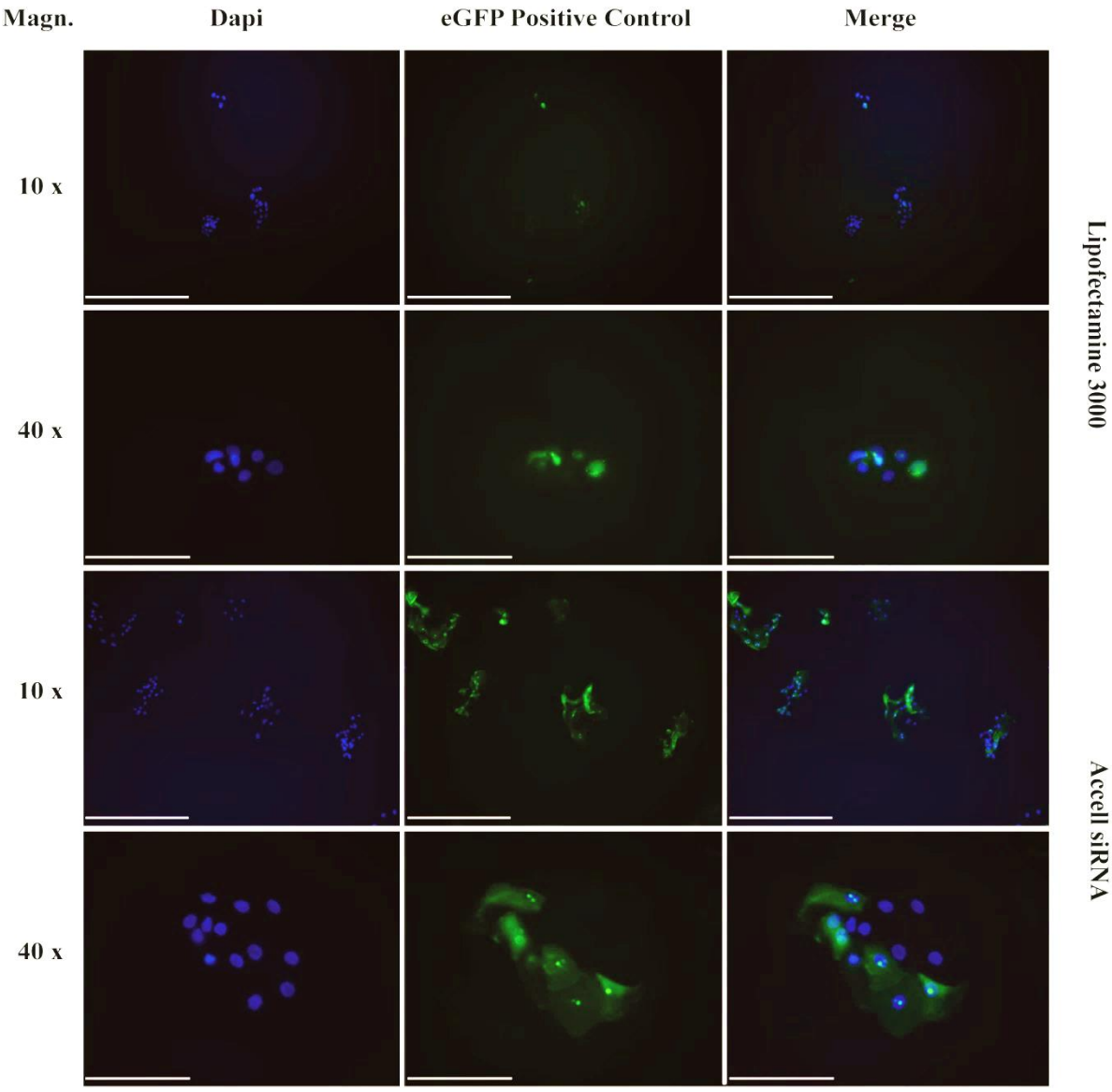

Figure 2.2. Non-viral transfection methods. Representative images of NFSKs transfected with either eGFP-tagged siRNA and Lipofectamine 3000 (two upper panels) or Accell non-targeting eGFP-tagged siRNA (two bottom panels) are shown. The scale bars represent 280 µm for the images at 10 x magnifications and 70 µm for the images at 40 x magnifications.

Table 2.3. Small interfering RNAs (siRNAs) used.

Target	Internal reference no.	Assay ID	Supplier
eIF3E	eIF3E 1	144785	Ambion
eIF3E	eIF3E 2	144784	Ambion
eIF4G2	eIF4G2 1	9765	Ambion
eIF4G2	eIF4G2 2	9945	Ambion
SREBP1	SREBP1 1	5045	Ambion
SREBP1	SREBP1 2	110742	Ambion
Negative Control	Not applicable	4390843	Ambion

2.1.5. Drug treatments

1mM stock solutions of drugs (see Table 2.4 for details) were prepared in DMSO (Sigma-Aldrich D8418). NFSKs were seeded at clonal density as detailed in Table 2.2 with inactivated J2 feeders (Table 2.1). 96 hours post seeding, the cultures were treated for 72 h with the relevant compounds. Final drug concentrations of between 0 and 80 nM were used. Media, supplemented with appropriate amounts of drugs, was changed daily. Plates were imaged before and after treatment using the Incucyte ZOOM (Essen Bioscience). To acquire clear images of whole plates, the feeder layer was removed for the duration of scans. New MMC-treated J2s were then applied before the treatment was started. At the end of treatment cells were either fixed or collected for protein immunoassays.

Table 2.4. Drugs and small molecule inhibitors used.

Name	Target	Supplier	CAS no.
Rapamycin	mTORC1	Sigma-Aldrich	53123-88-9
Torin 1	mTORC1/2	Cayman Chemical	1222998-36-8
Lovastatin	HMG-CoA reductase	Abcam	75330-75-5

2.1.6. Labelling of S-phase cells

In order to label cells in S-phase, keratinocyte cultures were treated with 1 µM EdU (Thermo Fisher Scientific A10044) in culture medium for 24 h. As the average division time for keratinocytes in culture is 15 h (Roshan *et al.*, 2016), a 24h incubation with EdU should ensure that all actively cycling cells are labelled.

Based on the cell cycle time distribution determined by live imaging, the proportion of EdU positive cells in a given colony can be used to assess a colony's fate. If more than 80% of cells within a colony are EdU positive (EdU+), it can be assumed a colony is expanding, otherwise a colony or an area is classified as dividing in the balanced mode.

2.1.6. Global transcription assay

In order to quantify levels of global RNA transcription, NFSKs were treated with 1 mM EU (Thermo Fisher Scientific E10345) for 1 h. After 1 hour the feeder layer was removed with vigorous washing using 1 x PBS and the NFSK colonies were fixed using 4% PFA (FD Neurotechnologies PF101) for 10 min at room temperature and then washed three times with 1 x PBS. Plates were stored at 4°C until staining was performed. As both EU and EdU are visualised using Click-iT chemistry (section 2.2 of the Materials and methods), for the global transcription assay, colonies were classified as either balanced or expanding based on Keratin1 (KRT1) expression. If at least 1 cell within a colony was KRT1 positive (KRT1+), the colony was classified as balanced. If no KRT1+ cells were present, the colony was branded expanding.

2.2. Immunocytochemistry and imaging

2.2.1. Staining of culture plates

Fixed cultures were permeabilised and blocked using PB-buffer (1 x PBS with 0.5% Triton X100 (BDH 28817.295), 0.25% FSG (Sigma-Aldrich G7765), 0.5% BSA (Sigma-Aldrich A8531) and 10% Donkey serum (Sigma-Aldrich D9663)) for 1 hour at room temperature. Primary antibodies (see Table 2.5) were incubated overnight at 4°C with PB-buffer. Plates were then washed three times, for 5 min each time, with 0.05% TWEEN 20 (Sigma-Aldrich P9416) in 1 x PBS. Secondary donkey antibodies conjugated with Alexa Fluor azides (Life Technologies) were incubated for 30 min at 1:500 dilution in PB-buffer. Plates were washed as previously and mounted in Vectashield Mounting Medium with DAPI (Vector labs H-1500) diluted 1:5 with 1 x PBS.

2.2.1.1. Zenon labelling kit

For direct immunofluorescence experiments, primary antibodies (anti-eIF3E and anti-eIF4G2) were labelled using Zenon labelling kit (Life Technologies Z-25407) following manufacturer's instructions. 2 µg of labelled antibodies were used per well of a 12-well plate and incubated overnight at 4°C and then the standard protocol was followed.

Table 2.5. Primary antibodies used for the immunofluorescent staining of culture plates.

Target	Host	Dilution	Clone	Supplier	Catalogue no.
ATF3	Rabbit	1:100	EPR19488	Abcam	ab207434
DNMT1	Rabbit	1:100	D63A6	NEB	5032S
eIF3E	Rabbit	N/A	Polyclonal	Abcam	ab36766
eIF4G2	Rabbit	N/A	D88B6	CST	5169
HES1	Rabbit	1:200	Polyclonal	Life Technologies	PA528802
Jarid2	Rabbit	1:100	EPR6357(2)	Abcam	ab192252
KEAP1	Rabbit	1:400	D6B12	NEB	8047S
Keratin 1	Rabbit	1:500	AF-87	Covance	PRB-149P
Keratin 17	Rabbit	1:200	D12E5	NEB	12509S
MafF	Goat	1:40	Polyclonal	Bio-Techne	AF3917
RAB7	Rabbit	1:50	EPR7588(B)	Abcam	ab126712
SRC-3	Rabbit	1:600	D1F11	NEB	5765S

2.2.1.2. EdU and EU detection

EdU and EU incorporation was detected using Click-iT EdU Alexa Fluor 488 Imaging Kit (Life Technologies C10337) and Click-iT RNA Alexa Fluor 488 Imaging Kit (Life Technologies C10329), respectively. Kits were used according to the manufacturer's instructions.

When used alongside an antibody-based immunofluorescent staining, Click-iT reaction was performed after the overnight incubation with the primary antibody, but prior to the incubation with the secondary antibody. When used with the Zenon-labelled antibodies, Click-iT was performed following an overnight incubation and before the final mounting with DAPI.

2.2.1.3. Lipid detection and imaging

For the lipid detection experiments, NFSKs were grown within multiwell plates with fibroblast feeders on 20 mm circle glass coverslips (Thermo Fisher Scientific CB00200RA020MNT0) sterilised with 70% ethanol. Overall, the same protocol was followed as for staining of culture plates. BODIPY 493/503 stain (Life Technologies D3922) at a final concentration of 10 µg/mL was used for visualising lipid droplets. Cholesterol distribution within cells was visualised using a Cholesterol Assay Kit (Cell-Based) from Abcam (ab133116), following manufacturer's instruction, and cell shapes were visualised using 1:500 dilution of Alexa Fluor 546 phalloidin (Thermo Fisher Scientific A22283).

2.2.2. Staining of frozen sections

2.2.2.1. Cryosectioning of human epithelium

Fresh abdominal skin samples were obtained from deceased organ transplantation donors in collaboration with Dr Kourosh Saeb-Parsy, Addenbrookes hospital, Cambridge (REC reference: 15/EE/0152 NRES Committee East of England - Cambridge South). A total of 6 samples, from both male and female donors, aged between 26 and 68, were used in this study. Where applicable subcutaneous fat was removed and approx. 0.5cm^2 squares of skin were embedded in Optimal cutting temperature compound (OCT) and then frozen on dry ice. OCT-embedded skin was cut into 10µm sections using a cryostat set to -18°C (Leica Biosystems CM1860). Prepared sections were mounted onto Polysine Adhesion Slides (Thermo Scientific J2800AMNZ) and stored at -80°C.

2.2.2.2. Immunofluorescence staining of frozen sections

Frozen sections were fixed with 4% PFA (FD Neurotechnologies PF101) for 10 min at room temperature, washed three times with 1 x PBS, and then incubated with 0.5% Triton X100 (BDH 28817.295), 0.25% FSG (Sigma-Aldrich G7765), 0.5% BSA (Sigma-Aldrich A8531) and 10% Goat serum (Sigma-Aldrich G9023) in 1 x PBS in humidified chamber for 1 hour at room temperature. Primary antibodies (see Table 2.6) were incubated overnight in humidified chamber at 4°C with 0.25% FSG in 1 x PBS. Sections were then washed three times in 1 x PBS, for 5 min each time. Alexa Fluor azide secondary goat antibodies (Life Technologies) were incubated for 1 hour in humidified chamber at 1:500 dilution with 0.25% FSG in 1 x PBS. Sections were then washed as previously, mounted with Vectashield Antifade Mounting Medium with DAPI (Vector Laboratories H-1200) and sealed with nail varnish.

Table 2.6. Primary antibodies used for the immunofluorescent staining of frozen sections.

Target	Host	Dilution	Clone	Supplier	Catalogue no.
eIF3E	Rabbit	1:2000	Polyclonal	Abcam	ab36766
eIF4G2	Rabbit	1:1000	D88B6	CST	5169
Keratin 14	Chicken	1:2000	Polyclonal	BioLegend	906001

2.2.2.3. Haematoxylin and eosin staining of frozen sections

Frozen sections were fixed with 4% PFA (FD Neurotechnologies PF101) for 10 min at room temperature. Sections were then incubated with haematoxylin (Merck 105174) for 10 s to colour cell nuclei and immediately rinsed twice with tap water. Eosin (Merck 109844) was then added for 5 s to stain eosinophilic cellular structures and rinsed briefly with tap water, before several washes in increasing concentrations of ethanol (70-100%) were performed. Finally, sections were soaked in xylene (Leica Biosystems 3803665) for 2 min at room temperature and mounted using a xylene-based mountant, CV Mount (Leica Biosystems 14046430011). Images were obtained using a NanoZoomer-XR slide scanner (Hamamatsu), and then processed using the NDP.view2 software (Hamamatsu).

2.2.3. Microscopy and image analysis

Immunofluorescent staining of 8 cell colonies was visualised on a Zeiss Axio Observer D1 microscope with Zeiss AxioVision software using 10 x, 20 x or 40 x objectives. Immunofluorescence staining of frozen sections and lipid droplets staining were visualised on Leica SP8 confocal microscope with Leica Application Suite X (LAS X) software using 20 x or 40 x objectives. Typical settings for acquisition of z stacks were: optimal pinhole, line average 3, scan speed 400 Hz and a resolution of 1024 x 1024 pixels. All the remaining immunofluorescent stainings were visualised on Leica DMi8 widefield microscope with LAS X software using 10 x or 20 x objectives. The H2B-GFP tracking experiments were performed on an Essen BioScience IncuCyte FLR machine, and later on the IncuCyte ZOOM system. Representative images were taken for illustrative purposes.

Obtained images were analysed in the IncuCyte software (EssenBiosystems), Volocity (PerkinElmer) and ImageJ. Figures were prepared using Adobe Illustrator and GraphPad Prism.

2.3. Molecular biology techniques

2.3.1. Nucleic acid preparation

2.3.1.1. RNA purification

Samples for RNA sequencing and qPCR analysis were collected and processed in the same manner. The feeder layer was removed by vigorous washing with ice cold 1 x PBS and RNA was extracted from the NFSKs using the RNeasy Mini Kit (Qiagen 74106) following the manufacturer's instructions.

Protocol was modified by replacing 70% ethanol with absolute ethanol and extending the elution step to 5 min to facilitate better recovery of total RNA. RNA concentrations were quantified using Qubit RNA Broad-Range Assay Kit (Thermo Fisher Q10210).

2.3.1.2. cDNA synthesis

cDNA synthesis was performed using the QuantiTect Reverse Transcription Kit (Qiagen 205311) with the amounts of RNA input constant within each experiment, ranging from 200 ng to 1 µg of purified RNA per reaction. Obtained cDNA samples were stored at -20°C.

2.3.2. Quantitative reverse-transcription PCR (RT-qPCR)

TaqMan Gene Expression Assay (Life Technologies) was used for RT-qPCR analysis. In this method, a pair of unlabelled primers supplied by Life Technologies is used in combination with a corresponding TaqMan probe to achieve maximal specificity. Standard cycling protocols for hydrolysis probe assays as advised by the manufacturer were followed. TaqMan probes used in the experiments are listed in Table 2.7.

Table 2.7. TaqMan probes used for the RT-qPCR.

Gene	Species	Amplicon Length	Assay ID	Supplier
ANXA2	Human	68	Hs00743063_s1	Thermo Fisher Scientific
CCND1	Human	57	Hs00765553_m1	Thermo Fisher Scientific
CCNG1	Human	82	Hs00171112_m1	Thermo Fisher Scientific
EIF3E	Human	104	Hs00266036_m1	Thermo Fisher Scientific
EIF4G2	Human	80	Hs00154952_m1	Thermo Fisher Scientific
GAPDH	Human	93	Hs02758991_g1	Thermo Fisher Scientific
ITGA2	Human	67	Hs00158127_m1	Thermo Fisher Scientific
IVL	Human	148	Hs00846307_s1	Thermo Fisher Scientific
KRT5	Human	133	Hs00361185_m1	Thermo Fisher Scientific
NAGK	Human	67	Hs00895033_m1	Thermo Fisher Scientific
S100A10	Human	113	Hs00751478_s1	Thermo Fisher Scientific
UBE2L3	Human	144	Hs00748530_s1	Thermo Fisher Scientific

2.3.3. Protein immunoassays

2.3.3.1. Extraction of proteins from keratinocytes

In a similar manner to the nucleic acid extraction protocol, the feeder layer was removed by washing with ice cold 1 x PBS. 500 µL of RIPA Lysis and Extraction Buffer (Thermo Fisher Scientific 89900) supplemented with cOmplete Mini EDTA-free Protease Inhibitor Cocktail (Roche 11836170001) was applied per well of a 6-well plate. Plates were incubated on ice for 30 min and then scraped with a cell scraper (Corning 3010). Cell lysates were spun at 4°C for 10 min at 10,000 RCF, after which supernatants were collected and analysed using capillary a based protein immunoassay.

2.3.3.2. Capillary based immune electrophoresis

Wes Simple Western system from Protein Simple was used in place of standard western blots. Wes is a gel-free and blot-free capillary-based immunoassay platform that integrates and automates the entire protein separation and detection process, ensuring better reproducibility than a standard western. What is more, Wes's broad dynamic range allows reliable quantitation of protein expression (Beekman *et al.*, 2018). Manufacturer's protocol was followed with the exception of the protein denaturation procedure. The duration of the denaturation step was increased to 10 min and the temperature was increased to 100°C to ensure complete and even denaturation between all samples. Primary antibodies were applied at dilutions detailed in Table 2.8.

Table 2.8. Primary antibodies used for Wes Simple Western analysis.

Target	Host	Dilution	Clone	Supplier	Catalogue no.
Akt	Rabbit	1:50	Polyclonal	CST	9272
eIF3E	Rabbit	1:200	Polyclonal	Abcam	ab36766
eIF4G2	Rabbit	1:200	D88B6	CST	5169
p70 S6 Kinase	Rabbit	1:20	p70	Bio-Techne	AF8962
Phospho-Akt (Ser473)	Rabbit	1:20	D9E	CST	4060
Phospho-S6 Kinase (Thr389)	Rabbit	1:20	p70	CST	9205
SREBP1	Mouse	1:12.5	2A4	Novus Biologicals	NB600-582
α-Tubulin	Rabbit	1:200	11H10	CST	2125

2.3.4. RNA sequencing

To assess changes in gene expression between the balanced and expanding mode colonies, RNA-seq was performed on samples collected at two selected time points post seeding. Samples were sent to the Sanger's sequencing core facility and the integrity of the RNA was assessed using the Eukaryote Total RNA Nano assay (Agilent) on a DE72902442 machine. After passing the quality control, samples were run on an Illumina HiSeq 2500 machine with the read length of 75 base pairs, paired end. Stranded RNA-seq (Standard with Oligo dT pulldown) library was chosen and 2 libraries were used per multiplex pool.

Bioinformatics analysis of the resulting raw data was carried out by Dr Tibor Nagy and Dr Swee Hoe Ong. Firstly, data was mapped using STAR 2.5.3a and the alignment files sorted and duplicate-marked using Biobambam2 2.0.54. The read summarisation was carried out using the htseq-count script from version 0.6.1p1 of the HTSeq framework. DESeq2 R package was used to identify differentially expressed genes between the two conditions. Hits reported by DESeq2 with corrected $p<0.05$ were considered significant. Data visualisation and downstream pathway analysis were performed using following R packages: org.Mm.eg.db, Pheatmap, RColorBrewer, clusterProfiler, GAGE and Pathview. Heat maps were generated from the ratio of TPM values of the treated sample over the average of the respective control samples.

2.5. Data analysis

2.5.1. Quantification of immunofluorescence

To analyse expression levels of selected proteins in cultured keratinocytes and cryosections of human skin, the appropriate fluorescence intensities were measured using Volocity (PerkinElmer) and ImageJ software. The mean fluorescence of an area or colony was normalised for the number of counted cells. In case of keratinocyte cultures, fluorescence was assessed by marking the whole colonies' and individual cells' perimeters to measure the mean fluorescence intensities across channels of interest. In case of stained cryosections, suprabasal and basal regions of the sections were compared, with detection of basal layer being facilitated by staining with a basal cell marker, Keratin 14.

2.5.2. Assessing colony survival and size distribution

To assess the colony size distributions, the number of nucleated cells per colony was determined by counting nuclei. Random fields of view were imaged and all colonies were counted. In case of experiments when drug or siRNA treatment was started after colonies were already established, only colonies of more than 6 cells were included in analysis. Cell densities were calculated by dividing the number of cells in a colony by the area measured by manually marking the colony's perimeter in Volocity software (PerkinElmer).

To assess colony survival, images obtained using the IncuCyte ZOOM system were analysed. For each condition, measurements of average colony area (μm^2), plate's confluence (%) and the number of colonies per well were obtained using the IncuCyte software. Then, experimental conditions were compared against a negative control and time points before and after treatment were analysed.

2.5.3. Statistical analysis

For all of the presented experiments, a minimum of 3 biological replicates were performed. Statistical analysis was performed using Microsoft Excel and Graphpad Prism software, with the exception of sequencing data. Column statistics were chosen and normality was assessed using D'Agostino-Pearson test. If data was normally distributed, a Student's unpaired t-test was performed and mean ± standard deviation (SD) is shown. If data was not normally distributed, a Mann Whitney test was performed and medians are presented instead, unless otherwise stated. Differences were considered significant and marked with * when $p<0.05$. Differences with p values of less than 0.01 were marked with **, and with $p<0.001$ were marked with ***.

Chapter 3 Two modes of proliferation have distinct molecular profiles

3.1. Chapter overview

Previous studies have shown that division of a single human epidermal progenitor cell can have three outcomes (Doupe and Jones, 2012). Two new proliferating cells, two differentiating cells, or one of each type can be produced following completion of the cell cycle. As discussed in the introduction to this thesis, Dr Amit Roshan, a former PhD student in the Jones laboratory, after analysing outcomes of thousands of such divisions, has identified two distinct modes of proliferation *in vitro* (Roshan *et al.*, 2016). In expanding mode, majority of divisions result in production of two new progenitor cells. This in turn leads to exponential population growth and formation of large colonies (normally 100-800 cells at 7 days). In balanced mode, equal numbers of cycling and differentiating cells are generated on average, leading to formation of small colonies (2-60 cells at 7 days). Those intrinsic modes of proliferation are inherited from the cell founding the colony (Roshan *et al.*, 2016). Interestingly, once an expanding colony reaches local confluence, the centre of the colony switches to the balanced mode, most likely in a cell density dependant manner. Since the two modes of proliferation and a confluence switch may underlie the remarkable ability of epidermal progenitor cells to reconstitute entire epithelium without overgrowth, the main aim of my project was to try to understand the molecular basis of these phenomena.

In order to study the molecular mechanisms which underlie the establishment and maintenance of the two modes of proliferation, I needed to develop a new robust approach, which would allow me to use high throughput techniques, such as RNA sequencing (RNA-seq). Utilising the pre-existing knowledge that the middles of large colonies, defined as all colony members other than the three cell wide layer known as the colony edge, switch from expanding mode to balanced mode several days post seeding, I have developed a way of studying the two modes of division in bulk cultures.

In this chapter, I will first describe how colony growth dynamics change over time, and how this temporal change can be used to represent the two modes of division. I will evaluate the timing of the middle colony switch using EdU labelling and qPCR based transcriptional profiling of cultures at different time points post seeding. Finally, I will discuss how using RNA-seq has allowed me to characterise the distinct molecular profiles of balanced and expanding cells.

3.2. Timing and cell density in the colony growth dynamics

To try and understand the molecular basis of the balanced and expanding modes of division, and the previously described switch between the two, I started by evaluating the growth dynamics of human keratinocytes in culture. I analysed NFSKs colonies between days 5 and 8 post seeding (Figure 3.1A). Firstly, I looked at EdU incorporation in colonies exceeding 10 cells in size (Figure 3.1B). The cut-off was chosen, so that my analysis can be focused on expanding mode colonies, which, given their exponential growth, should all be larger than 10 cells in size at day 5 post seeding (Roshan *et al.*, 2016). When cells are treated with EdU, the compound is only incorporated into the cells that are undergoing S-phase during the treatment period (Buck *et al.*, 2008). Based on the cell cycle distributions characterised by Roshan et al., I could assume that a 24 hour EdU treatment would ensure that all dividing keratinocytes are labelled. Also, remembering, that majority of cell divisions of expanding mode cells result in generation of two dividing daughters, regions with the majority of EdU positive cells can be classified as expanding (Roshan *et al.*, 2016). Therefore, in my analysis, I assumed that if the middle third of a colony had more than 80% of EdU positive cells, the colony had not switched its behaviour and was expanding. If there were less than 80% of EdU positive cells in that region, the colony has switched its proliferation mode towards balanced. 60 colonies were assessed per time point. An average of 35% of analysed colonies displayed balanced mode behaviour at day 5 post seeding. The situation was largely different towards the end of the experiment, with virtually all middle thirds of colonies larger than 10 cells in size displaying balanced mode behaviour at days 7 and 8 post seeding (Figure 3.1C).

To determine further growth characteristics of keratinocyte colonies, I have assessed the number of cells per colony, colony area and cell density for 60 colonies per time point between days 5 and 7 post seeding. The measurements were performed over the whole colony, not just the switching middle. As expected, the number of cells per colony is increasing over the course of the experiment. The colony growth appears to be exponential, which is characteristic of the expanding mode colonies that I was aiming to focus on mostly (Figure 3.1D). Interestingly, the increase in colony area happened at a faster rate than the increase in the cell count (Figure 3.1E). Consistent with this observation, there was a modest but statistically significant decrease in the cell density (cells/μm^2) in large colonies between days 6 and 7 (Figure 3.1F). This is likely to reflect the rise in the number of differentiated cells, which are larger in size, which occurs as the middle of the expanding colony switches towards balanced mode of division. Taken together, these results indicate that middle colony switch is likely to occur between days 6 and 7 post seeding.

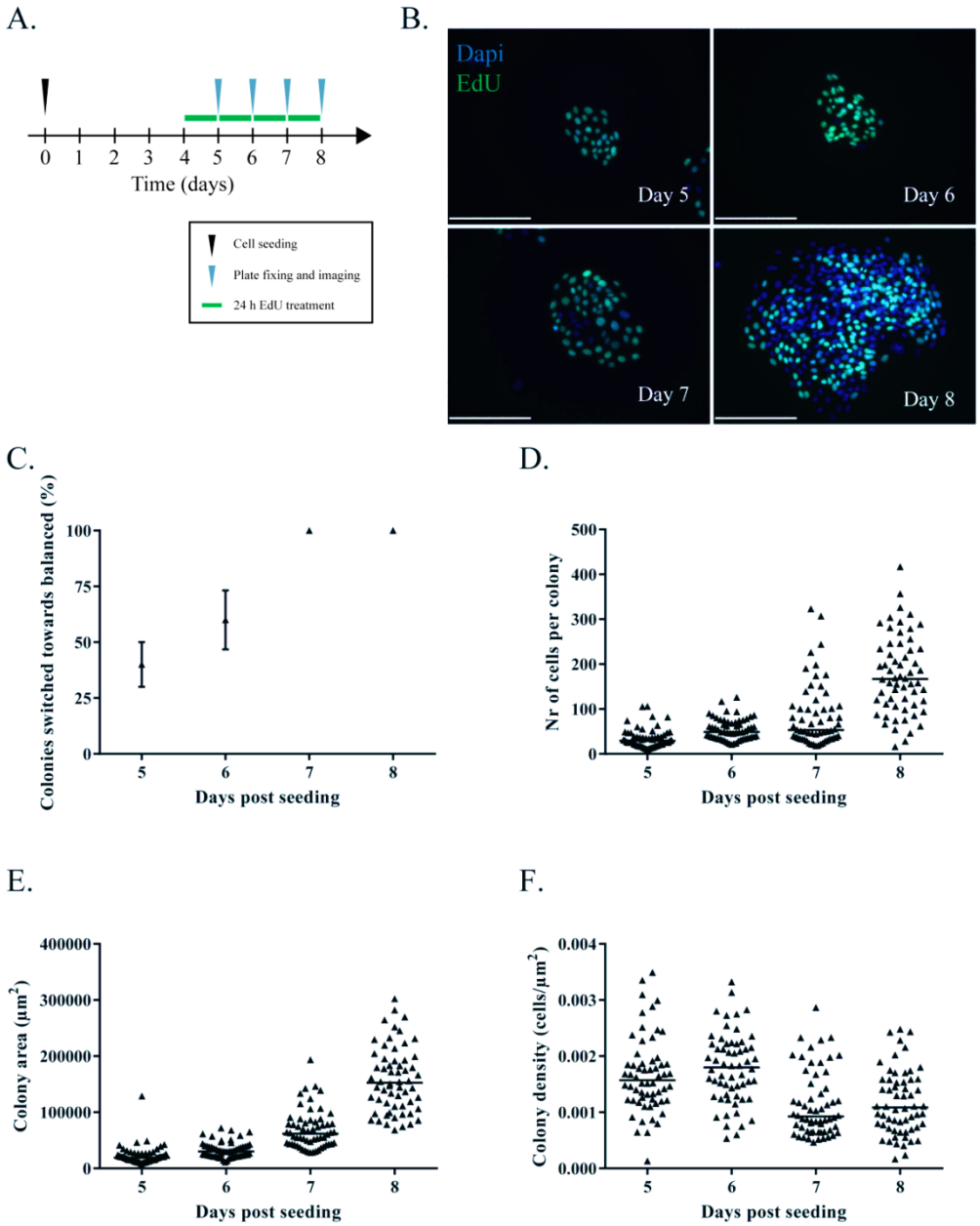

Figure 3.1. Colony growth kinetics in keratinocyte *in vitro* cultures. **A:** Experimental outline. **B:** Representative images of colonies fixed at different time points labelled with EdU (green) and Dapi (blue). Scale bar represents 60 µm. Only colonies of 10 or more cells in size were included in the analysis. Presented day 5 and day 6 colonies would be classified as expanding, since all of the cells in their middles are EdU positive. Presented day 7 and day 8 colonies would be classified as switched towards balanced mode, since, respectively, 60% and 50% of cells in their middles are EdU positive. **C:** Percentage of colonies switched towards balanced mode at different time points post seeding. By day 7, all analysed colonies have switched. **D:** Changes in colony size distribution over time (measured as a number of cells per colony). **E:** Changes in colony area over time. **F:** Changes in cell density (cells/µm^2) within colonies over time. There is a significant drop in colony density between days 6 and 7 ($p<0.0001$ 2-tailed Mann Whitney). N=60 colonies per time point. Performed in 3 biological replicates.

3.3. Changes in transcriptional profiles of keratinocyte cultures over time

Results presented so far confirm the existence of a middle colony switch phenomenon and indicate the time by which it occurs. Nonetheless, microscopic analysis provides only a limited insight into the mechanism of the switch and the two modes of division. I wanted to evaluate transcription in expanding and balanced mode cells. RNA-seq analysis could be used to provide a broad overview of the expression profiles of the two proliferation modes. However, in order to obtain sufficient amounts of high quality RNA, I needed to establish bulk culture models of the two proliferation modes. Using the switch phenomenon could potentially allow me to do just that, as just before the switch happens, the fact that expanding colonies are growing at a faster rate would ensure that majority of the cells coming from a culture plate would be in the expanding mode. After the switch, since middles of the expanding mode would switch towards balanced mode, the plate would now be dominated by cells proliferating balanced mode along with differentiated cells (Figure 3.2). The fact that day 7 cultures contain a mix of balanced mode cells and differentiated cells is the main limitation of this assay, as I cannot resolve changes due to differentiation from those due to the expanding to balanced switch in proliferating cells

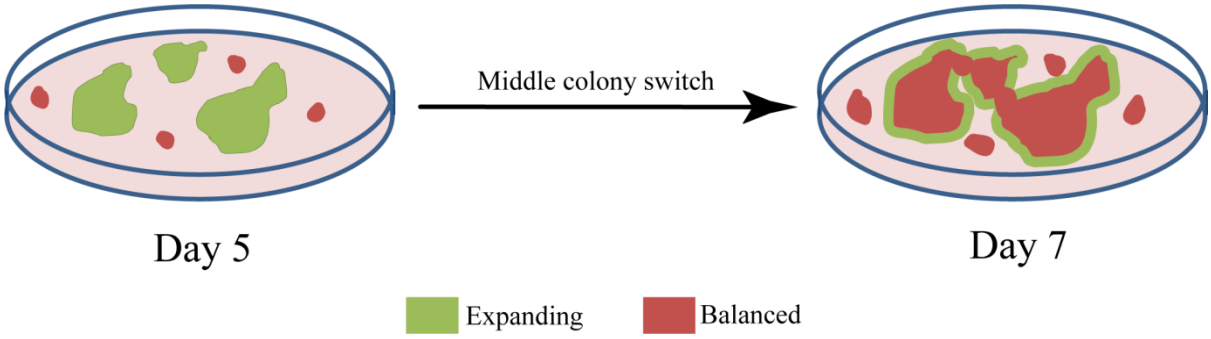

Figure 3.2. Schematic representation of the middle colony switch.

In order to test this hypothesis, I have performed RT-PCR profiling of samples obtained from bulk NFSK cultures collected between days 3 and 8 post seeding (Figure 3.3A and Figure 3.4A). I have included transcripts encoding basal cell markers (Figure 3.3B and Figure 3.4B (Langsenlehner *et al.*, 2006; Moll *et al.*, 1982), keratinocyte differentiation markers (Figure 3.3C and Figure 3.4C (Broome, Ryan and Eckert, 2003; Ma and Ozers, 1996)), and cell cycle markers (Figure 3.3D and Figure 3.4D (Murray, 2004)). I have repeated the analysis using two housekeeping genes highly expressed in keratinocytes (Thierry-Mieg and Thierry-Mieg, 2006), *NAGK* (Figure 3.3) and *UBE2L* (Figure 3.4). Both approaches showed similar patterns in gene expression over the course of the experiment. Amongst basal cell markers, *ITGA2* remains constant, while *KRT5* shows a brief increase at day 7 and decreases again at day 8. Importantly, there is a sharp sustained increase in differentiation markers at day 7, coinciding with a decrease in cell proliferation markers, suggesting that the middle colony switch happens at this time.

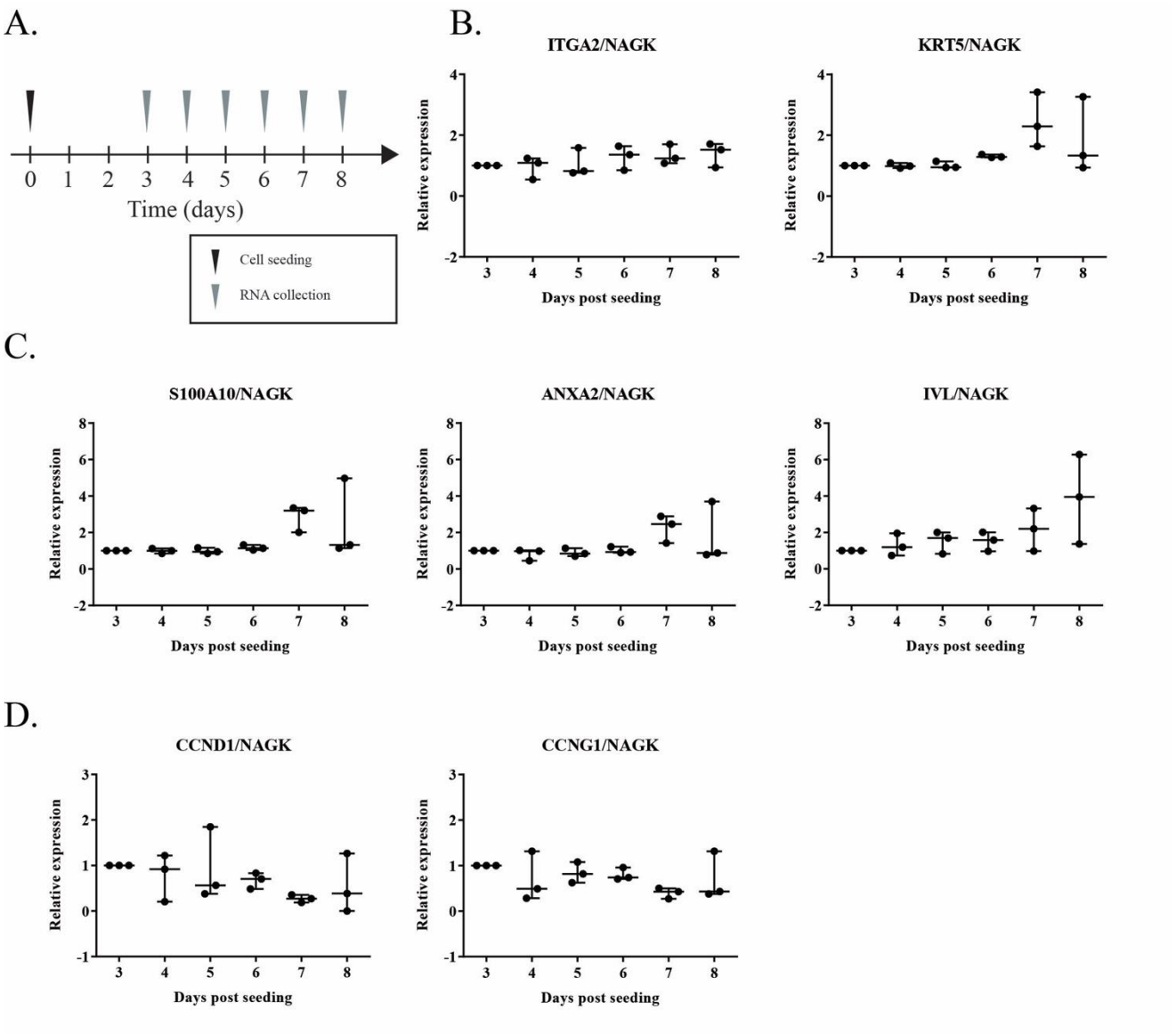

Figure 3.3. Changes in transcriptional profiles of keratinocyte cultures over time (normalised to NAGK). **A:** Experimental outline. **B:** Expression of known basal keratinocyte markers over time. **C:** Expression of known differentiation markers over time. There is an upregulation of all three differentiation markers happening at day 7 post seeding. **D:** Expression of known proliferation markers over time. 3 biological replicates analysed per time point. No statistically significant differences in expression profiles were detected.

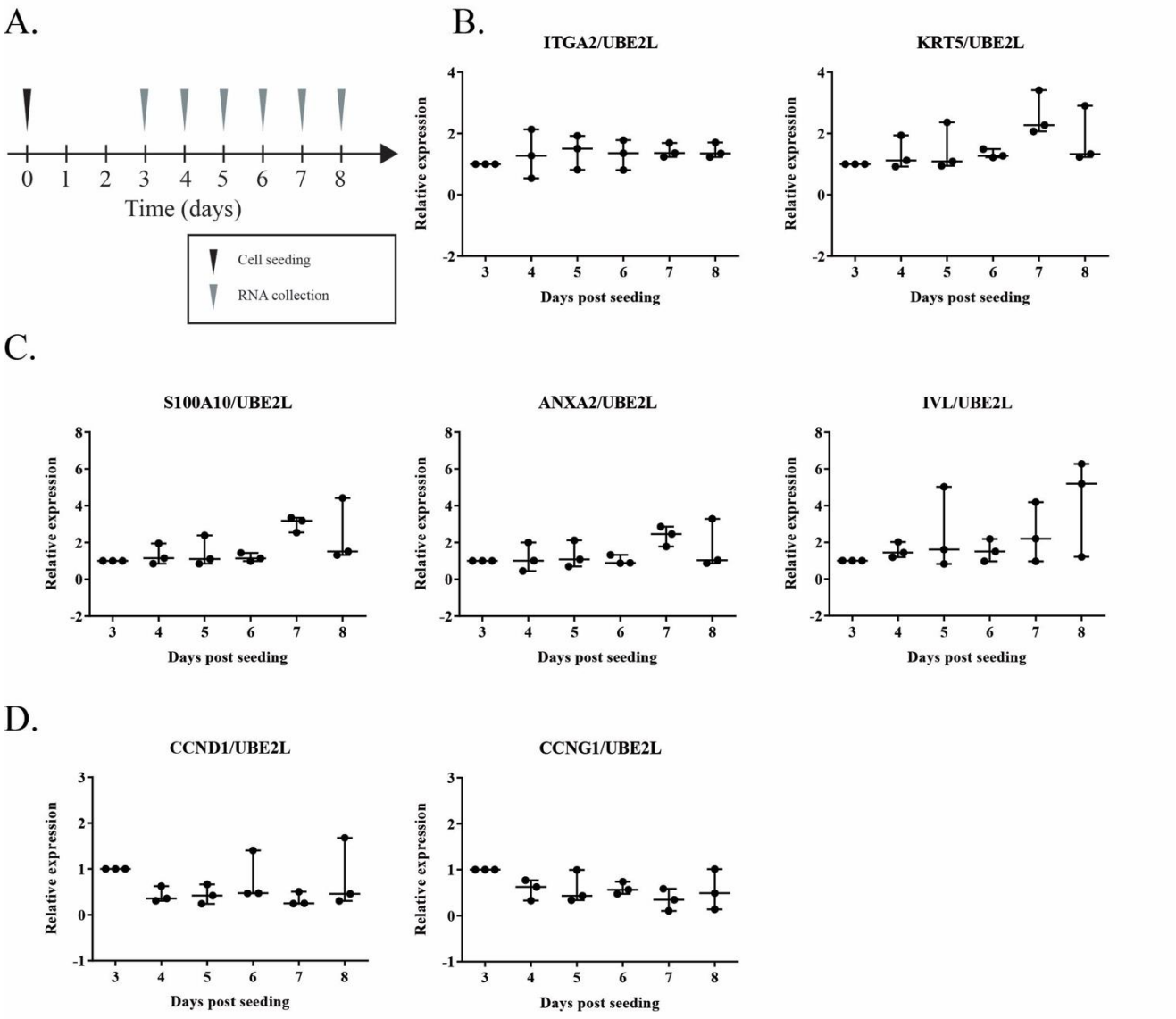

Figure 3.4. Changes in transcriptional profiles of keratinocyte cultures over time (normalised to UBE2L). **A:** Experimental outline. **B:** Expression of known basal keratinocyte markers over time. **C:** Expression of known differentiation markers over time. There is an upregulation of all three differentiation markers happening at day 7 post seeding. **D:** Expression of known proliferation markers over time. 3 biological replicates analysed per time point.

3.4. Pre and post-switch cultures correspond to expanding and balanced modes of proliferation

Imaging of growing keratinocyte colonies, together with EdU labelling and qPCR analysis allowed me to select time points at which cultures are enriched for expanding mode cells (day 5) and for balanced mode cells (day 7). For the RNA-seq analysis, I have collected total RNA samples from 6 biological replicates of day 5 and day 7 cultures. For cell collection, use of trypsin was avoided to prevent stress-induced change in the transcription profiles. Following RNA extraction and purification, samples were submitted to the Sanger Institute's RNA sequencing pipeline. Library preparation and Illumina sequencing and read alignment were performed by the pipeline staff. The subsequent analysis of the RNA-seq data was performed with the help of Dr Swee Hoe Ong.

Initial clustering of the RNA-seq data has confirmed that day 5 and day 7 samples have largely distinct transcriptional profiles (Figure 3.5). Principal Component Analysis (PCA) of the differential expression data revealed that a single sample from day 5 (NFSK_d5c) appeared to be clustering with day 7 samples (Figure 3.5B). Biologically, it could be the case that this particular culture has switched early and hence exhibits a transcriptional profile characteristic of later time points. Geometric coefficient of variation of the data, which is a measure of dispersion of the data (Kirkwood, 1979), confirmed that sample NFSK_d5c is transcriptionally closer to day 7 samples. To avoid excluding this sample from further analysis, sample NFSK_d5c will be treated as an additional replicate for day 7 (Figure 3.6).

Presented heatmap and PCA data indicates that day 5 and day 7 samples exhibit different transcriptional profiles (Figure 3.6). To further evaluate these differences, I have analysed what proportion of genes are differentially expressed between day 7 and day 5 datasets (Figure 3.7). In this analysis a normalised read count is plotted against fold change of expression. The further the point corresponding to a particular gene is from the central axis, the more differentially expressed it is between the two samples. The analysis has indicated that a large number of genes showed significant changes in their expression, with some being activated or downregulated more than 100000 fold. As the fold change in expression levels needed for statistically significant difference to be observed depends on the total number of particular reads, a gradient of p values was analysed across the samples with varying read numbers. This allowed for assignment of differentially expressed genes (shown in red in Figure 3.7). These can then be mapped to corresponding biological processes to study which cellular processes are altered in each of the two modes of division.

A.

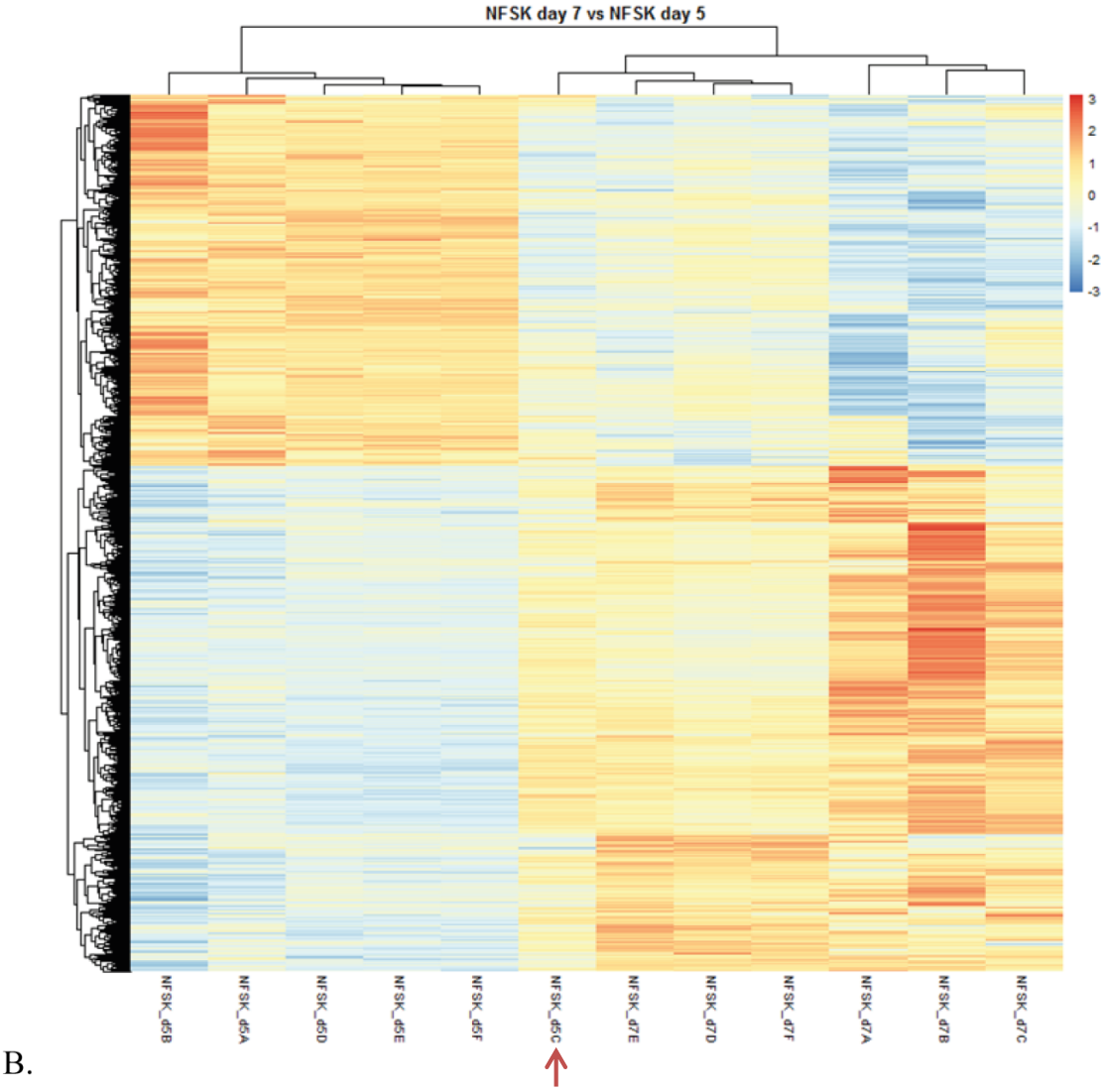

B.

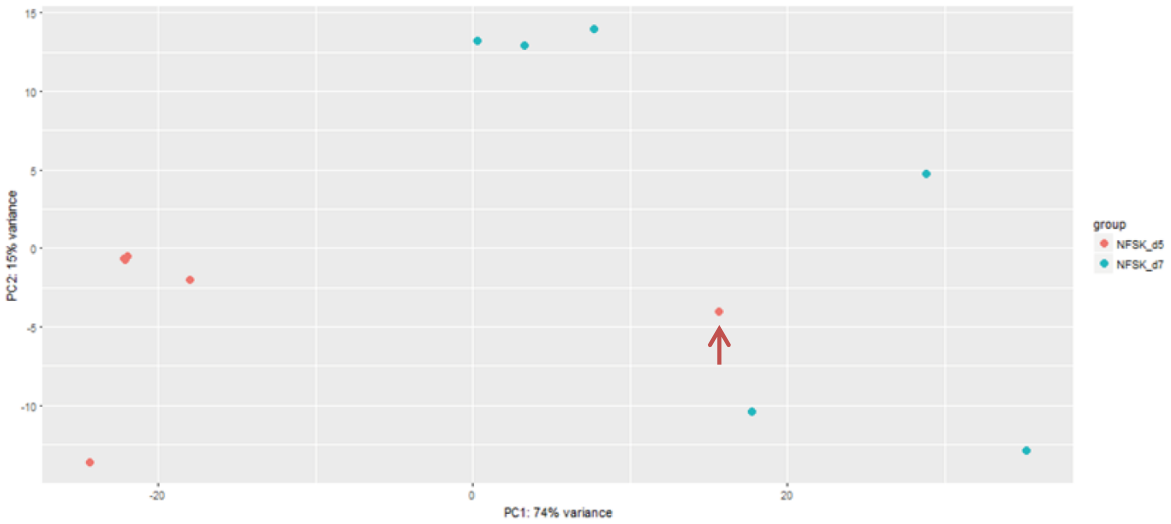

Figure 3.5. Differential gene expression in day 7 *versus* day 5 samples.**A**: Heatmap of the RNA-seq data. **B**: Principal component Analysis plot of the RNA-seq data. Day 5 samples are shown in orange; day 7 samples are shown in blue. Red arrows highlight the outlier sample.

A.

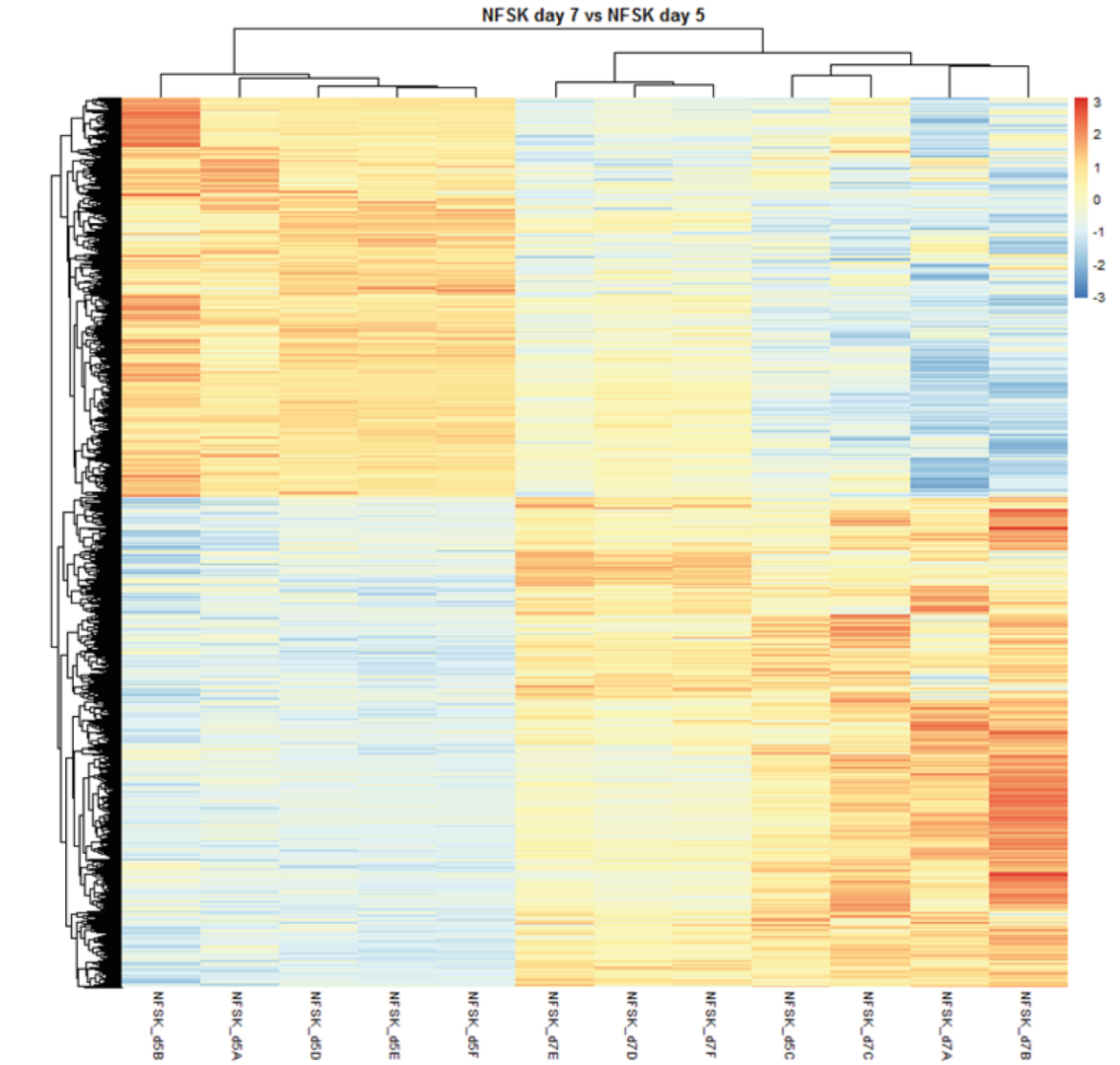

B.

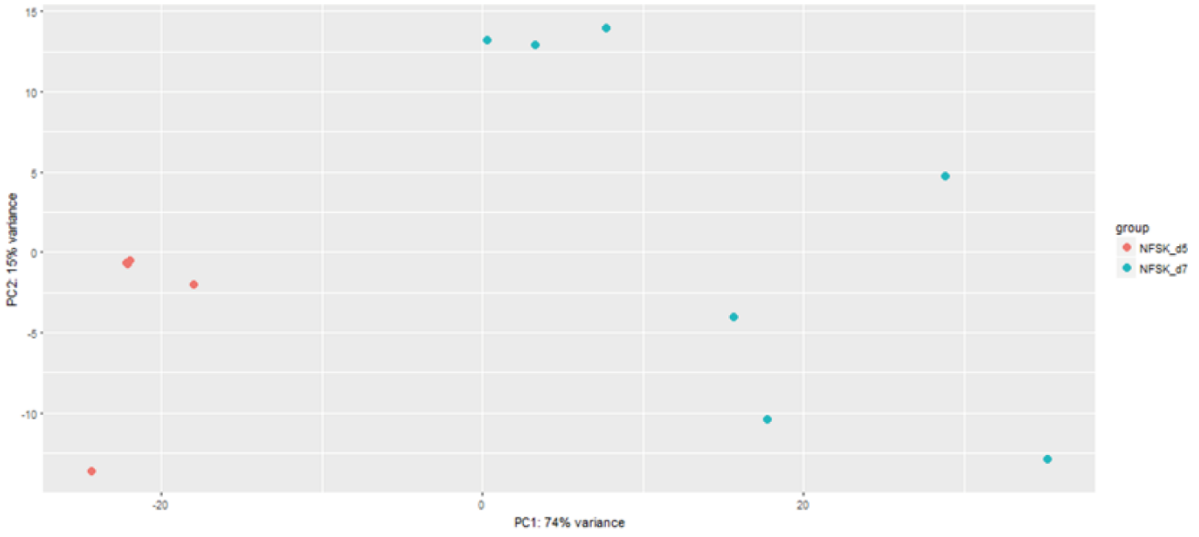

Figure 3.6. Differential gene expression in day 7 *versus* day 5 samples (corrected). **A**: Heatmap of the RNA-seq data. **B**: Principal component Analysis plot of the RNA-seq data. Day 5 samples are shown in orange; day 7 samples are shown in blue.

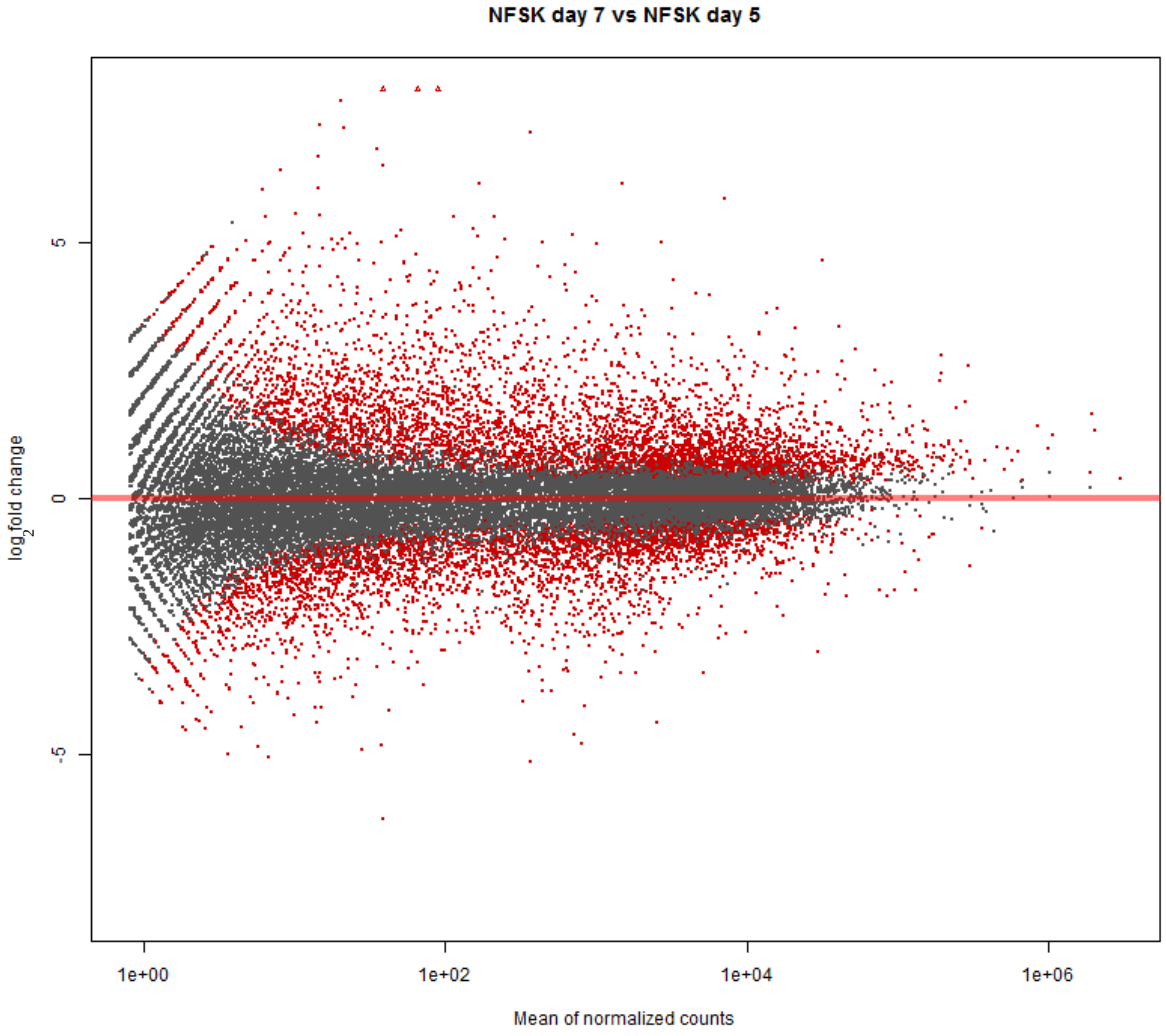

Figure 3.7. MA plot of normalised RNA-seq data showing differential gene expression between f day 7 and day 5 samples. Differentially expressed genes are shown in red.

Having established that day 5 and day 7 cultures exhibit distinct transcriptional profiles, I wanted to investigate the biological reason behind this difference. My hypothesis was that the reason for the differential gene expression between the two groups is the proportion of balanced and expanding proliferating cells and differentiating cells in each of them. As previously outlined, pre-switch cultures may contain predominantly expanding cells, while post-switch cultures may be formed mainly from balanced ones (Figure 3.2). Therefore, if the hypothesis is correct, the transcriptional profiles of the pre and post-switch cultures should largely resemble these of expanding and balanced colonies, although the accumulation of differentiating cells post switch will mean that all the findings need to be validated at a single cell level. Moreover, the differentiation, likely to be associated with balanced state colonies, may lead to some variability within transcriptomes from day 7 cultures. This may be reflected by clear separation of these datasets by PC2 on Figure 3.6 which is not so evident for day 5 cultures. To evaluate my theory I have analysed expression profiles for a set of pathways associated with the balanced and expanding states in day 5 and day 7 colonies. This analysis was performed using both mapping of the RNAseq data onto KEGG pathway graphs, using Pathview, an R package for pathway-based data integration and visualisation (Luo and Brouwer, 2013), and by performing specific staining experiments which validate the results of the RNA-seq experiment. This validation is particularly important as the RNA-seq analysis may be affected by certain batch effects as these seen for one of the day 5 cultures which is more similar to the day 7 ones (see Figure 3.5).

Firstly, I analysed enrichment or depletion of reads associated with the progression of the cell cycle (Figure 3.8). Previous experiments indicated that balanced NFSK colonies exhibit lower levels of cell cycle progression associated transcripts (Roshan *et al.*, 2016). This is likely to be associated with larger number of differentiating cells in these colonies. My analysis has indicated that most of the cell cycle progression associated reads studied are downregulated in day 7 cultures compared to the day 5 ones. Particularly consistent downregulation was observed across cyclins and cyclin dependant kinases. These are required to initiate progression of different cell cycle stages (Murray, 2004). Moreover, I have detected upregulation of *WEE1*, which is known to act as an inhibitor of mitosis entry (Nurse and Thuriaux, 1980). Together, this data indicates that at day 7, cell cycle progression is inhibited, suggesting a larger proportion of balanced cells in these cultures.

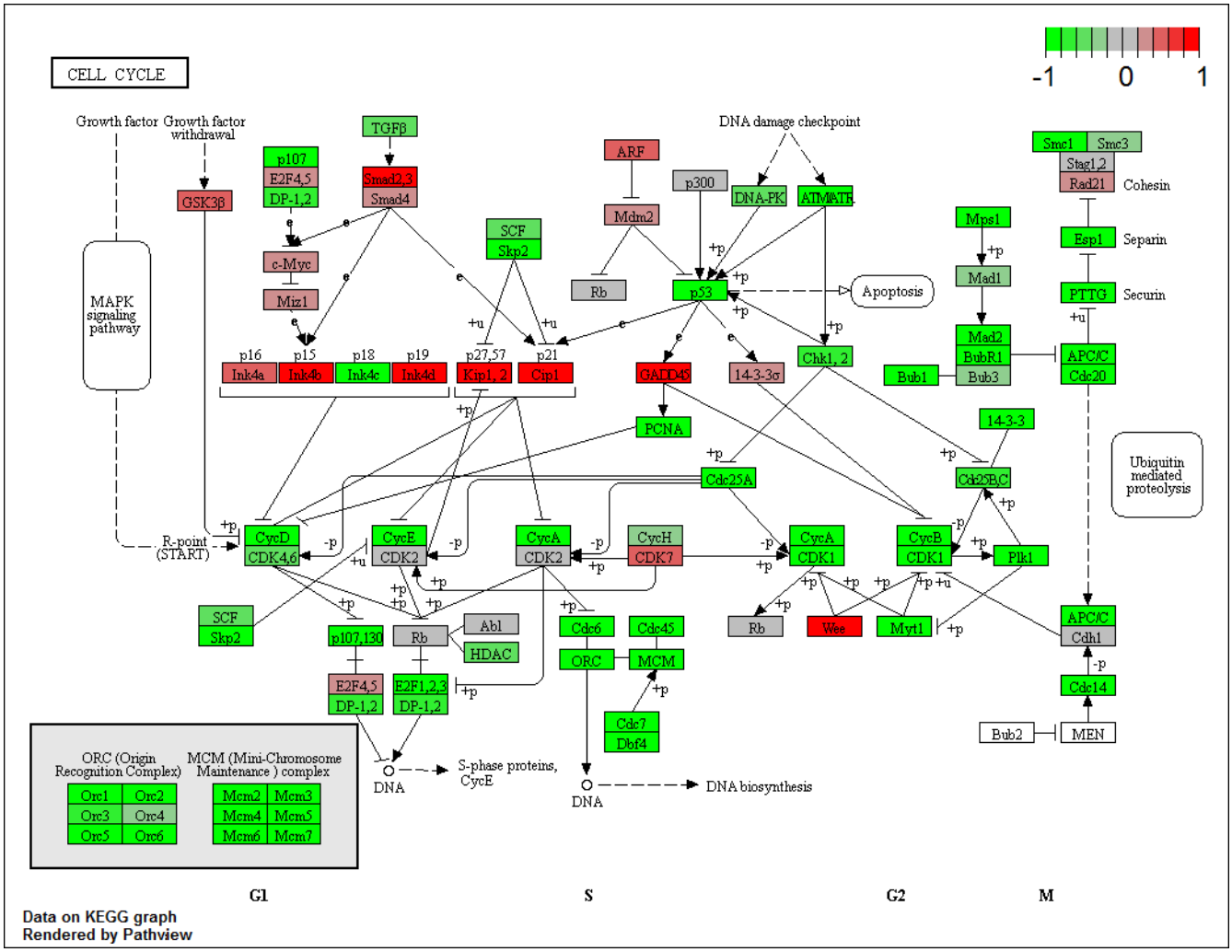

Figure 3.8. Differential expression of genes involved in cell cycle progression.Day 7 *versus* day 5 RNA-seq data is visualised on KEGG graph, prepared using Pathview R package. Genes upregulated at day 7 compared to day 5 are shown in red, downregulated genes are shown in green.

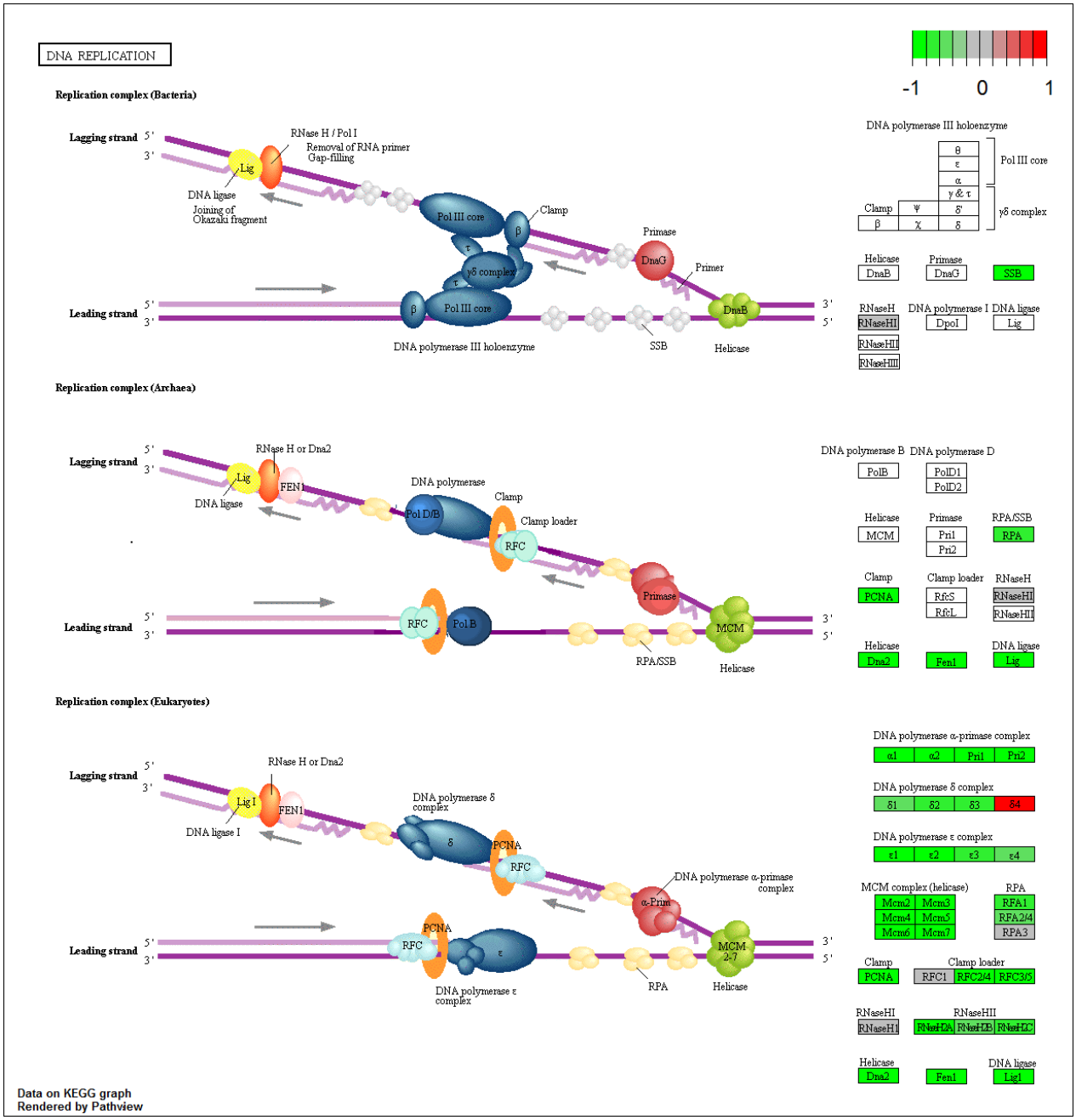

Figure 3.9. Differential expression of genes involved in DNA replication. Visualisation of day 7 *versus* day 5 RNA-seq data. KEGG graphs were prepared using Pathview R package. Genes upregulated at day 7 compared to day 5 are shown in red, downregulated genes are shown in green.

In addition to cell cycle progression, a strong consistent inhibition was observed across reads coding for members of the origin recognition complex (ORC)(Bell and Dutta, 2002). To further evaluate this link to DNA replication, I have analysed differential expression of reads associated with members of the DNA replication fork (Figure 3.9). Once again, I have observed consistent downregulation of these reads in day 7 samples compared to the day 5 ones. Together, this data indicates that RNA-seq profiles of day 5 cultures represent predominantly highly dividing expanding mode cells, whereas day 7 cultures may be associated with a lower proportion of dividing cells, consistent with them being mainly balanced.

The indication that day 5 cultures seem to be associated primarily with the expanding state and that the day 7 cultures may be mainly linked to the balanced one is until now based solely on mapping the RNA-seq results onto specific pathways of interest. However, the simplest explanation is that the changes are due to the accumulation of differentiated cells at day 7. In order to assess the extent of keratinocyte differentiation at day 7, and to provide external validation for the quality of the RNA-seq analysis, I have identified 3 genes for which reads are highly enriched at day 7 compared to day 5 and performed immunostaining for their protein products at both time-points. For my analysis I have selected AFT3 (1.017045134 log2FoldChange, p=2.58E-05, Figure 3.10A), KRT17 (1.133693674 log2FoldChange, p=4.04E-07, Figure 3.10B) and SRC3 (0.301640244 log2FoldChange, p= 0.01, Figure 3.10C). These genes were selected as, in addition to being enriched in the day 7 cultures, the expression of these genes was previously associated with keratinocyte differentiation in culture (Wu *et al.*, 2010; Lewis *et al.*, 2014; Hawker *et al.*, 2007) and they were observed to be differentially expressed in a microarray analysis of individual 8-cell colonies of cultured NFSKs (Roshan *et al.*, 2016). The results of my analysis indicate that for all three proteins studied their levels were significantly higher in day 7 colonies compared to the day 5 ones. In addition to providing validation for the results of the RNA-seq analysis this experiment provides important confirmation that the enrichment or depletion in reads observed in RNA-seq is likely to correlate with the levels of respective proteins.

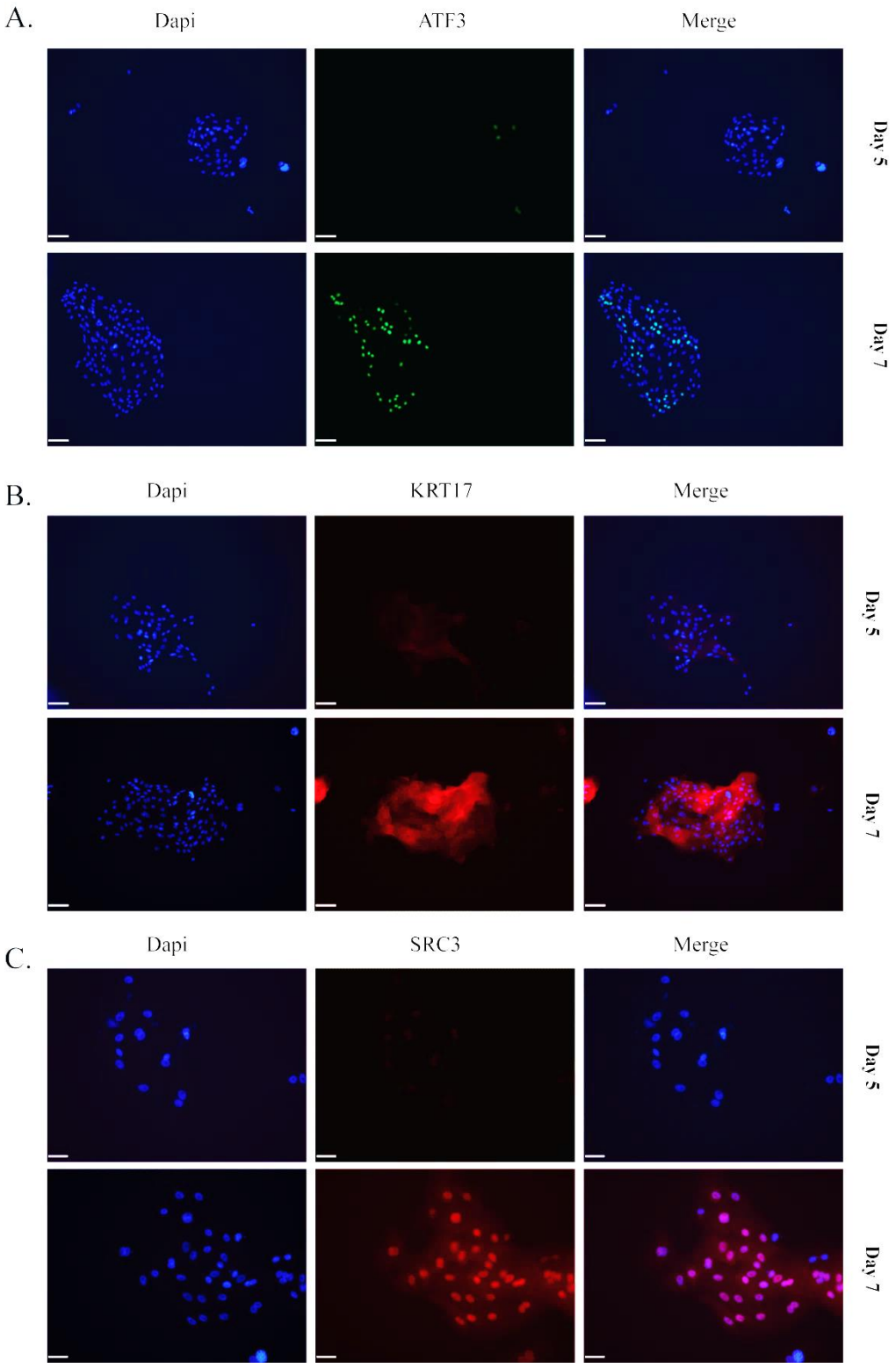

Figure 3.10. Immunostaining for keratinocyte differentiation markers at day 5 and day 7. Representative images of colonies over 15 cells in size fixed at day 5 and day 7 are shown in all panels. **A:** Colonies labelled with an anti-ATF3 antibody (green) and Dapi (blue). Scale bar represents 100 µm. **B:** Colonies labelled with an anti-KRT17 antibody (red) and Dapi (blue). Scale bar represents 100 µm. **C:** Colonies labelled with an anti-SRC3 antibody (red) and Dapi (blue). Scale bar represents 48 µm. Each staining was repeated 3 times. For each replicate, a minimum of 20 colonies per time point were assessed.

3.5. Levels of translation and lipid biosynthesis associated transcripts are increased in balanced mode cultures

In order to identify candidate pathways for further validation, I wanted to look more closely at the molecular signatures of each of day 5 and day 7 cultures. First, I looked at the GO enrichment analysis of my RNA-seq data (Figure 3.11). GO enrichment analysis allows functional analysis of RNA-seq data by looking at read enrichment in certain biological processes known as GO terms (Mi *et al.*, 2013). Not surprisingly, cell cycle progression (GO:0044843, p.adjust= 1.72e-06) and DNA replication (GO:0006270, p.adjust= 1.45e-08) were amongst processes which differed most significantly between day 5 and day 7 samples. Strikingly, top 10 hits from the GO enrichment analysis were dominated by processes related to protein synthesis (Figure 3.11), including translation initiation (GO:0006413, p.adjust= 2.45e-08), ribosome biogenesis (GO:0042254, 2.45e-08) and rRNA processing (GO:0006364, 1.40e-13). Since previous work in our laboratory has already indicated that global translation levels may contribute to the establishment of the balanced mode or keratinocyte differentiation (Roshan *et al.*, 2016), observing the upregulation of translation-associated transcripts in day 7 samples has convinced me to investigate the importance of translation in keratinocyte cell fate determination in more detail.

To visualise the scale of changes in expression levels of transcripts associated with translation, I have looked at detailed pathway analysis of ribosome biogenesis (Figure 3.12). Vast majority of transcripts encoding structural proteins of the large and small ribosomal subunits are upregulated in day 7 compared to day 5 samples. One of the signalling pathways which may be involved in the control of the observed upregulation of ribosome biogenesis associated transcripts is mTOR pathway. The mammalian target of Rapamycin (mTOR) is a kinase, which, through a complex signalling network, is involved in control of several cellular processes, including ribosome biogenesis and hence protein synthesis (Mayer and Grummt, 2006). Analysis of changes in mTOR signalling between day 5 and 7 cultures indicates that its positive regulators are upregulated at day 7, and its inhibitors are downregulated, indicating overall mTOR pathway stimulation (Figure 3.13). If mTOR signalling is indeed involved in progression towards the balanced state, other processes controlled by this pathway, for example lipid biosynthesis, should be also affected (Laplante and Sabatini, 2009). Indeed sterol biosynthetic processes (GO:0016126, p.adjust= 0.01) and cholesterol biosynthetic processes (GO:0006695, p.adjust= 0.01) were also significantly upregulated in day 7 compared to day 5.

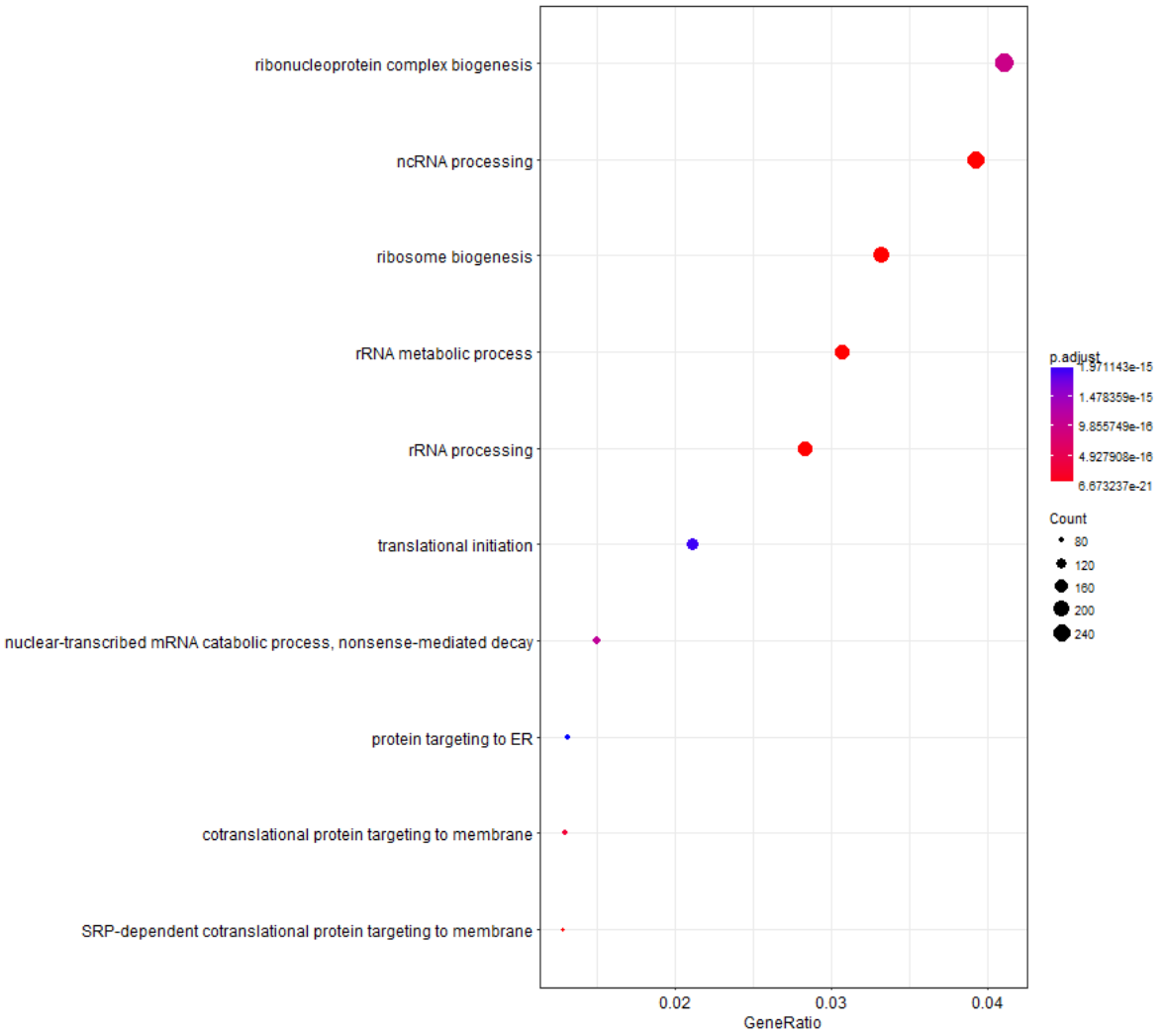

Figure 3.11. GO enrichment analysis of day 7 *versus* day 5 RNA-seq data. Top 10 hits revealed by the GO enrichment analysis are listed.

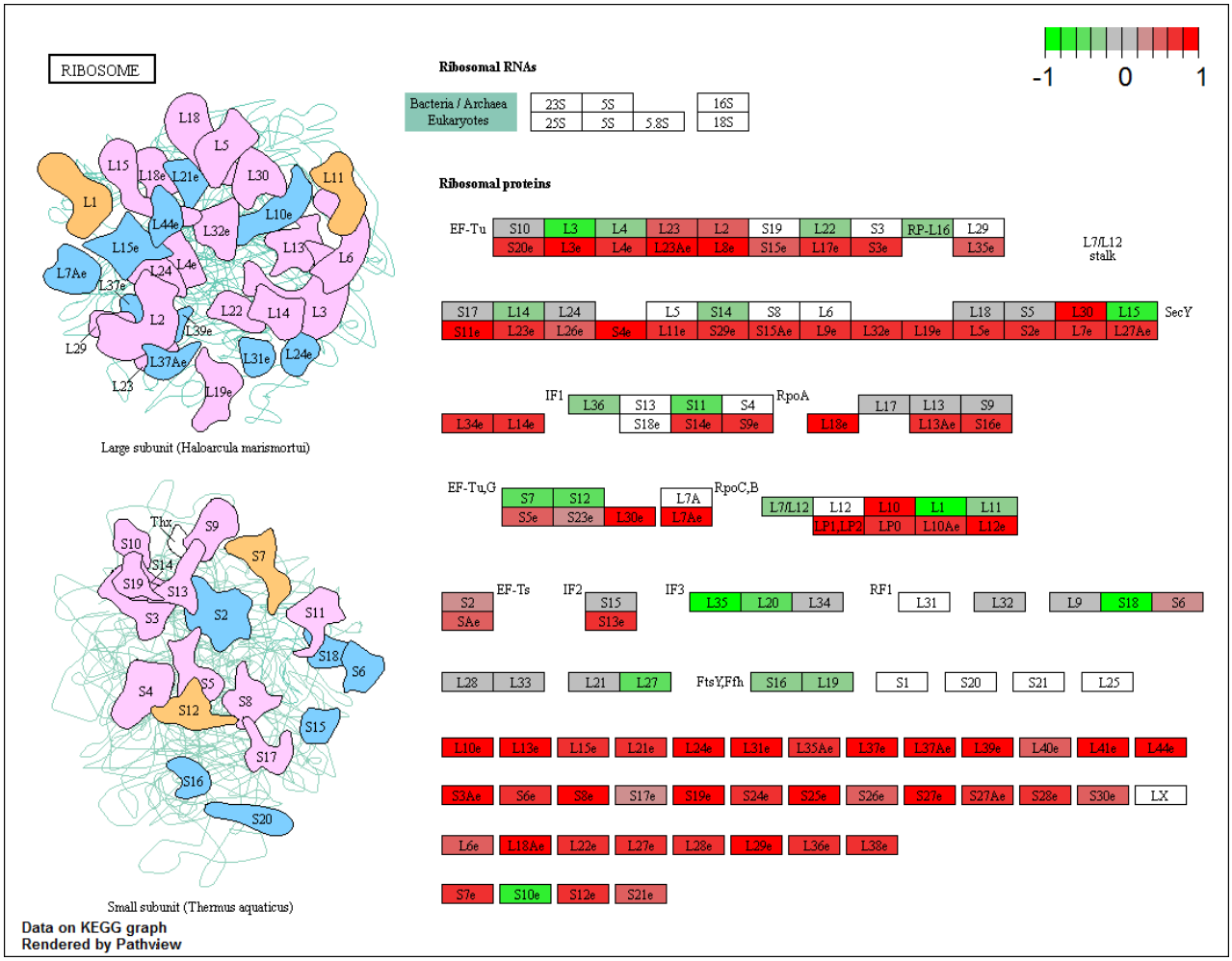

Figure 3.12. Differential expression of genes involved in ribosome biosynthesis. Visualisation of day 7 *versus* day 5 RNA-seq data. KEGG graphs were prepared using Pathview R package. Genes upregulated at day 7 compared to day 5 are shown in red, downregulated genes are shown in green

.

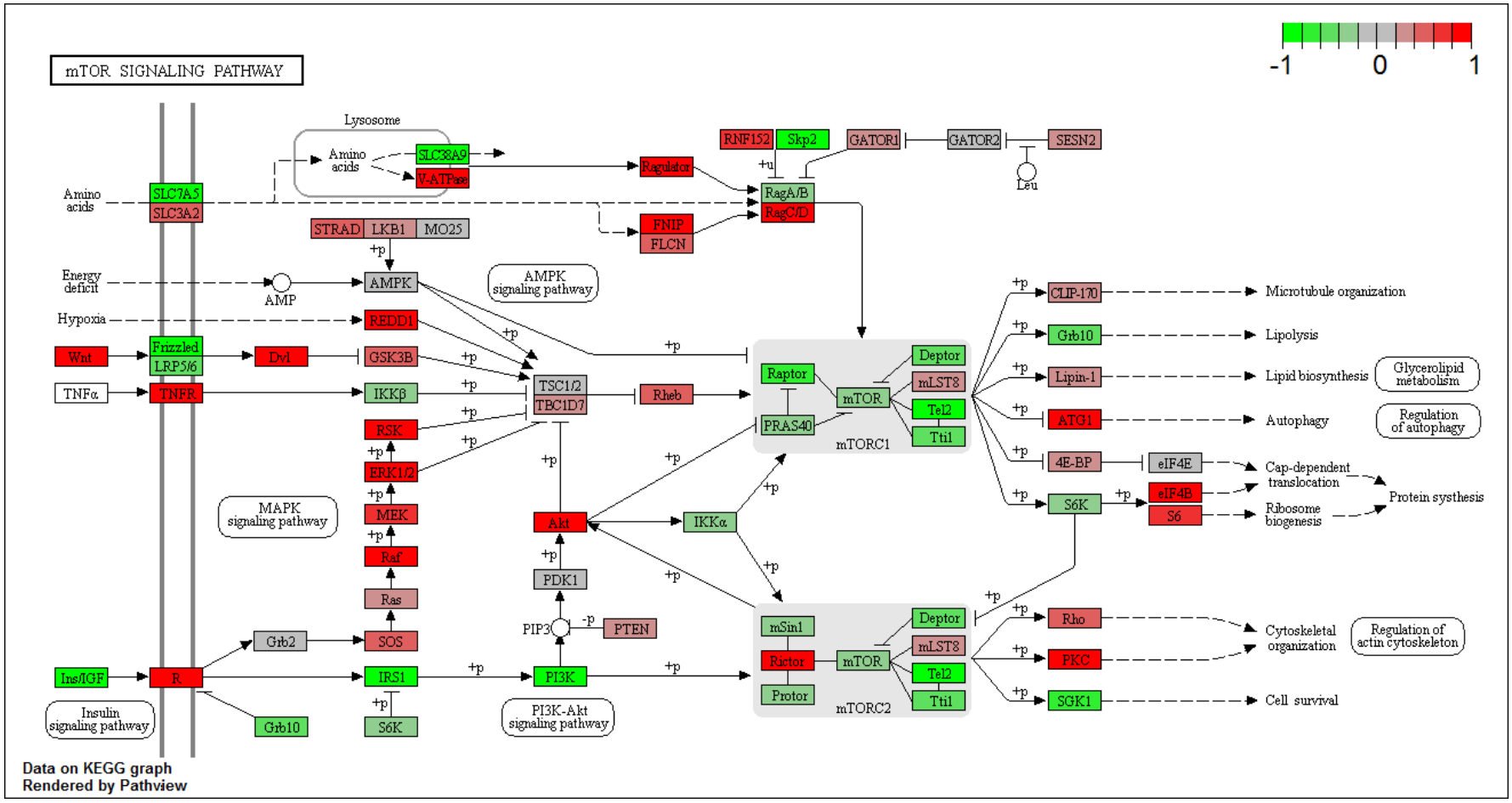

Figure 3.13. Differential expression of genes involved in mTOR signaling pathway. Visualisation of day 7 *versus* day 5 RNA-seq data. KEGG graphs were prepared using Pathview R package. Genes upregulated at day 7 compared to day 5 are shown in red, downregulated genes are shown in green.

3.6. Discussion

At the start of this chapter I described the changes in growth dynamics of developing keratinocyte cultures. My analysis has indicated that between days 5 and 8 of colony growth, both the kinetics of its growth and rate of its area increase change (Figure 3.1). Using EdU labelling I was able to observe that this alteration is primarily caused by a switch in the proliferative capacities of cells localised in the middle third of a growing colony (Figure 3.1B and C). The observed switch towards the balanced state has been previously reported, however, the exact timing at which it happens may be affected by culture conditions, supporting the hypothesis that it is confluence-dependant (Roshan *et al.*, 2016). Indeed, loss of cell confluence upon events such as tissue damage is known to stimulate proliferation by activating cell division (Martin, 1997). This observation provides further evidence that the reversible change between balanced and expanding modes of division is likely to have a switch-like nature.

Next, I wanted to analyse the transcriptional profiles of the pre and post-switch cultures in order to better understand the differences between the two proliferation types. Based on the qPCR profiling data (Figure 3.3 and Figure 3.4), I selected day 5 and day 7 time points as models of expanding and balanced modes of proliferation. RNA-seq analysis of 6 replicates of day 5 and day 7 samples has confirmed that these cultures show discrete transcriptional profiles and that the differences are likely to be either a representation of the discrepancies between the two proliferation modes or reflect early differentiation (section 3.4). In particular, processes such as stimulation of cell cycle progression and DNA synthesis were downregulated in day 7 cultures, suggesting they are representative of the balanced mode (Figure 3.8 and Figure 3.9). Reassuringly, similar differences in transcriptional profiles were already reported from a microarray analysis of individual 8-cell colonies of cultured NFSKs (Roshan *et al.*, 2016). Importantly, my analysis provides advance over the previous study as it analyses the transcriptional profiles of cells at two distinct time points and uses RNA-seq which unlike the microarray analysis, investigates the entire transcriptome, not selected sequences. This enables analysis of entire signalling and metabolic pathways. Although analysis of bulk cultures seems to provide a good snapshot of the transcriptional profiles of the two proliferation modes, this approach is unlikely to reflect the true complexity and heterogeneity of the studied populations. In the next chapters I will try to determine whether the differences in transcriptome identified using RNA-seq are truly due to changes in proliferation mode, or rather a consequence of accumulation of differentiated cells.

The approach chosen by me would be well complemented with the use of single cell RNA profiling. Such experiments were already performed in epithelial tissues, including a single cell RNA-seq analysis of mouse hair follicle cells (Joost *et al.*, 2016). This work has identified as many as 25 different cellular subpopulations. It is possible that some of the detected subpopulations might represent a gradient between the extremes of balanced and expanding cultures that were detected in my work. Hopefully, it should be possible to perform a similar single cell analysis on day 5 and day 7 cultures in the near future.

One of the most pronounced differences in the transcriptional profiles of the two proliferation modes revealed by both, my RNA-seq analysis and previously reported micro-array (Roshan *et al.*, 2016), was that the putative balanced mode cells had much higher levels of mRNA associated with translation as compared to the expanding group. Increase in global translation in the balanced mode cells was further confirmed in a fluorescence based O-propargyl-puromycin global translation assay (Roshan *et al.*, 2016). Together these results suggest a key role played by translation in either progression towards balanced mode or keratinocyte differentiation.

Performing a more detailed pathway-based analysis of my RNA-seq data allows me to speculate that the observed transcriptional phenotypes are influenced, directly or indirectly, by mTOR signalling (Figure 3.13). The mTOR pathway is a key regulator of mammalian metabolism and physiology, and has been reported to play a role in cell fate determination (Liakath-Ali *et al.*, 2018; Sampath *et al.*, 2008). In the next chapters of my thesis, I will look at three specific processes, all controlled by mTOR signalling and all differentially expressed in the RNA-seq dataset, which may play a role in keratinocyte cell fate determination. In Chapter 4, I will focus on the role of transcription and translation in the establishment of the balanced mode of proliferation and cell differentiation. In Chapter 5, I will attempt to evaluate the involvement of lipid biosynthesis in the same processes.

Chapter 4 Level of translation affects colony's proliferative mode

4.1. Chapter overview

The molecular profiling experiments described in Chapter 3 confirmed that the transcriptional profiles of balanced and expanding cells differ. Genes involved in translation were amongst the most differentially expressed in the RNA-seq dataset, with significantly higher levels of translation associated transcripts detected in balanced mode cells compared with expanding ones. This observation is in line with previous findings from our laboratory, where a microarray analysis of 8-cell colonies revealed an increase in translation in the balanced colonies, which was later confirmed using an OP-puro-based global translation assay (Roshan *et al.*, 2016). Moreover, a recent publication by another research group has also emphasised the role of eukaryotic translation in epidermal homeostasis (Liakath-Ali *et al.*, 2018). While the link between translation and keratinocyte cell fate determination has been proven before, the exact nature of this relationship remains unknown. I wanted to know how early in a colony's development changes in translation occur, and whether a colony's fate could be switched by altering translation.

To address these questions, I needed to identify the molecular markers of the colony's proliferation mode, building on data obtained from the RNA-seq and microarray analyses. As there was such a striking difference in translation between the two proliferation modes, I selected two genes involved in translation, eukaryotic translation initiation factors 3E (*EIF3E*) and 4G2 (*EIF4G2*), to investigate further. These factors both work as part of larger complexes and are required for several steps in the initiation of protein synthesis. While the eIF3 complex positions mRNA near the exit site of the 40S ribosome subunit, thus promoting the assembly of the pre-initiation complex, the eIF4G complex mediates circularisation and activation of mRNA by binding the poly(A) tail via an accessory protein (Klann and Dever, 2004).

In this chapter I will first describe how, using a combination of immunofluorescence and live cell imaging, I have demonstrated that eIF3E and eIF4G2 can be used to distinguish between the balanced and expanding mode cells at a very early stage of colony growth. This suggests a colony's fate is set early on. Secondly, using a global transcription marker, I will show that the increase in translation in balanced mode colonies is associated with an increase in global transcription. Finally, I will explain how the use of RNA interference allowed me to knock-down eIF3E and eIF4G2 in cultured keratinocytes, leading to an apparent switch in the colony's proliferative potential following the eIF4G2 knock-down. This key finding suggests that global translation levels or the actual process of translation initiation may determine the cell fate of human keratinocytes.

4.2. Levels of selected eIFs correspond to colony growth dynamics

RNAseq analysis showed that there were significantly higher levels of *EIF3E* and *EIF4G2* transcripts in cultured balanced colonies compared to expanding ones. My first goal was to determine if one or both of the selected eIFs could be used as a molecular marker of colony's proliferation mode. To achieve this, neonatal foreskin epidermal keratinocytes (NFSKs) were grown *in vitro*, EdU labelled to mark cells in S-phase, fixed and immunostained for eIF4G2 and eIF3E (Figure 4.1 and Figure 4.2). A 24 h treatment allowed me to detect the majority of the proliferating cells, based on cycle time distribution determined by live imaging (Roshan *et al.*, 2016). Colonies were assigned as balanced or expanding based on the proportion of EdU positive cells in the colony. For the purpose of this experiment, I made an assumption that a colony with more than 80% of cells labelled as EdU +ve would likely be an exponentially dividing expanding colony, because at this early stage during colony development it is very rare to observe differentiating cells that have exited the cell cycle in this type of colony. In contrast, on average half of cells in a balanced colony would be differentiating, wherefore a colony with a proportion of diving cells smaller than 80% would be balanced (Figure 4.1A and Figure 4.2A). Fluorescence intensities were measured for each colony for both eIF4G2 (n = 150 colonies) and eIF3E (n = 150 colonies) (Figure 4.1C and Figure 4.2C). Data analysis showed that for both eIF3E and eIF4G2 there was a statistically significant increase ($p<0.0001$ 2 tailed unpaired t test) in the expression levels of both of the translation-associated proteins in the balanced versus expanding colonies.

Since I was comparing homogenous expanding colonies in which all cells were proliferating with heterogeneous balanced colonies containing both proliferating and differentiating cells, I then looked at fluorescence intensities of single cells within 20 balanced colonies to assess this heterogeneity and to see if there is a difference in expression of the eIFs of interest in dividing and differentiating cells coming from a single colony (Figure 4.1D and Figure 4.2D).

The analysis revealed significantly higher expression of both eIF3E and eIF4G2 within the non-dividing (EdU -ve) cells as compared to the dividing ones (EdU +ve) ($p< 0.0001$ 2-tailed Mann Whitney) reflecting the trend seen at a whole colony level. These results would suggest that an increase in in these proteins is potentially an early marker of differentiation.

To see if the differences seen at the whole colony level were purely due to the higher proportion of differentiating cells in the balanced mode colonies, or if maybe proliferating cells in the balance colonies are 'primed' towards differentiation, I decided to quantify the levels of eIFs in the EdU positive cells to assess if there were differences between balanced and expanding colonies within the dividing cells. I analysed the levels of eIF3E and eIF4G2 fluorescence in single EdU +ve (dividing) cells in both balanced and expanding colonies (Figure 4.1E and Figure 4.2E), and for both eIF3E and eIF4G2 proteins there was a significant increase in expression ($p< 0.0001$ 2-tailed Mann Whitney) in dividing cells coming from balanced versus expanding colonies. This suggests that there is something intrinsically different between the dividing cells in colonies with two distinct proliferative modes.

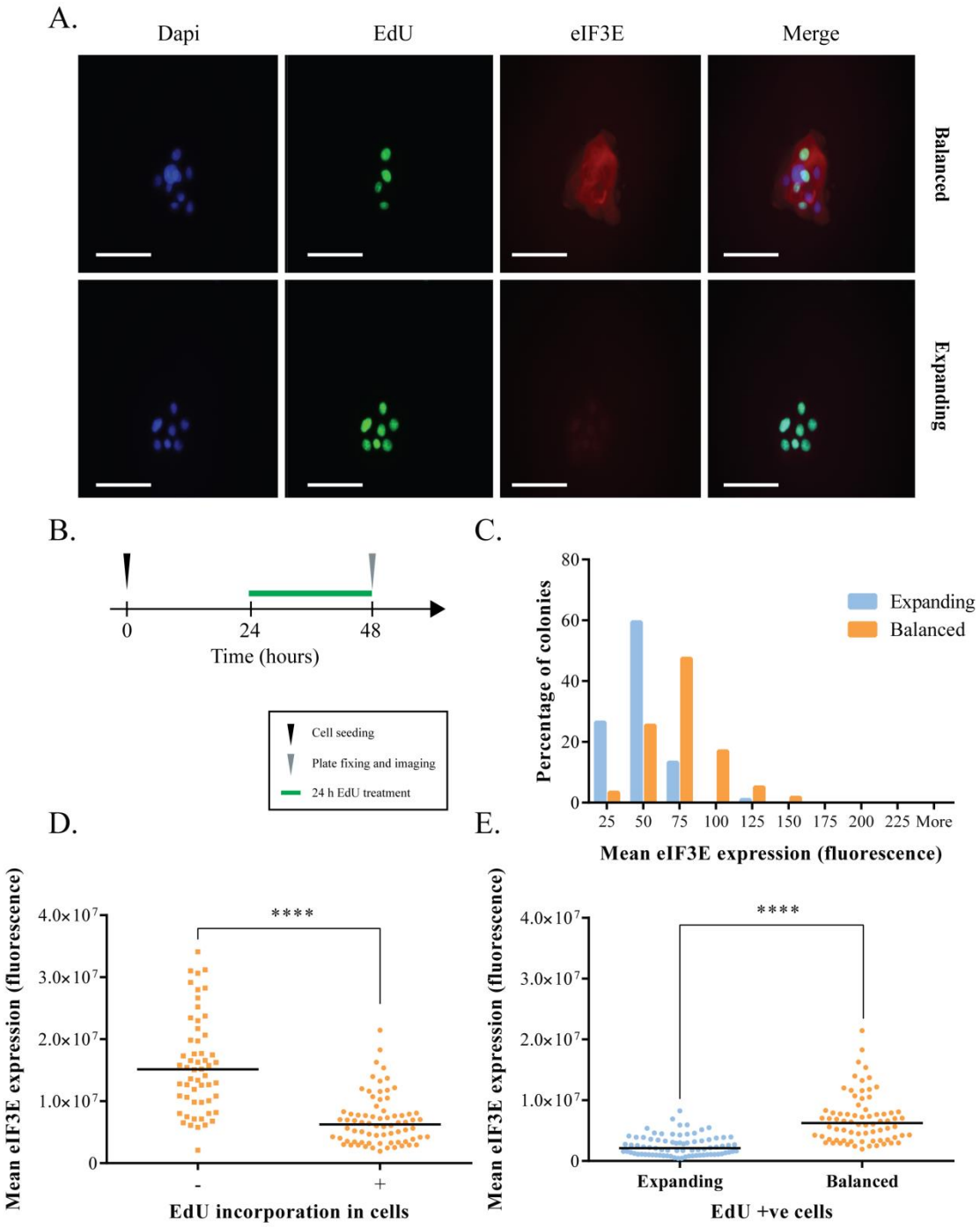

Figure 4.1. Quantification of eIF3E protein expression in balanced and expanding modes. **A**: Representative images of balanced and expanding colonies labelled with anti-eIF3E antibody (red), EdU (green) and Dapi (blue). Scale bar represents 60 µm. **B:** experimental outline. Fluorescence intensities were analysed for whole colonies (**C**, $p<0.0001$ 2-tailed t-test), for single cells within balanced colonies (**D**, $p<0.0001$ 2-tailed Mann Whitney) and dividing (EdU +ve) cells from both colony types (**E**, $p<0.0001$ 2-tailed Mann Whitney). 150 colonies across 3 biological replicates were analysed at the whole colony level, and 20 colonies of each type were analysed at the single cell level.

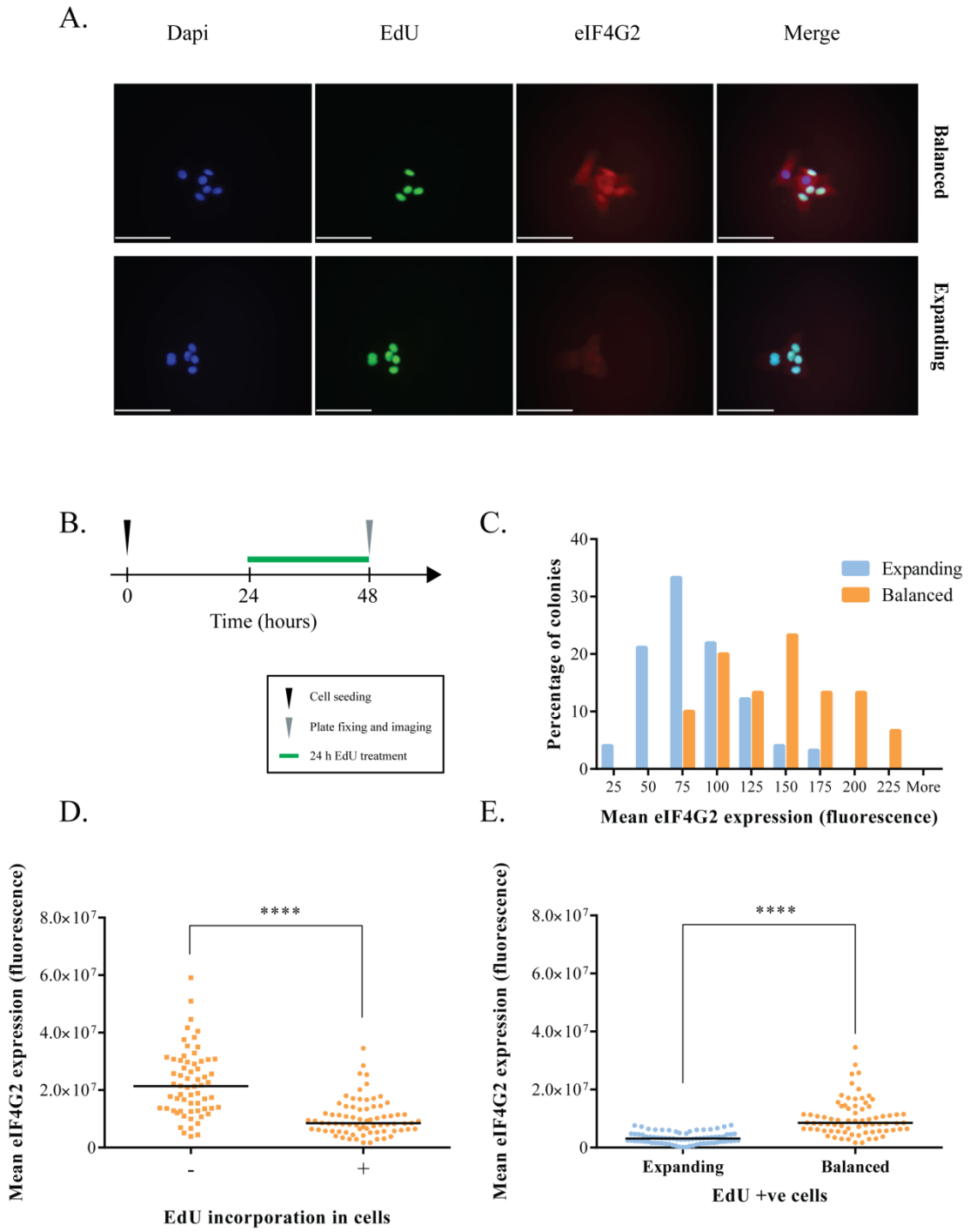

Figure 4.2. Quantification of eIF4G2 protein expression in two proliferative modes. **A**: Representative images of balanced and expanding colonies labelled with anti-eIF4G2 antibody (red), EdU (green) and Dapi (blue). Scale bar represents 60 µm. **B:** The timeline of the experiment. Fluorescence intensities were first analysed for the whole colonies (**C**, $p<0.0001$ 2-tailed t-test), then for single cells within the balanced colonies (**D**, $p<0.0001$ 2-tailed Mann Whitney), and dividing (EdU +ve) cells from two types of colonies (**E**, $p<0.0001$ 2-tailed Mann Whitney). 150 colonies across 3 biological replicates were analysed at the whole colony level, and 20 colonies of each type were analysed at the single cell level.

4.3. A colony's fate may be set after the first cellular division

Immunostaining of 6-10 cell keratinocyte colonies has shown that the levels of eIF3E and eIF4G2 differ significantly between differentiating and dividing cells coming from a single colony. Moreover, for these two factors there was also a significant difference in protein expression between dividing cells coming from colonies with different proliferative potential. Together these findings suggest that the level of translation, and more specifically levels of certain eIFs, can be used as an early predictor of a cell's proliferative mode and differentiation state. In order to assess how early these differences in the levels of translation arise, a 2-cell colony staining experiment was set up. NFSKs were grown *in vitro* at clonal density and fixed 18 h post seeding. This early time point was based on live imaging data (Roshan *et al.*, 2016) and should allow me to analyse pairs of sister cells within a few hours of cell division. Cells were immunostained for eIF4G2, which was showing a wider distribution of staining intensity, potentially allowing higher sensitivity at the single cell level, imaged and then levels of fluorescence were compared between the sister pairs (Figure 4.3).

Comparison of the expression ratio between sister pairs has revealed 64% of screened NFSKs had a very similar level of eIF4G2 expression to their sister (using a cut off of <1.5 fold comparing the two cells, based on the distribution of IF values). However the remaining 36% of pairs were heterogeneous, with one sister having a higher expression of eIF4G2 than the other. This outcome is in line with the results of the *in vitro* tracking experiments performed previously in our laboratory (Roshan *et al.*, 2016). Live tracking revealed that only around 10% of colonies in any culture are expanding, and these could correspond to pairs of two low eIF expressing cells. The remaining 90% of colonies are balanced and of these about 35% are going to give 2 differenting cells, 35% 2 dividing cells and about. 30% one of each kind (Roshan *et al.*, 2016).

Focussing on the absolute values of eIF4G2-associated fluorescence in the sister pairs with similar ratios of expression shows that there are two groups; pairs with high levels of eIF4G2 expression and those pairs with low levels of expression (Panels A and D in Figure 4.3). It is tempting to speculate that as I have already shown eIF4G2 is associated with differentiation (Figure 4.1 and Figure 4.2) these 3 groups could be categorised into early stage balanced colonies (heterogenous expression), early stage expanding colonies (low homogenous expression) and balanced colonies where both cells have committed to differentiation (high homogenous expression).

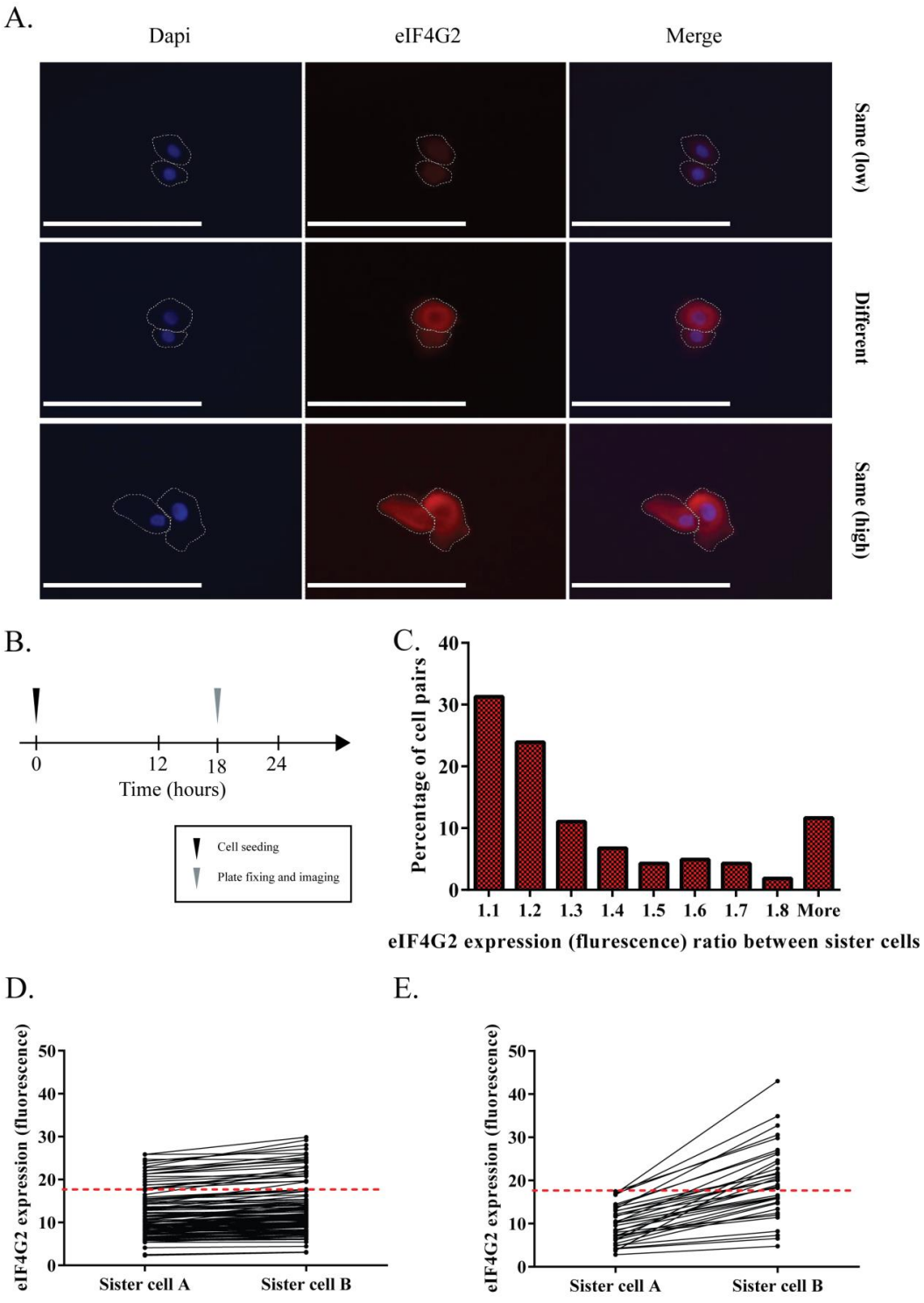

Figure 4.3. Expression of eIF4G2 in 2-cell colonies. **A**:Representative images of sister pairs stained for eIF4G2 (red) and Dapi (blue). Scale bar represents 60 µm. **B**: Experimental outline. **C**: Ratio of fluorescence intensity between sister cells (n=60 pairs). Sister pairs with ratio >1.5 are defined as heterogeneous. eIF4G2 expression (fluorescent intensity) in homogeneous (**D**) and heterogeneous (**E**) sister pairs. Lines link pairs of sister cells. The red line indicates the highest observed expression of eIF4G2 of the lower expression sister in the heterogeneous pairs.

4.4. Increase in translation is coupled with increase in transcription

Both eIF3E and eIF4G2 seem to be good candidates for markers of the colony's proliferation mode. Building on that, I wanted to see if increase in translation is associated with an increase in global transcription levels. To test this, I looked at the level of incorporation of an alkyne-modified nucleoside, 5-ethynyl uridine (EU), into freshly synthesised mRNA. EU was given to NFSKs for 1h, after which cells were fixed and the amount of labelled RNA was detected using Click-iT chemistry. In the eIF staining experiment, EdU detection was used for discriminating the proliferation modes. Unfortunately, EdU is also detected using Click-iT reaction and the two assays are incompatible. To mitigate this issue, a different approach to discriminate between different colony types was needed.

Keratin 1 (KRT1) is an early marker of differentiation in keratinocytes and is not usually expressed in proliferating cells (Takazawa *et al.*, 2015). Expanding colonies at the 6-10 cell stage are composed of dividing cells only and should have low KRT1 levels. To test this, NFSKs were grown *in vitro*, EdU treated, fixed and immunostained for KRT1. Colonies were scored for KRT1 expression and classified based on the proportion of EdU positive cells within a colony (Figure 4.4). 96% of colonies classified as balanced contained at least one KRT1 positive cell, and 86% of colonies classified as expanding did not contain any KRT1 positive cells. Based on the results of this experiment, I set my criteria that any colony with at least one KRT1 positive cell would be categorised as balanced and all the others would be expanding.

To quantify the levels of global transcription in balanced and expanding colonies, NFSKs were cultured for 48 h, treated with EU, fixed and immunostained for KRT1 (Figure 4.5). Fluorescence relating to EU incorporation was quantified for balanced and expanding whole colonies (Figure 4.5C). A significant increase ($p < 0.0001$ 2-tailed unpaired t test) in global transcription levels was observed in the balanced versus expanding colonies. In a single cell analysis, EU levels in differentiating (KRT1 +ve) and proliferating (KRT1 -ve) cells within balanced colonies were measured (Figure 4.5D), and showed a subtle yet statistically significant increase in global transcription levels in differentiating cells ($p=0.0142$ 2-tailed Mann Whitney test). However, there was a clear difference between the non-differentiated (KRT1 -ve) cells comparing the different colony types, with higher EU levels in balanced type colonies (Figure 4.5E, $p < 0.0001$ 2-tailed Mann Whitney).

This data may suggest that the global transcription level, measure as EU incorporation, goes up before KRT1 in keratinocyte differentiation, although it could also reflect a difference in EU levels in cycling cells in the two modes of proliferation.

Overall, similarly to the levels of eIF3E and eIF4G2, which also differed between dividing cells from different colony types, the higher global transcription level in cycling keratinocytes coming from balanced colonies versus the ones coming from expanding colonies, and the fact that the level of transcription is further increased in differentiating cells, together suggest that the ability of a progenitor cell to produce daughters of different proliferative capacity may be set before the decision to divide is made.

A.

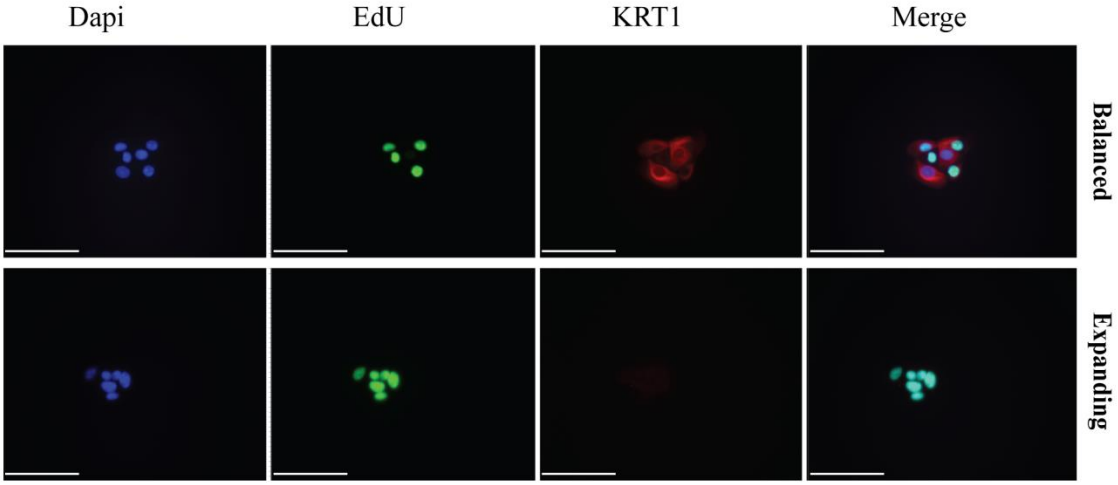

B.

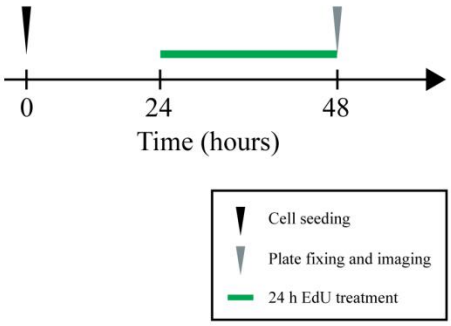

C.

	At least one KRT +ve cell	No KRT +ve cells
Balanced colonies	96%	4%
Expanding colonies	18%	82%

Figure 4.4. Keratin1 expression in balanced and expanding colonies. **A**: Representative images of balanced and expanding colonies with EdU (green) or KRT1 (red) staining. Scale bar represents 60 µm. **B**: Experimental outline. **C**: Table detailing KRT1 expression in balanced and expanding colonies. 96% of balanced colonies contain 1 or more Keratin 1 expressing cell, however this is the case for only 18% of expanding colonies.

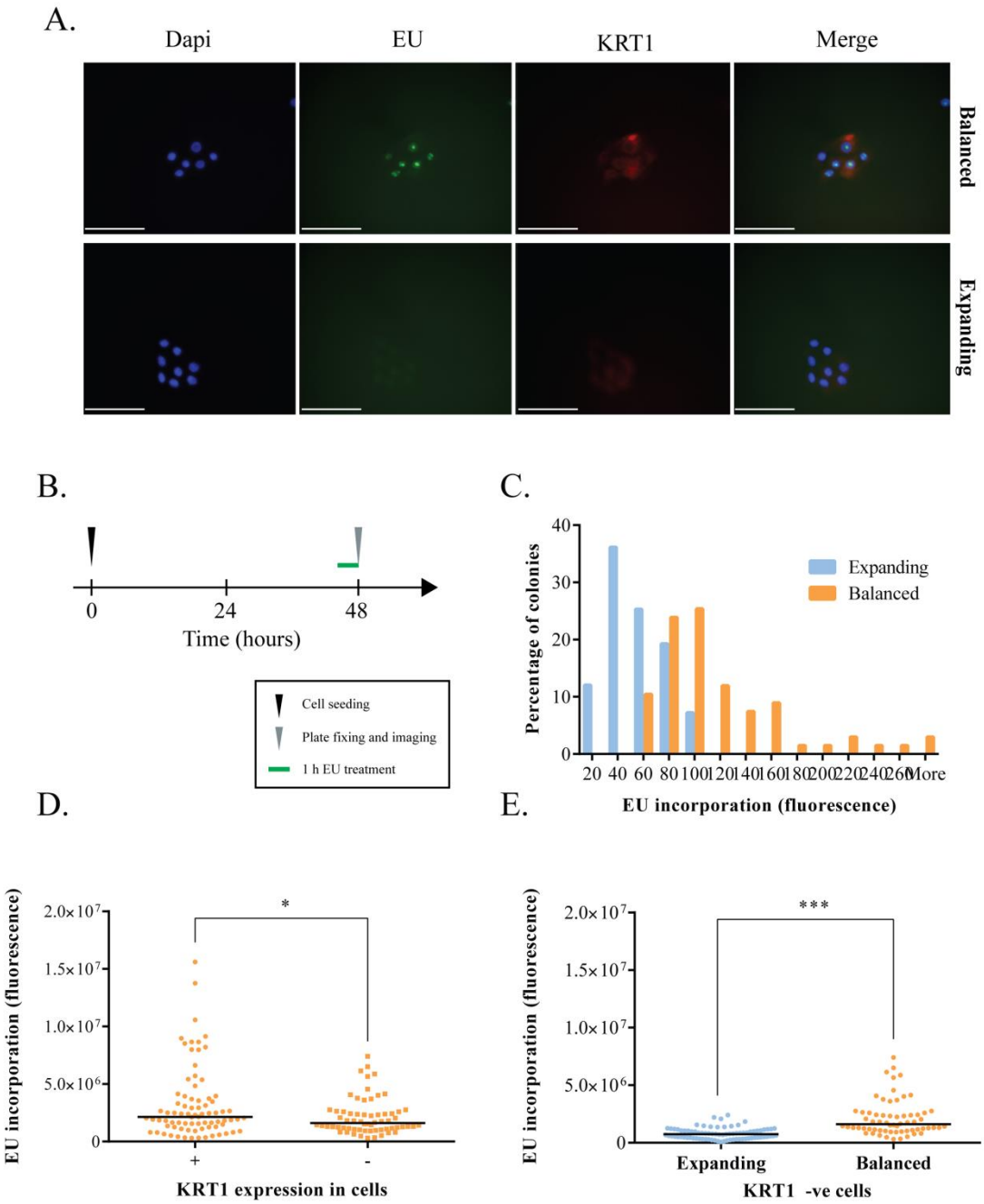

Figure 4.5. EU incorporation in balanced and expanding colonies. **A**: Representative images of balanced and expanding colonies categorised based on expression of KRT1 (red). EU (green) and Dapi (blue). **B**: Experimental outline Fluorescence intensities for whole colonies differed significantly between the colony types (**C**, $p<0.0001$ 2-tailed t-test), while the difference between differentiating (KRT1 +ve) and dividing (KRT1 -ve) cells within balanced colonies (**D**) was less pronounced but statistically significant ($p=0.0142$ 2-tailed Mann Whitney). **E**: EU incorporation levels in cycling cells (KRT -ve) coming from different types of colonies (**D**, $p< 0.0001$ 2-tailed Mann Whitney). 150 colonies across 3 biological replicates were analysed per experiment. Scale bars represent 60 µm.

4.5. Colony's proliferation mode can be predicted in live cells

While EdU and KRT1 are useful tools for the classification of colonies, there are several drawbacks to consider. They can only be used on fixed cells and both are prone to some degree of mis-annotation when categorising dividing and differentiating cells, with some of the balanced colonies being consequently classified as expanding. Ideally, I would like to be able to predict what fate a cell will follow at an early point in colony formation to enable us to identify markers before cells fully commit to differentiation. To achieve this, I became involved in developing a tool based on dilution of GFP fused to histone 2b (H2B-GFP), which should allow us to predict the cell fate of eight-cell colonies.

For this experiment, H2B-GFP infected NFSKs were live tracked using an IncuCyte live imaging system. Colonies were scored for H2B-GFP associated fluorescence after reaching 8 cells in size. Live tracking allowed me to revisit same colonies after 7 days and assess whether they are balanced or expanding based on their size. Previous work in our laboratory has shown that expressed H2B-GFP is stable and its fluorescence is halved during cell division (fluorescently labelled histones are divided equally between daughter cells, Figure 2.1 in Chapter 2). By definition, in expanding colonies the majority of cells are dividing. Hence, at 8-cell stage, fluorescence should be similar across the whole colony For balanced 8-cell colonies, cells would show different levels of fluorescence depending on the number of full cell cycles they have undergone (Figure 4.6A and B). I have employed this principle to accurately predict ($p < 0.0001$ 2-tailed Mann Whitney test) whether a colony at the 8-cell stage will grow to be a large expanding colony or a much smaller balanced one (Figure 4.6C).

After determining that H2B-GFP dilution can be used to predict a colony's proliferative potential, I wanted to test if we could still see differences in levels of transcription and translation in colonies classified using this approach. NFSKs were first infected with the H2B-GFP construct and induced using Doxycyclin. Cells expressing H2B-GFP were then flow-sorted into 96-well plates and growing colonies were tracked using the IncuCyte. When colonies reached 8-cells in size, they were treated with EU, fixed, stained for eIF3E and imaged. H2B-GFP was used to classify colonies as either balanced or expanding, and eIF3E expression and EU incorporation in individual cells was analysed. Analysis revealed that cells coming from balanced colonies have significantly higher levels of both eIF3E expression (Figure 4.7C, 0.0170 2-tailed Mann Whitney test) and EU incorporation (Figure 4.7D, $p < 0.0001$ 2-tailed Mann Whitney test) than cells coming from expanding colonies.

Observed differences in eIF3E expression and EU incorporation are in line with results obtained by analysis of fixed colonies classified using EdU incorporation and KRT1 expression. Therefore, using three independent colony classification techniques I have demonstrated that balanced and expanding colonies differ in the level of eIFs expression and global transcription at both colony and single cell level, which makes these observations robust in the *in vitro* system. Thus, next I wanted to assess whether similar patterns of expression can be observed *in vivo*.

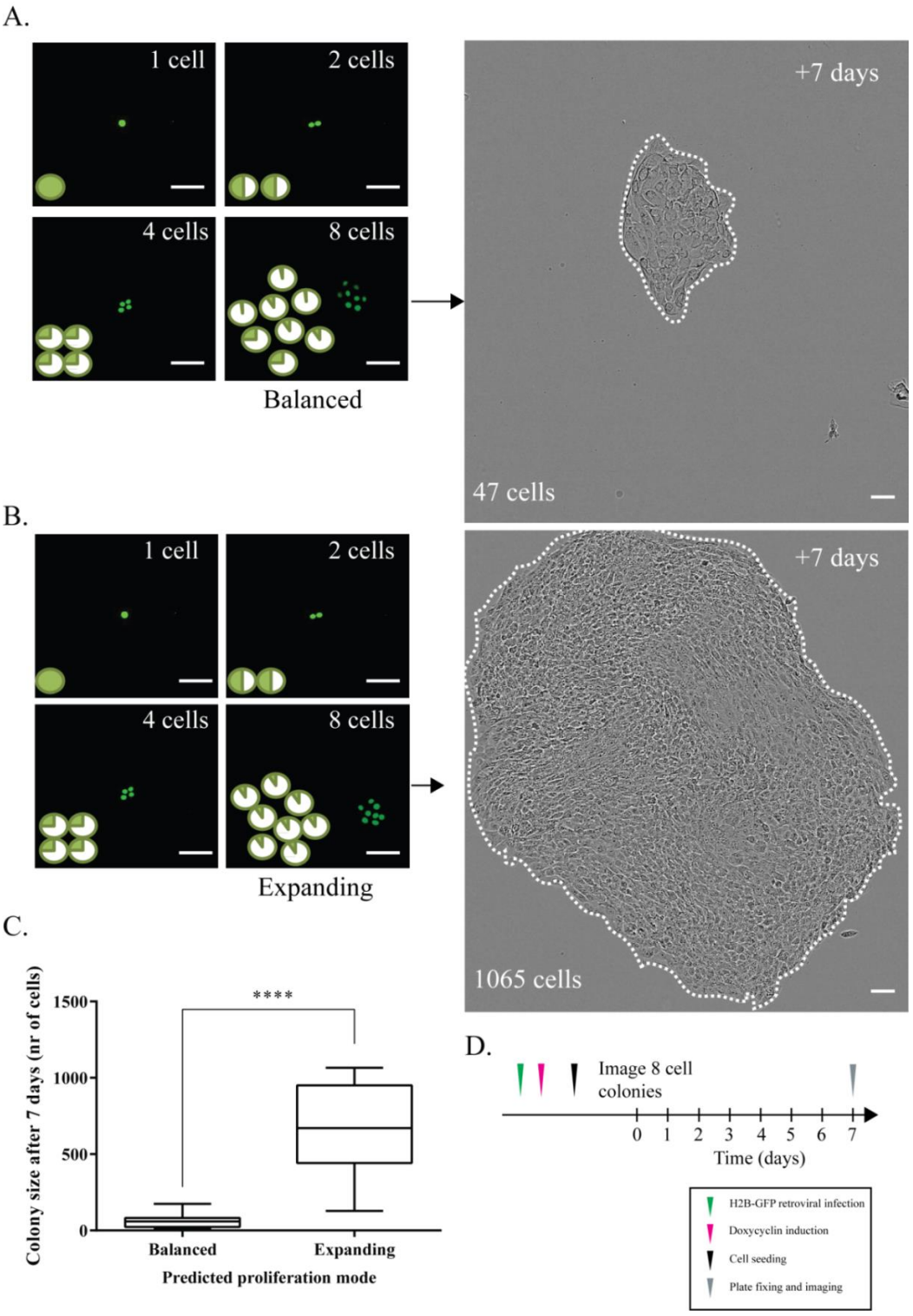

Figure 4.6. Tracking H2B-GFP dilution to predict a colony's proliferation mode. In balanced colonies some cells stop dividing before the colony reaches 8 cells in size, leading to variable levels of H2B-GFP expression (**A**). **B**: At an early stage, all cells within an expanding colony are dividing; hence similar levels of H2B-GFP expression are observed (**B**). Scale bars represent 60 µm. **C**: Colony size at one week. Proliferation mode determine by H2B GFP dilution at 8-cell stage. N= 36. Colony proliferation mode was predicted with high accuracy (**C**, $p < 0.0001$ 2-tailed Mann Whitney test). **D**: Experimental outline. The H2B-GFP construct is described in Chapter 2 section 2.1.3

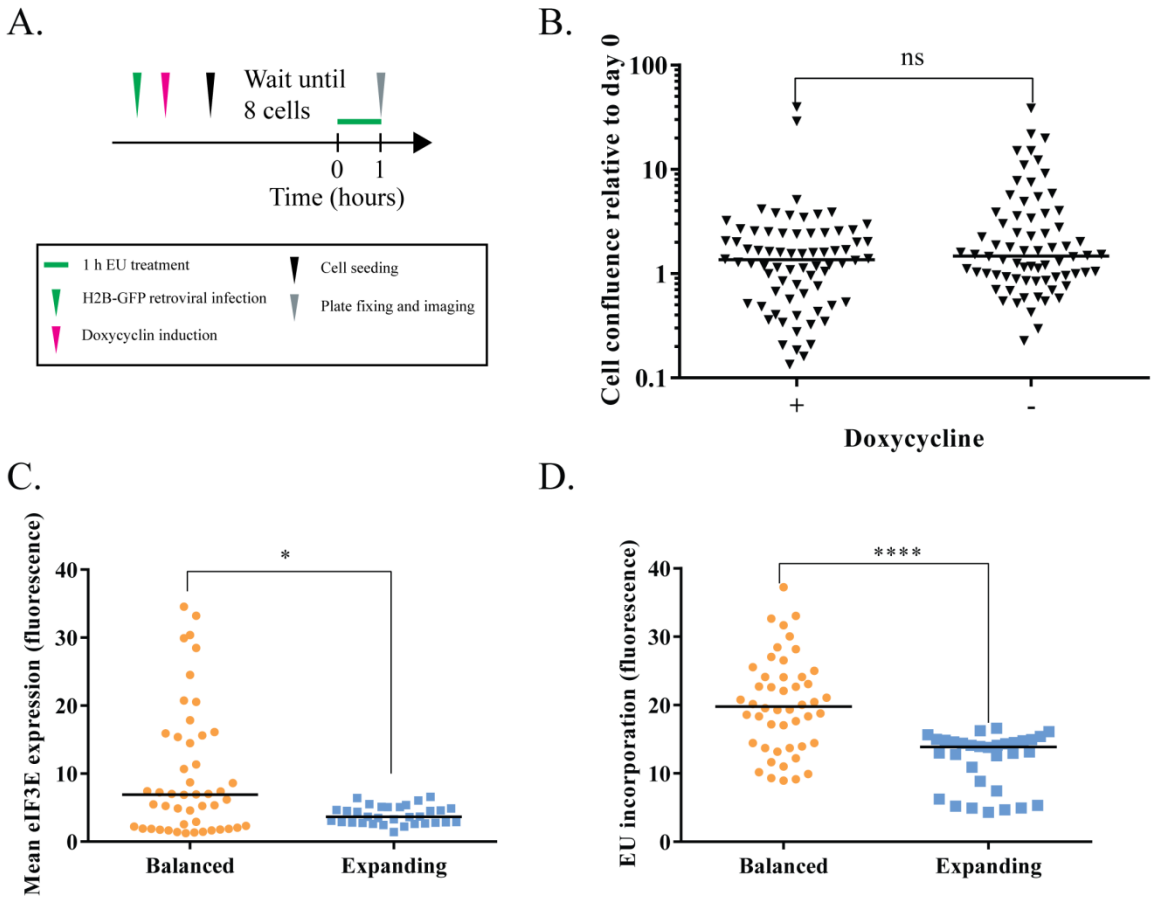

Figure 4.7 eIF3E staining and EU incorporation in H2B-GFP labelled colonies. **A**: Experimental outline. **B**: Doxycycline (used to induce expression of H2B-GFP) has no effect on keratinocyte growth (**B**). Levels of eIF3E (**C**) and EU (**D**) in 30 colonies classified as balanced or expanding based on H2B-GFP dilution. In both cases there was an increase in expression in the balanced colonies similar to that observed when classifying with EdU and KRT1 (**C**, 0.0170 2-tailed Mann Whitney test and **D**, $p < 0.0001$ 2-tailed Mann Whitney test).

4.6. Levels of translation are increased in differentiating cells *in vivo*

As eIF3E and eIF4G2 levels were significantly different between balanced and expanding colonies *in vitro* I wanted to see if we could observe a similar increase *in vivo*. Samples of abdominal skin from organ transplantation donors were cryosectioned and immunostained with either eIF3E or eIF4G2 to assess the level of translation. Keratin 14 (KRT14) was also used to label the basal layer of the tissue, which normally contains all proliferative keratinocytes in adult mammalian epidermis (Diociaiuti *et al.*, 2018; Kim *et al.*, 2017; Kocher *et al.*, 2017). Sections were also stained with haematoxylin and eosin to confirm that the samples were grossly normal. In all cases a contiguous basal layer and several layers of stratifying keratinocytes are clearly visible. Interestingly, despite being obtained from donors of similar ethnicity, the thickness and overall appearance varied significantly between the epidermal samples from different donors and this relationship was not directly correlated to donor's age (Figure 4.8).

eIF3E and eIF4G2 staining intensity was compared between Keratin 14 positive (proliferating) and negative (differentiating) areas (Figure 4.9 and Figure 4.10). Based on the results of the *in vitro* experiments, I would expect to see lower levels of both eIFs in the proliferative cells than in the differentiating ones, meaning that, if our assumption is correct, there should be lower levels of eIF3E and eIF4G2 in the KRT14 +ve basal layer than in the KRT14 –ve suprabasal layer. For all samples analysed, expression of eIF3E (Figure 4.9C) and eIF4G2 (Figure 4.10C) was lower in the KRT14 +ve basal layer than in the KRT14 –ve region. All measurements were normalised for the number of cells contained in the analysed region to account for the fact that a single basal layer is compared to a suprabasal region, which is composed of multiple layers. In all cases, the expression of both eIFs was higher in the suprabasal layers than in the basal one, corresponding to the higher level of differentiation in the suprabasal region, however the actual ratios varied from 1.5 to 3.5 fold (Figure 4.9D and Figure 4.10D). This suggests there is a high degree of variability between samples.

Nevertheless, the observed trend is maintained between samples and donors, suggesting that eIF3E and eIF4G2 are both good markers of keratinocyte cell fate, as they increase with differentiation. It would be interesting to look at individual cells within the basal layer to see if they are heterogeneous in the levels of eIFs expression, however it was impossible to assess that with high enough certainty using sections of frozen tissue.

A.

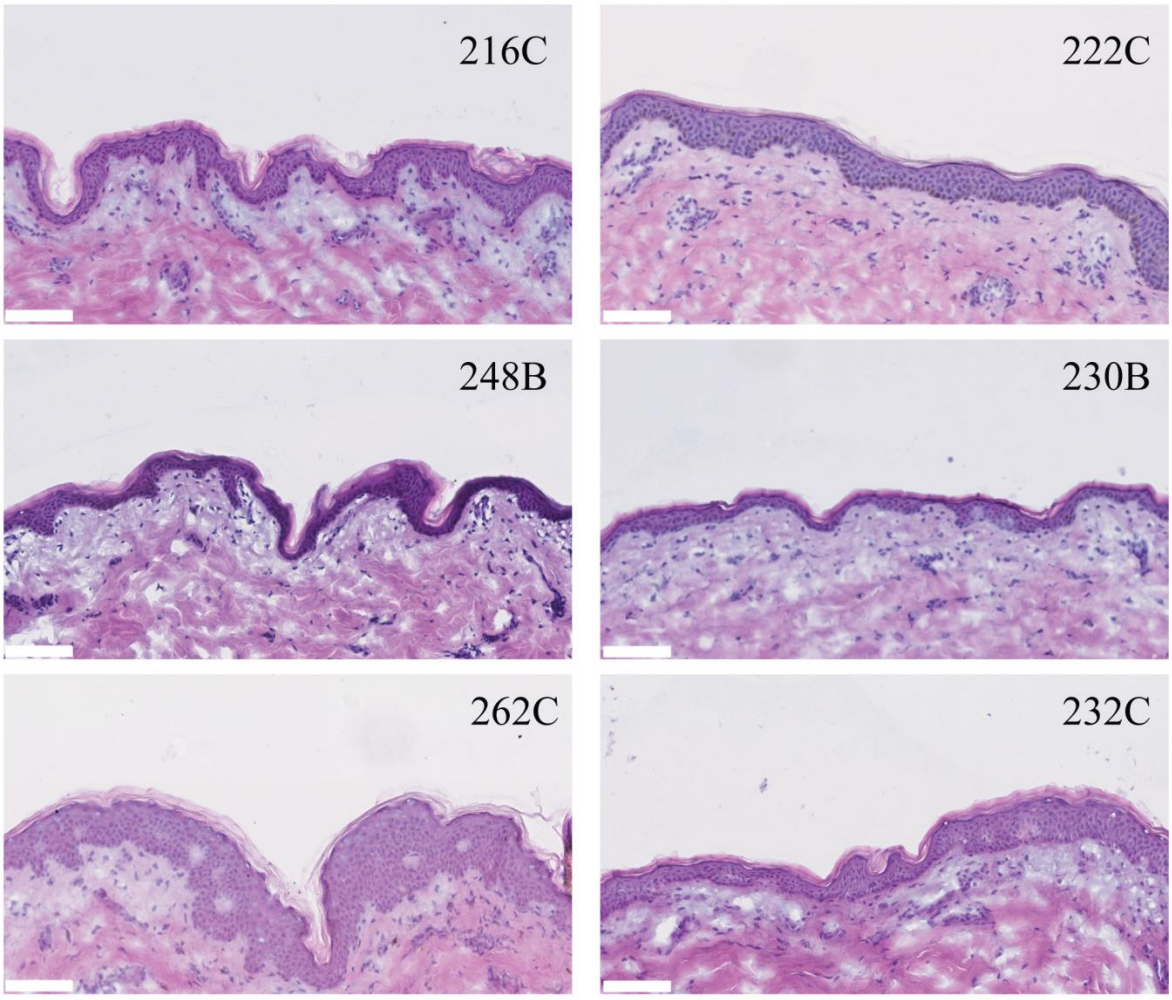

B.

Sample ID	Sex	Age (years)	Ethnicity
216C	Female	67	Caucasian
222C	Male	68	Caucasian
230B	Male	54	Caucasian
232C	Male	45	Caucasian
248B	Female	57	Caucasian
262C	Female	26	Caucasian

Figure 4.8 Hematoxylin and eosin staining of human epithelium. **A**: Representative images of H&E stained cryosections of human skin. Samples from female donors are presented in the left column, and samples from male donors are shown on the right. Scale bars represent 100 µm. **B**: Summary of donor details.

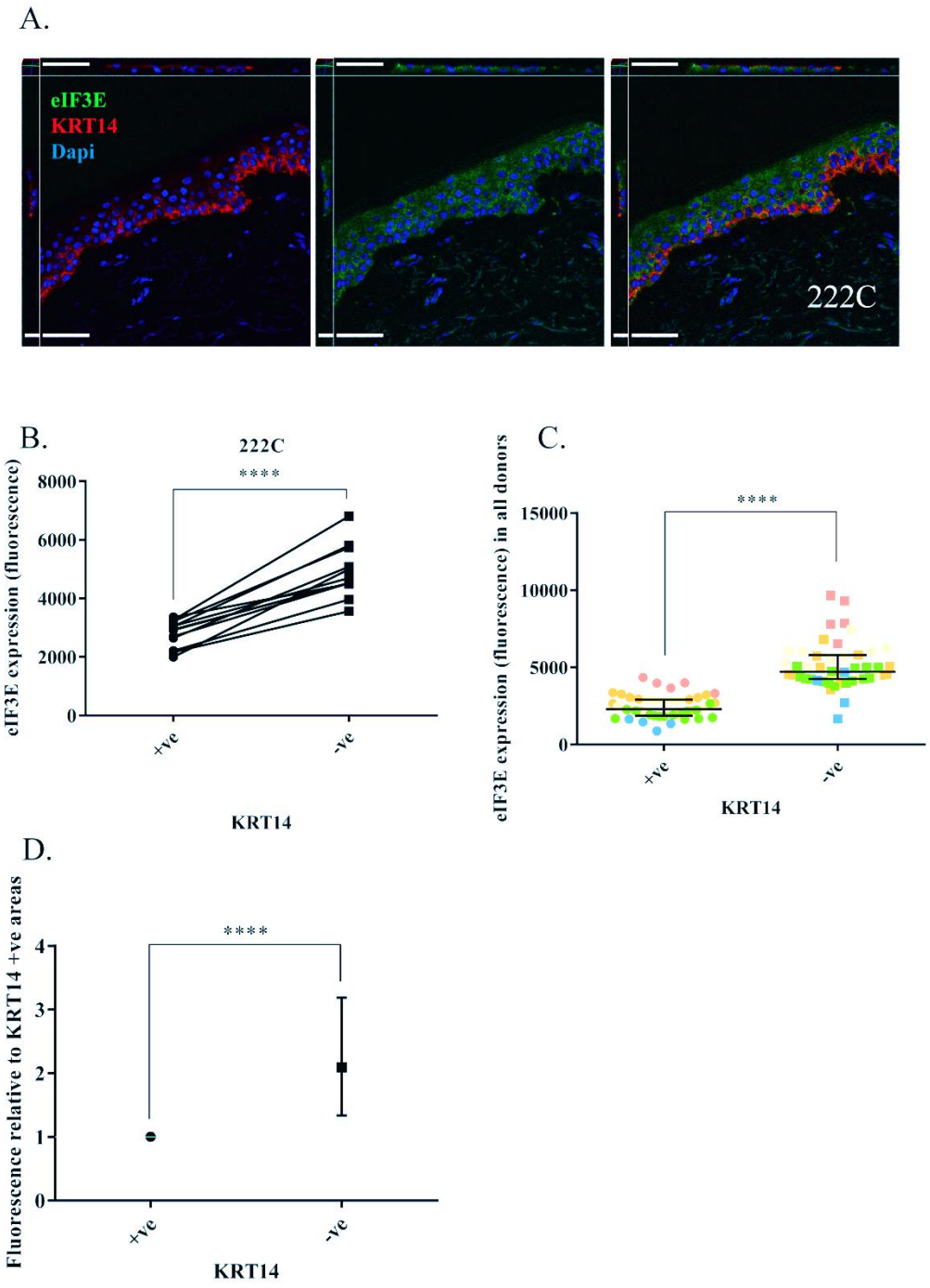

Figure 4.9. eIF3E staining of sections of human skin. **A**: Representative images of a single sample. eIF3E (red), KRT14 (green) Dapi (blue). Scale bars represent 70 µm (x and z axis) and 15 µm (y axis). **B**: Quantification of eIF3E expression in KRT14 positive and negative areas from a single patient. **C**: Individual quantification for each sample. Different colours represent different individuals. (n= 6 donors, a minimum of 4 areas/ person). Pooled measurements from all donors are shown in Panels **C** and **D**. Levels of eIF4G2 are significantly higher in the KRT14 –ve regions for all analysed samples ($p < 0.0001$ 2-tailed Mann Whitney test).

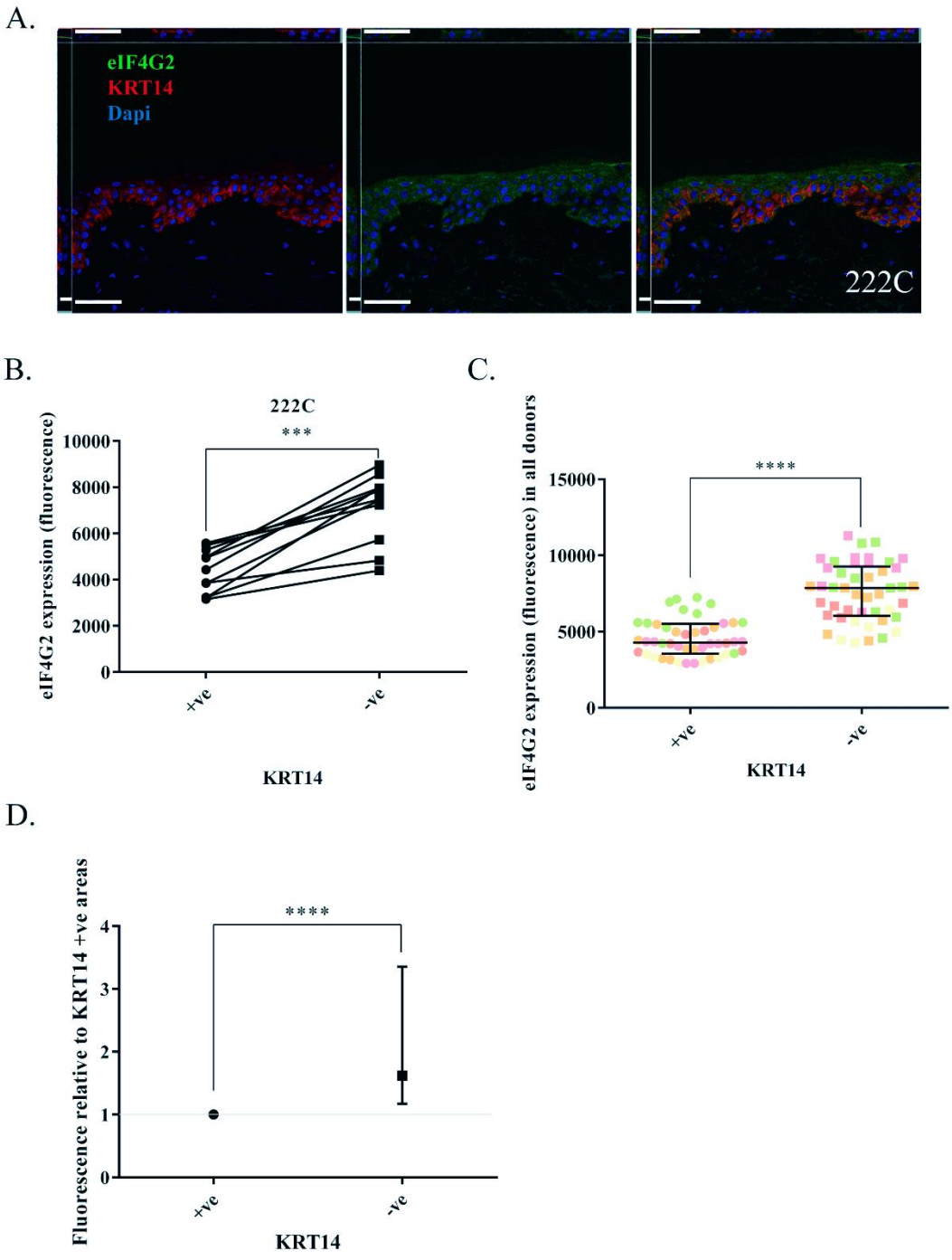

Figure 4.10. eIF4G2 staining of sections of human skin. **A**: Representative images of two different samples. eIF4G2 (red), KRT14 (green) Dapi (blue). Scale bars represent 70 µm (x and z axis) and 15 µm (y axis). **B**: Quantification of eIF4G2 expression in KRT14 positive and negative areas from two different individuals. **C**: Individual quantification for each sample. Different colours represent different individuals. (n= 6 donors, a minimum of 4 areas/ person). There are significant differences in levels of eIF4G2 expression between the KRT14 +ve and-ve regions for individual donors (**B**, 0.0006 and 0.0023 respectively 2-tailed Mann Whitney test), as well as for samples from all donors pooled together (**D** and **C**, $p < 0.0001$ 2-tailed Mann Whitney test).

4.7. Partial inhibition of translation promotes keratinocyte proliferation *in vitro*

Results of the staining and sequencing experiments presented so far in this thesis indicate that the level of translation, and more specifically the levels of eIF3E and eIF4G2, can be used as an early predictor of a cell's proliferative mode and differentiation state. Nevertheless, based solely on this data, it is still unclear whether the observed peak in translation is a trigger or rather a consequence of differentiation.

To assess this, I have performed siRNA-mediated knock-down of eIF3E and eIF4G2 in keratinocyte cultures, using two targeting siRNAs and a scrambled siRNA control. NFSKs were seeded at clonal density and, after 48 h, feeders were removed before either a targeting or control siRNA was applied for a further 48 h (Figure 4.11A). To ensure that there was no toxicity from the knockdown, plates were imaged pre and post treatment. The percentage of surviving colonies was the same whether a targeting or a control siRNA was applied (Figure 4.11B). For eIF3E at 48 hours there was a 72-85% knockdown in the mRNA levels for both siRNA compared to control and at 96 hours there was a 50 - 60% decrease in protein levels as assessed by capillary immuno-electrophoresis. For eIF4G2 at 48 hours there was a 67 - 75% knockdown in the mRNA levels for both siRNAs compared to control and at 96 hours there was a 60 - 70 % decrease in the protein amount (Figure 4.11 and Figure 4.12).

Immunostaining for the two translation initiation factors 48 hours after addition of the siRNA showed that there was a reduction in eIF3E and eIF4G2 expression in the knock-down cultures. This proved that not only was there an effective protein knock-down, but also that both antibodies used for staining are accurately targeting the protein of interest (Figure 4.13B, Figure 4.14B). I also stained the colonies with a differentiation marker KRT1. For both eIF4G2 and eIF3E while there was no significant difference in the number of KRT1 expressing cells, there was an apparent shift in colony size distribution between the knock-down and control cultures, suggesting a change in colonies' proliferation mode (Figure 4.13C and D). This shift in colony size further highlights the importance of post-silencing analysis of eIF3E and eIF4G2 using immunostaining (Figure 4.13). While the controls for mRNA and protein levels of eIF3E and eIF4G2 may vary due to changes in colony proliferative mode and metabolism, the direct measurement of eIF3E and eIF4G2 with antibodies provides a non-biased evidence confirming successful knock-down.

If NFSKs are being pushed towards expanding mode, any differences in size distribution would be amplified as the colonies grew; therefore I repeated the experiment but allowed the colonies to grow for 5 days after the knockdown (Figure 4.14). This time, for both siRNAs targeting eIF4G2, there was a clear significant reduction in the level of Keratin1 expression (Figure 4.14C).

Additionally, there was a significant shift in the colony size distribution towards larger colonies in the eIF4G2 knock-down cultures compared to the control ones (Figure 4.14D). Despite an effective knock-down at both RNA and protein levels, similar effects were not observed in the eIF3E knock-down cultures. Taking this into the consideration, it is possible that while both translation initiation factors seemed to be good markers for colonies' proliferative mode, only eIF4G2 appears to play a significant role in its establishment or maintenance.

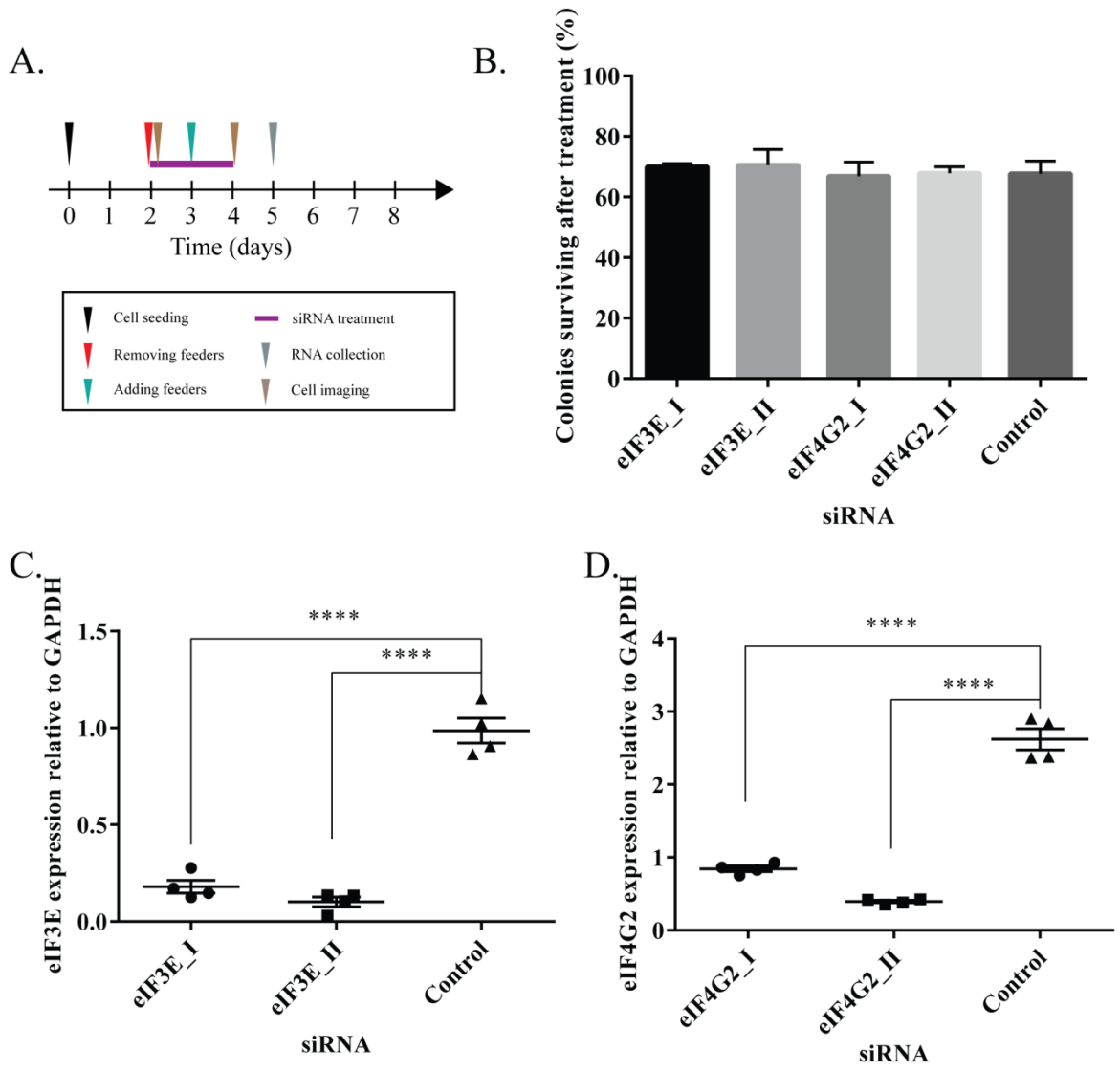

Figure 4.11. Assessment of efficacy of siRNA knockdown of eI4G2 and eIF3E at mRNA level A: Experimental outline. B: Assessment of toxicity of siRNA treatment. Quantification of *eIF3E* (C) and *eiF4G2* (D) mRNA levels 48 hours post knockdown. Expression was normalised to GAPDH (C and D, $p < 0.0001$ 2-tailed Mann Whitney test). Experiment was performed in 4 replicates.

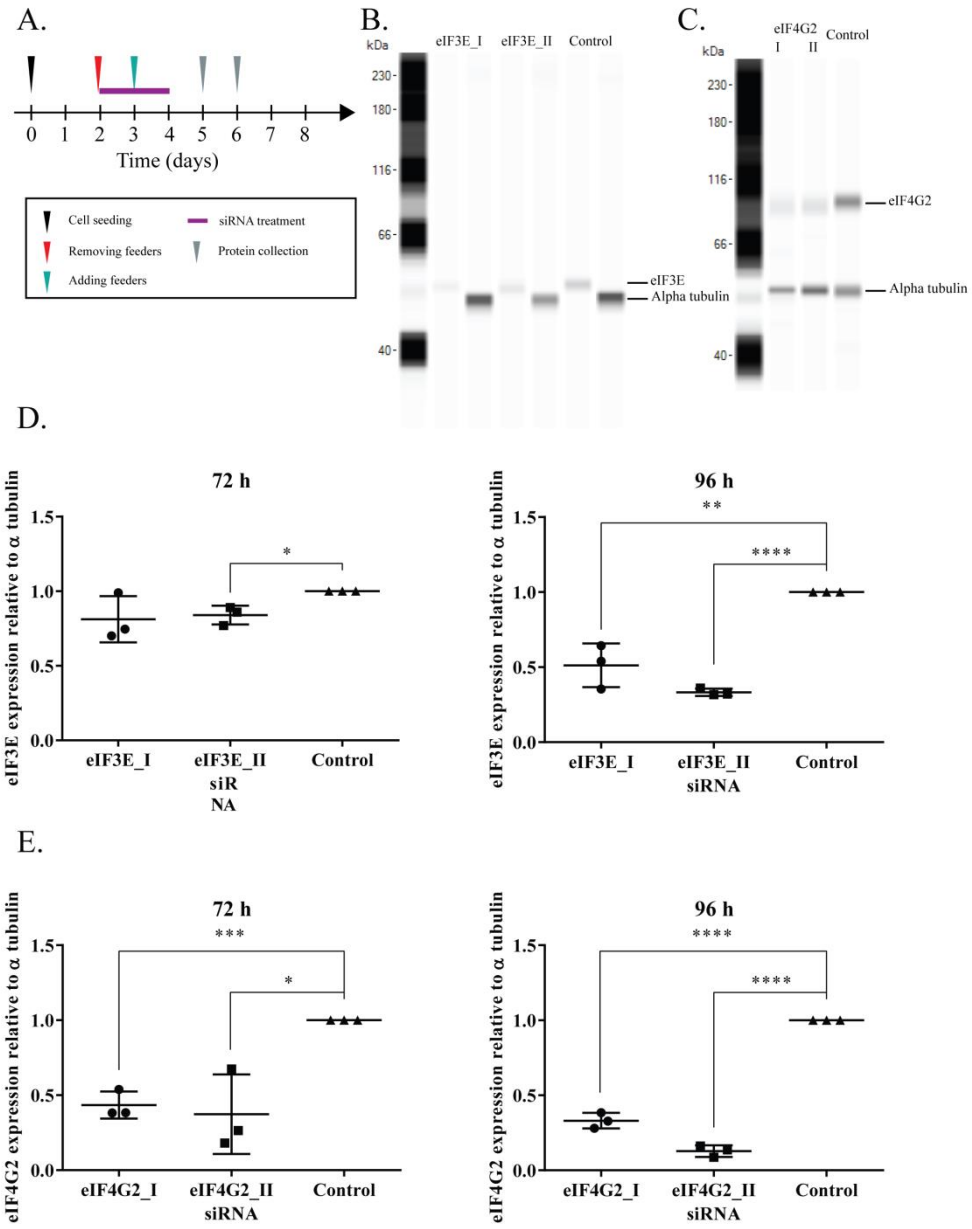

Figure 4.12. Assessment of efficacy of siRNA knockdown of eI4G2 and eIF3E at protein level A: Experimental outline B and C: Representative images from the capillary immunoassay system used to quantify protein expression (lysates from 72 hours post knockdown). Quantification of eIF3E (D) and eIF4G2 (E) protein levels at 72 and 96 hours post knockdown. *p=0.0148, **p=0.0044, ***p=0.0004, ****p< 0.0001 2-tailed Mann Whitney test. Experiments performed in 3 replicates.

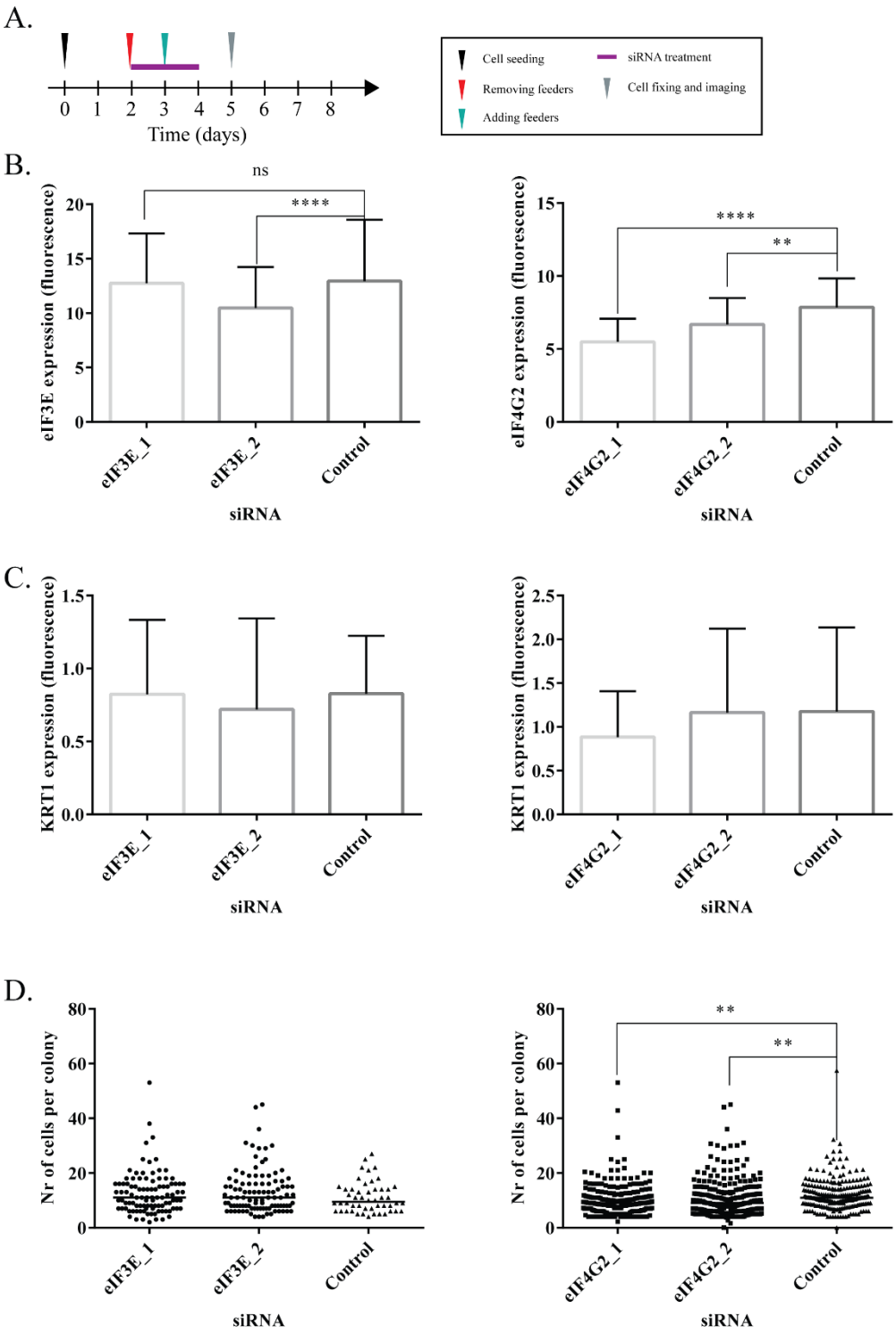

Figure 4.13. Colony behaviour 48 hours after knock-down. **A**: Experimental outline. **B:** Quantification of eIF3E and eIF4G2 48 hours after knockdown. In most cases a significant reduction in expression was observed. **C**: There was no significant difference in KRT1 expression post knockdown for either eIF3E or eIF4G2. A modest increase in colony size was observed for eIF4G2 but no eIF3E post knockdown (**D**). ** p=0.0011 2-tailed Mann Whitney test. Experiments were performed in 4 biological replicates.

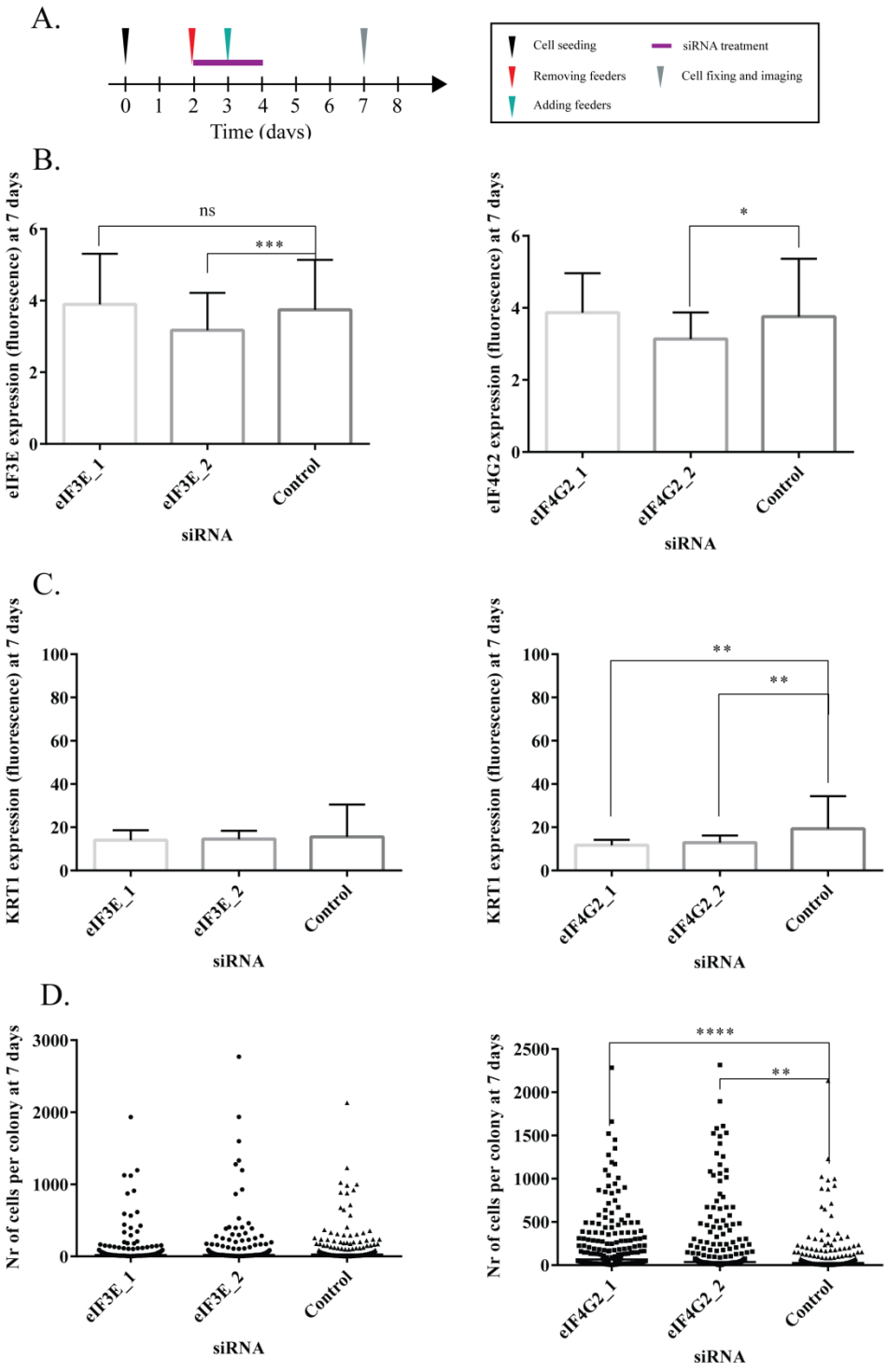

Figure 4.14. Colony behaviour after knock-down at day 7 post seeding. **A**: Experimental outline. **B:** Quantification of eIF3E and eIF4G2 5 days after knockdown. The production of both eIFs is recovering to a normal level (**B**). RNA-silencing of eIF4G2 clearly affects keratinocyte proliferation and differentiation state, manifested by reduced expression of a differentiation marker KRT1 (**C**), and increased number of large colonies observed 5 days post treatment (**D**). 2-tailed Mann Whitney test was used to assess significance. ** p=0.007 2-tailed Mann Whitney test. Experiments were performed in 4 biological replicates.

4.8. Discussion

In this chapter I have further evaluated the distinct transcriptional and translational profiles displayed by cultured human keratinocytes. My work has provided further evidence that the balanced and expanding colonies differ in their transcriptional and translational profiles. This analysis was made possible as I was able to distinguish between balanced and expanding colonies at the 8-cell stage using specific markers for translation (Figure 4.1 and Figure 4.2) and a global transcription marker (Figure 4.5). In addition, the H2B-GFP assay is able to predict if a developing colony will go on to be expanding or balanced (Figure 4.6).

In line with data obtained from RNA-seq and microarray analysis, the levels of eIF4G2 and eIF3E proteins were found to be significantly higher in balanced colonies than in expanding ones. This observation was consistent for both entire colonies and single cells. This develops and is consistent with the work of Roshan *et al*. who showed that balanced 8 cell colonies had higher levels of global translation. My work has further shown that alongside an increase in translation, balanced colonies have an increase in global transcription, as assessed using an EU-based assay. This increase in anabolic processes in the balanced mode dynamics might be associated with cell differentiation, as previously demonstrated in mouse embryoid bodies derived from mouse ES cells (Sampath *et al.*, 2008). Moreover, this hypothesis can be supported by the observed increase in translation in differentiating keratinocytes localised in the suprabasal layer of stained epithelial samples from human donors (Figure 4.9 and Figure 4.10).

When evaluating balanced and expanding colonies, the main concern is that we are comparing heterogeneous and homogenous populations. Balanced colonies contain dividing and differentiating cells, whereas expanding colonies are composed purely of proliferating cells. Thus, it was crucial to investigate whether dividing cells, present in both modes, differ between the two colony types. I have observed significant differences in transcription and translation levels for proliferative cells coming from expanding and balanced colonies (Figure 4.1E, Figure 4.2E). This implies that dividing cells of different proliferation modes are innately distinct. This difference may arise from intrinsic factors within the cells, which is supported by the fact that proliferation mode is inherited through generations (Doupe *et al.*, 2010; Klein *et al.*, 2011).

However, in larger colonies, it may be influenced by external factors, such as confluence and interactions with the extracellular matrix (Connelly *et al.*, 2010; Nanba *et al.*, 2013), which is in line with findings presented in Chapter 3, where the density-dependant switch in the proliferation mode is discussed.

So far, I have been focusing on defining the characteristics that differentiate balanced and expanding colonies. Based on the results of staining and sequencing experiments, we cannot unarguably say whether what we observe is a causative agent or just a result of a cell committing to one mode. What it tells us is that increase in translation is a signature of balanced proliferation mode. What it does not address is whether this increase in translation is a result of surge in differentiation or whether it is needed to establish balanced colonies. However, this question is partially answered by the results of the siRNA knock-down experiment (Figure 4.13 and Figure 4.14). When translation was partially inhibited by knocking down expression of eIF4G2, the number of large colonies observed was significantly increased compared to a non-targeting control. Importantly, since the same percentage of colonies survives treatment whether a targeting or a scrambled siRNA is added (Figure 4.11B), the observed shift in colony sizes is unlikely to be caused by selectively killing one kind of colonies but rather by affecting the proliferative fate of targeted colonies. Similar results were observed in a previous study by (Nanba *et al.*, 2013), when keratinocytes were treated with a translation inhibitor, Rapamycin. Following treatment cells could not enter the balanced mode and divided in an exponential manner, suggesting causative relationship. The relationship between the mTOR pathway, which is targeted by Rapamycin, and the cell's proliferative mode will be further investigated in Chapter 5.

It is puzzling why if both eIF3E and eIF4G2 seemed to be accurate markers of cell proliferative mode and differentiation state, knocking down eIF4G2 and not the other factor had a direct effect on colony size distribution and differentiation (Figure 4.14). Of course, even though both factors are involved in initiation of translation, each one plays a distinct role as part of larger processes, with eIF4G2 being mainly involved in cap recognition, and eIF3E playing a role in ribosomal assembly and mRNA activation (Klann and Dever, 2004). Alternatively, it is possible that the difference in the level of protein knockdown observed between eIF3E and eIF4G2 may be a reason for this result.

One way of looking at what exactly happens when each of the factors is knocked-down would be performing an RNA-seq or Ribosome profiling experiment (Ribo-Seq). This may provide evidence for the importance of the two eIFs in different pathways, as it would allow as study the change in expression profile following knockdown. Ribo-seq would give as more information, as this technique makes it possible to isolate and sequence the RNA molecules that are being processed by the ribosome in order to monitor the translation process. In case of my project, it would tell me whether knocking down eIF3E and eIF4G2 affects translation at a global scale or whether specific transcripts are selectively not translated. Moreover, it could help me to answer the question why knocking down eIF4G2 seems to affect progenitor fate while knocking down eIF3E does not.

Overall, the work presented in this chapter has focused on the role of two specific Eukaryotic translation initiation factors in switching between balanced and expanding modes of proliferation, which *in vivo* would most likely correspond to the switch between tissue maintenance and tissue repair processes. However, since my RNA-seq analysis, as well as studies performed by other groups (Liakath-Ali *et al.*, 2018; Walko *et al.*, 2017), have shown that differences between different modes of division in human keratinocytes are not limited to a single pathway or process, I would next like to focus on more global processes. Therefore, in the next chapter I will look in more detail at the role of global translation and lipid biosynthesis in progenitor fate determination, as both processes have been highlighted by the RNA-seq.

Chapter 5 Increase in lipid biosynthesis is a hallmark of keratinocyte differentiation

5.1. Chapter overview

Being the outermost layer of human skin, epidermis constitutes the main barrier between the body and the outside environment. It is therefore crucial that this barrier is sufficient to prevent invasion by pathogens and water loss, which is especially important given that humans live in a highly variable, terrestrial environment. The protective functions of the skin are ensured to a great extent by a formation of a water impermeable lipid layer, which is formed by differentiating keratinocytes(Akiyama *et al.*, 2008). Thus increase in lipid biosynthesis has for a long time been considered as one of the factors involved in keratinocyte differentiation (Ponec *et al.*, 1987).

In line with that, it was also not surprising that my RNA-seq analysis described earlier in this thesis has showed a significant increase in transcripts associated with lipid biosynthesis in day 7 samples when compared to day 5 ones. Nevertheless, I wanted to see if this increase is indeed just a consequence of increase in keratinocyte differentiation, or rather an important prerequisite for the establishment of balanced fate.

In this chapter I will first show that the increase in lipid biosynthesis, suggested by the results of RNA-seq analysis, is resulting in enrichment in neutral lipids in day 7 cultures. Next, I will describe the effects of inhibition of cholesterol biosynthesis using both, a pharmaceutical and a RNAi approach. Finally, I will look more globally at the control of lipid biosynthesis, and will assess the effects of mTOR signalling inhibition, which is also involved in the control of this process (Laplante and Sabatini, 2009), on the proliferative capacity of cultured keratinocytes.

5.2. Levels of neutral lipids are increased in mature keratinocyte cultures

The RNA-seq analysis discussed in Chapter 3 has indicated that there is an increase in the level of transcripts associated with lipid biosynthesis in cultures collected at day 7 compared to day 5 samples. Since the transcriptomic analysis was performed on bulk cultures, which contain a mixture of differentiated and proliferative cells, the observed trend, if real, could have two possible explanations. Namely, it could either mean that balanced mode cells exhibit higher levels of lipid biosynthesis or that there is more lipids synthesised in the differentiated keratinocytes, which are more prevalent in day 7 cultures. Based on previous studies of keratinocyte differentiation, which strongly indicate that increase in lipid synthesis and incorporation is a requirement for efficient keratinocyte differentiation *in vitro* (Ponec *et al.*, 1987; Bikle *et al.*, 2010) and *in vivo* (Tan *et al.*, 2018; Schweiger *et al.*, 2009), the latter explanation seems more likely.

A staining experiment was performed in order to visually assess if the observed increase in lipid biosynthesis associated transcripts in day 7 cultures is directly translated into a higher level of lipid biosynthesis and incorporation in these cells (Figure 5.1). Keratinocyte colonies fixed at days 5 and 7 post seeding (Figure 5.1A) were labelled with a neutral lipid dye, BODIPY 493/503, which allows detection of neutral lipid droplets, including triglycerides and cholesterol esters (Qiu and Simon, 2016). Phalloidin was used to visualise cell shapes and to allow the assessment of the localisation of the neutral lipid inclusions. The experiment was repeated 3 times, and a total of 60 colonies were assessed per time point. There was no BODIPY signal detected in any of the assessed day 5 colonies (Figure 5.1B). Interestingly, in day 7 cultures, multiple neutral lipid inclusions were detected, showing as bright green granules localised in a close vicinity to the nuclei (Figure 5.1C).

These results indicate that colonies containing a larger proportion of differentiating cells (day 7 cultures) exhibit stronger BODIPY staining and therefore may contain larger amounts of neutral lipids. These neutral lipids may include cholesterol and may therefore be in line with the RNA-seq analysis which has indicated that the transcripts associated with biosynthesis pathway of these particular lipids were significantly up regulated in day 7 cultures (Chapter 3). Together, this may suggest that the increase in neutral lipid biosynthesis may be required for the effective keratinocyte differentiation and potentially may be involved in the establishment of the balanced mode of proliferation.

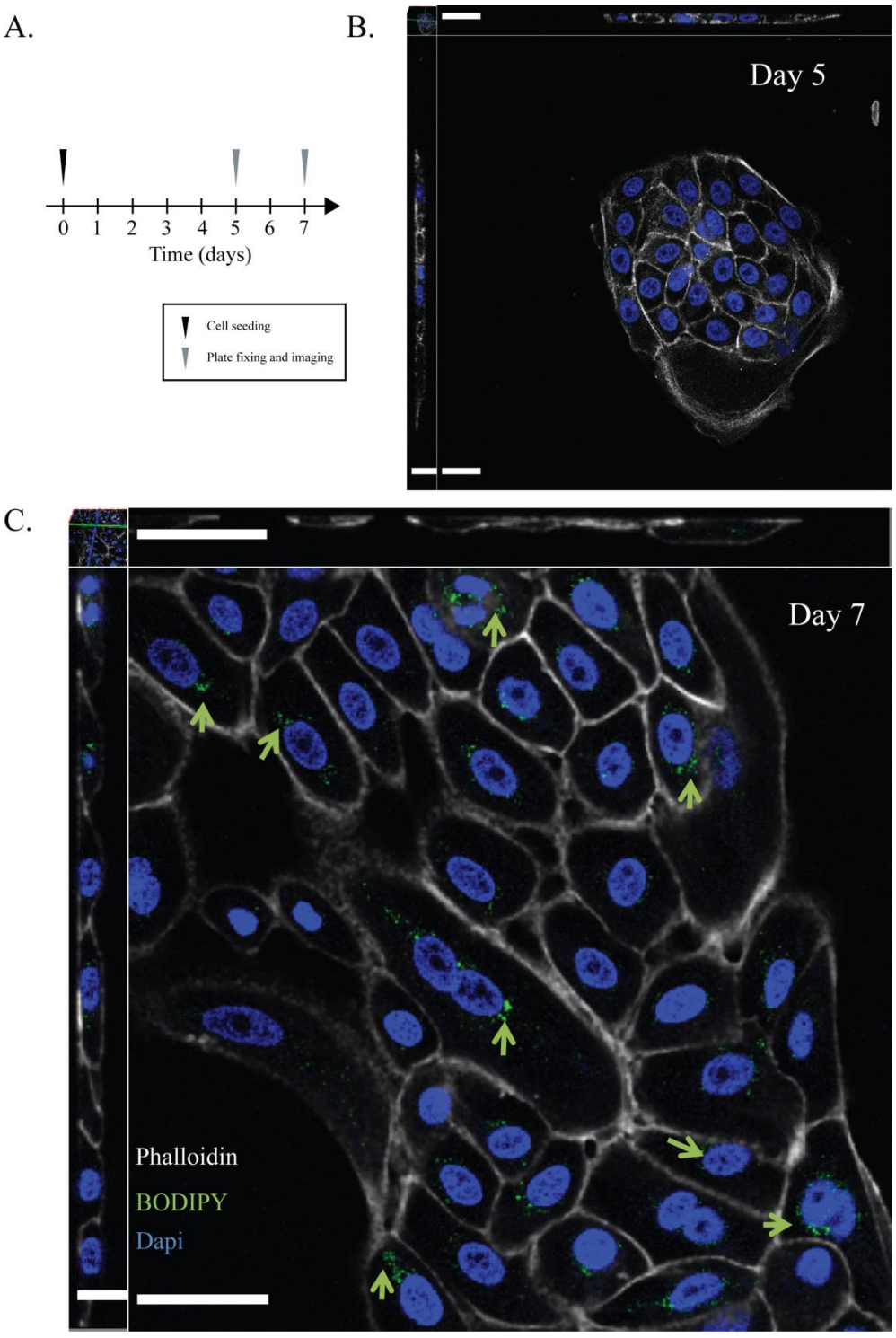

Figure 5.1. Neutral lipid staining of day 5 and day 7 cultures. **A**: Experimental outline. **B**: Representative image of a colony fixed at day 5 post seeding. **C**: Representative image of a colony fixed at day 7 post seeding. Cultures were labelled with Phalloidin (white), BODIPY (green) and Dapi (blue). Scale bars represent 50 µm (x, y axis) and 30 µm (z axis).Green arrows indicate areas with high levels of neutral lipid staining. Experiment was performed in 3 replicates. Each time, 20 colonies were assessed per time point.

5.3. Sterol biosynthesis is unlikely to be involved in keratinocyte cell fate determination

As previously discussed, the RNA-seq analysis has indicated that multiple lipid biosynthesis associated transcripts were upregulated in day 7 cultures when comparing with the day 5 ones. Transcripts encoding 3-hydroxy-3-methylglutaryl-CoA reductase (HMGCR) were amongst of the most differentially expressed ones (1.1 log2FoldChange, p=6.95E-05). HMGCR is a master regulator of cholesterol synthesis pathway in mammals and is a target of pharmaceuticals aimed at lowering blood cholesterol levels in humans (Allenbach *et al.*, 2014; Jones *et al.*, 1998). I have decided to use one of such inhibitors, namely Lovastatin, to inhibit HMGCR activity in keratinocyte cultures. My hypothesis was that if the spike in cholesterol synthesis is indeed required for the establishment of the balanced mode *in vitro*, the Lovastatin mediated inhibition of HMGCR activity may have an influence on the colonies' proliferative potential. Possibly, it could cause keratinocytes to divide in an expanding manner by inhibiting the switch towards the balanced mode.

To test this hypothesis, keratinocyte cultures were treated with varying concentrations of Lovastatin between day 4 and day 7 post seeding. The dose range is based on studies of Lovastatin treatment effects on cultured human keratinocytes (Kim *et al.*, 2011; Lu *et al.*, 2015). Experiment was repeated three times with two wells per each drug concentration used. Following the treatment the cultures were washed to remove the feeders and imaged using IncuCyte (Figure 5.2A). To assess the cytotoxicity of Lovastatin I have quantified the number of colonies per well at the end of the treatment using IncuCyte image analysis software (Figure 5.2B). In this analysis, I have observed no significant difference in the number of colonies surviving the treatment with up to 80 µM Lovastatin (2-way ANOVA test). Next, I looked at the proportion of the well area occupied by cells at the end of the treatment (percentage confluence, Figure 5.2C) and average colony areas post treatment (Figure 5.2D). Both colony area and percentage confluence decreased with increasing drug concentrations. This decrease could be explained by either colonies becoming more compact, with individual cells taking up less area, or because on average there are less cells per colony. The visual assessment of images used for IncuCyte analysis seems to disprove the first possibility as colony density remained the same between different experimental conditions (Figure 5.2E).

Taken together, this data indicates that Lovastatin treatment alone is insufficient to prevent switch of colony proliferative mode towards balanced. However, these results alone do not disprove the importance of cholesterol synthesis in keratinocyte differentiation.

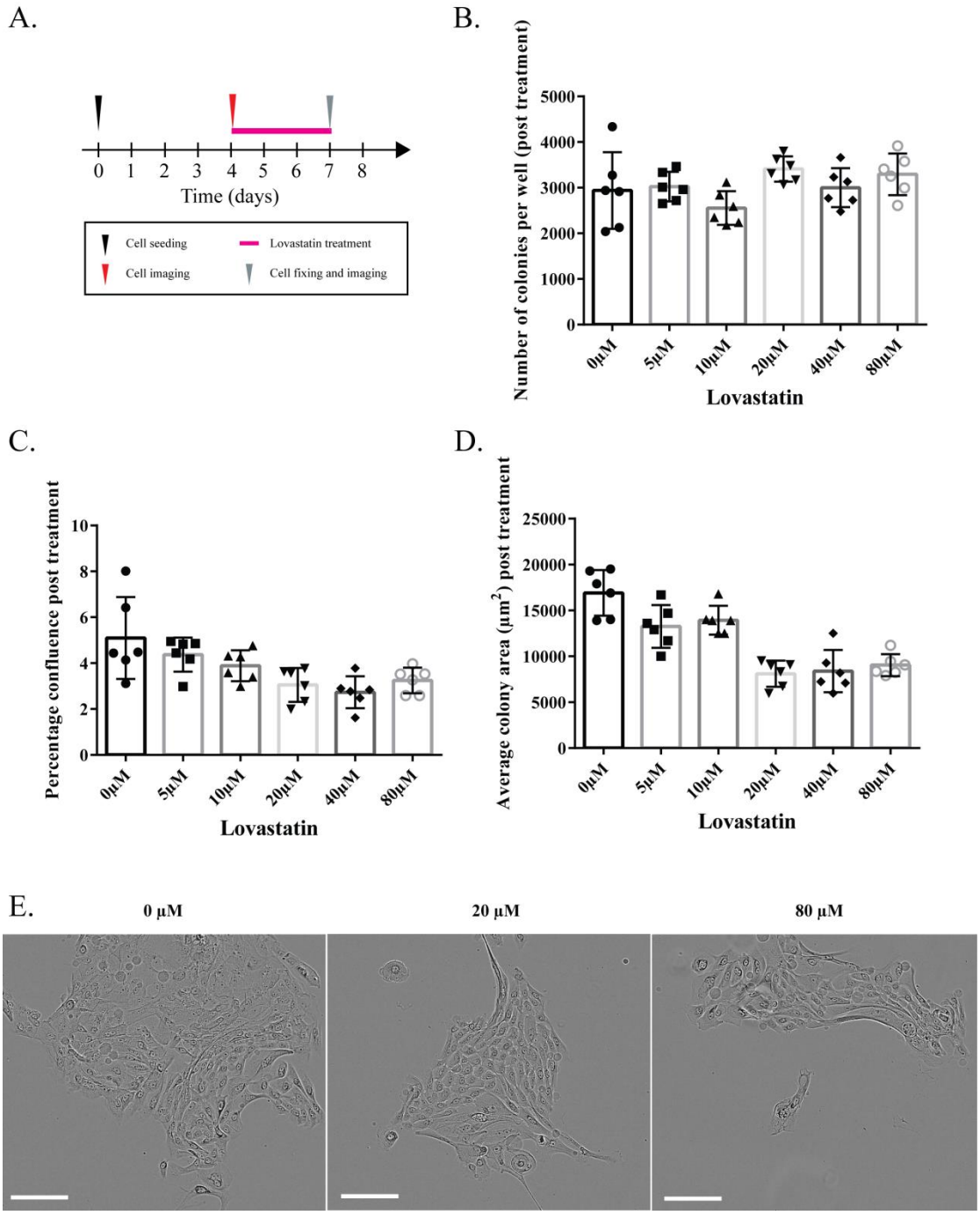

Figure 5.2. Lovastatin treatment of keratinocyte cultures. **A**: Experimental outline. **B**: Number of colonies per well surviving the Lovastatin treatment at varying drug concentrations. **C**: Percentage confluence of day 7 wells. **D**: Average colony area at day 7. Cultures treated with between 20 µM and 80 µM of Lovastatin show a statistically significant decrease in average colony area compared to lower doses (2-way ANOVA test). **E**: Representative images of cultures at varying drug concentrations (0 µM, 20 µM and 80 µM) captured at day 7. Scale bars represent 80 µm.

To further investigate if cholesterol levels have a direct impact on the colonies' proliferative mode, I decided to evaluate additional lipid biosynthesis associated transcripts in day 5 and day 7 RNA-seq data. Sterol regulatory element-binding protein 1 (SREBP1) s associated with cholesterol metabolism and SREBP1 encoding transcripts were also differentially expressed between day 7 and day 5 samples (1.0 log2FoldChange, p=1.1E-03). The protein is a transcription factor involved in the control of expression of sterol biosynthesis genes (Brown and Goldstein, 1997).

To evaluate the impact of SREBP1 signalling on keratinocyte growth in culture, I have tested two different siRNAs. The experimental procedure was similar to the one used in the RNAi knock-downs of eIF3E and eIF4G2 described in Chapter 4 (Figure 5.3A) and the experiments were repeated three times. An effective knock down at RNA level of 50 - 90% was observed for the two targeting siRNAs used at both 48 h (Figure 5.3B) and 72 h (Figure 5.3C) as compared to a scrambled siRNA control. Total protein sample was extracted from the cultures at 72 h post siRNA treatment (Figure 5.4A). A capillary based immunoassay has revealed a decrease in SREBP1 levels for both targeting siRNAs used as compared to a scrambled siRNA control, across all three replicates of the experiment (Figure 5.4B and C).

Having established that a successful SREBP1 knock down at both RNA and protein level was achieved, I wanted to investigate the impact of SREBP1 downregulation on keratinocyte growth and proliferative potential. Keratinocytes were grown for 5 days following addition of siRNAs before being imaged on an IncuCyte (Figure 5.5A). First, the number of colonies surviving treatment was assessed for both targeting siRNAs and a scrambled control (Figure 5.5B). No significant differences in colony survival were observed between the experimental conditions (2-way ANOVA). Next, the percentage confluence and the average colony area were assessed (Figure 5.5C and D), and again no significant differences were detected (2-way ANOVA). This suggests that in this experimental setup, disturbance of SREBP1 has no observable effect on keratinocyte growth potential.

Taken together, the results from the Lovastatin treatment experiment and the SREBP1 knock-down, suggest that the increase in sterol biosynthesis indicated by the RNA-seq data may not be directly involved in the control of keratinocyte proliferation, whereas it is still possible that it is needed for keratinocyte differentiation. Moreover, these results do not disprove the involvement of other lipid biosynthesis pathways in the keratinocyte cell fate determination.

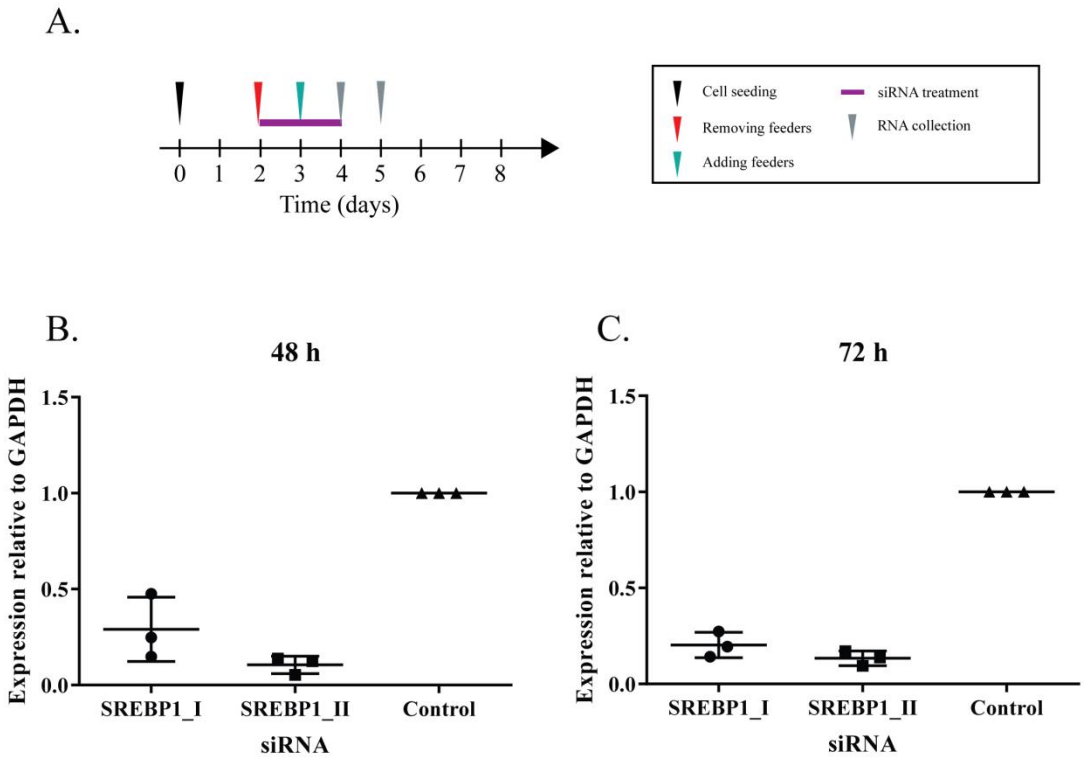

Figure 5.3. Efficiency of the SREBP1 knock-down at the RNA level. **A**: Experimental outline. **B**: SREBP1 expression relative to GAPDH at 48 h after addition of siRNAs. **C**: SREBP1 expression relative to GAPDH at 72 h after addition of siRNAs. Experiments were repeated 3 times.

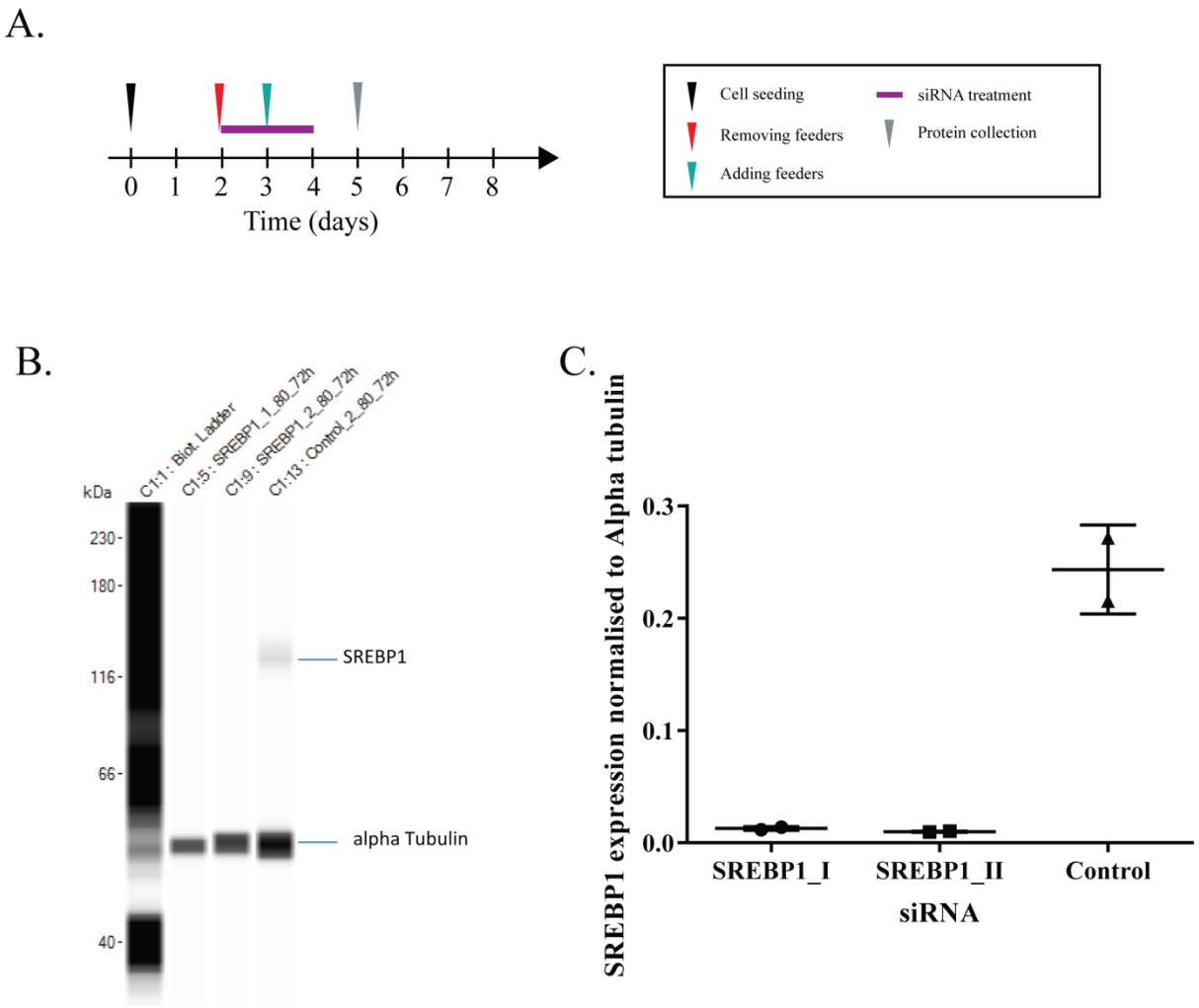

Figure 5.4. Efficiency of the SREBP1 knock-down at the protein level. **A**: Experimental outline. **B**: Visual representation of the capillary-based immunoassay results for a single replicate of the SREBP1 knock-down experiment. **C**: SREBP1 protein levels relative to alpha-Tubulin at 72 h after addition of siRNAs. Experiments were repeated 3 times.

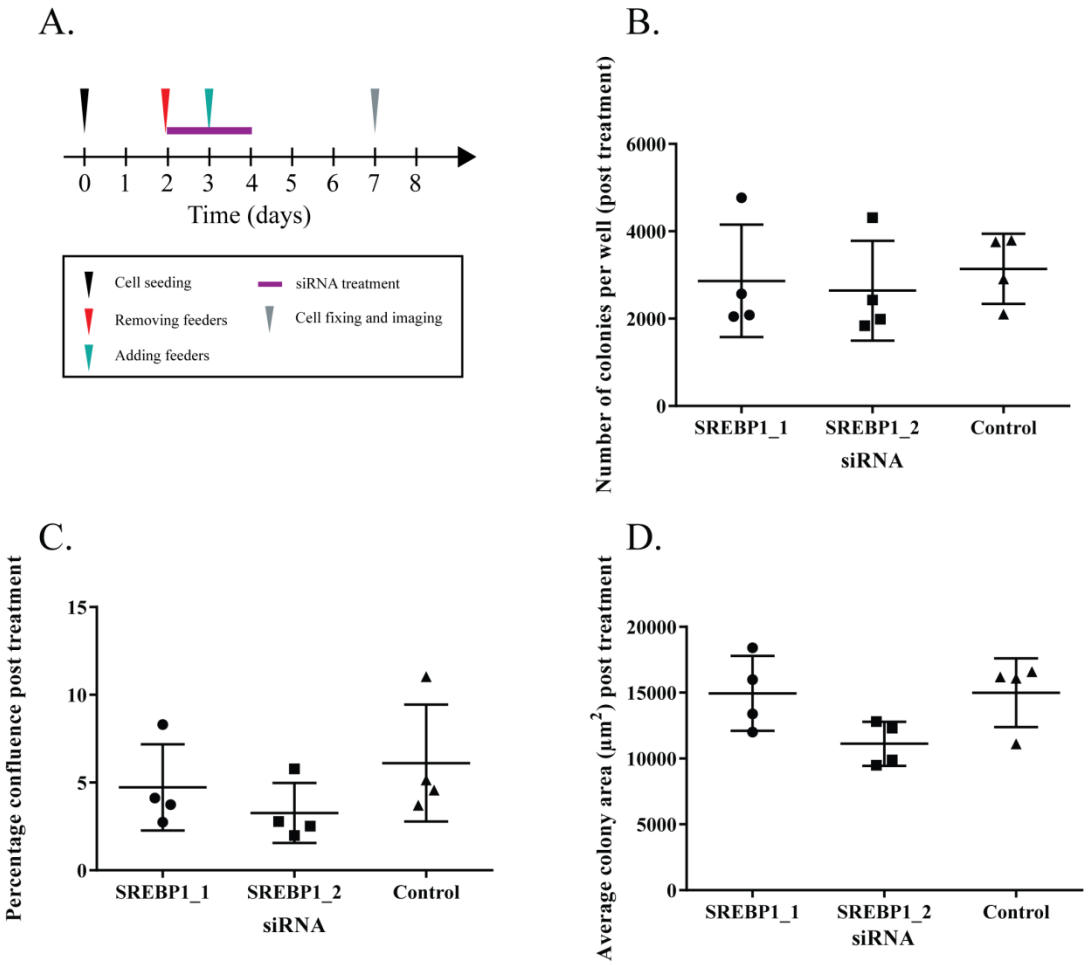

Figure 5.5. Colony phenotype following SREBP1 knock-down. **A**: Experimental outline. **B**: Number of colonies per well surviving the siRNA treatment. **C**: Percentage confluence of day 7 wells. **D**: Average colony area at day 7. Experiments were repeated 4 times.

5.4. Inhibition of mTOR signalling is not sufficient to change progenitor fate

Results presented in section 5.3 of this Chapter indicate that sterol biosynthesis may not be directly involved in the establishment of balanced mode colonies. This was demonstrated by inhibition of two key sterol biosynthesis pathway regulators, HMGCR and SREBP1. Transcripts associated with the mTOR signalling pathway, acting upstream of these two sterol biosynthesis regulators, were also observed to be unregulated in the RNA-seq dataset comparing day 7 and day 5 keratinocyte cultures. Interestingly, in addition to being involved in the control of sterol synthesis, mTOR is also involved in the control of the translation process (Figure 5.6) (Shao, Evers and Sheng, 2004; Roux *et al.*, 2007; Laplante and Sabatini, 2009). My previous experiments have indicated that silencing of a translation initiation factor eIF4G2 may have an effect on the keratinocyte proliferation mode. Unlike in cells where sterol biosynthesis was inhibited, silencing of eIF4G2 resulted in a shift of colony size distribution towards larger colonies. When considered together with the RNA-seq results, this suggests that it is relevant to investigate the effects of mTOR signalling on the keratinocyte proliferative mode.

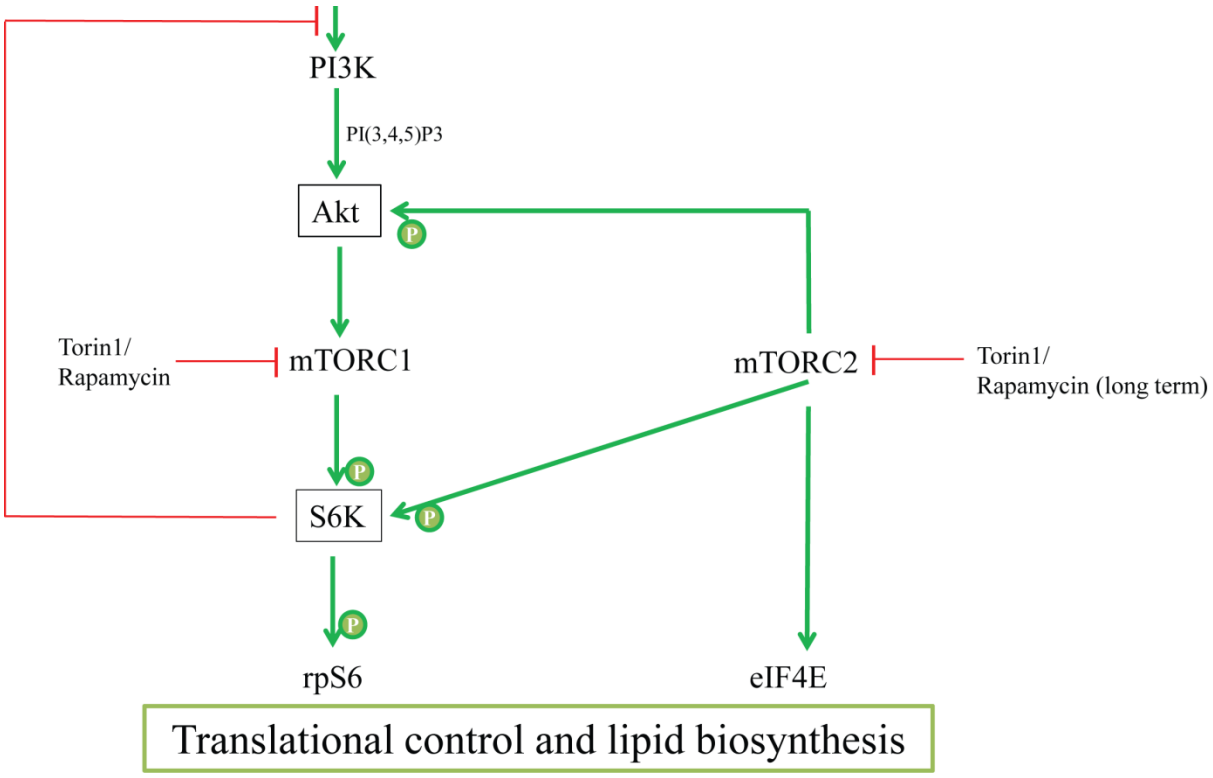

Figure 5.6. mTOR signalling pathway. Events of phosphorylation are indicated by green arrows. Inhibition is indicated by red lines.

The main regulator in the mTOR signalling pathway is protein mTOR which acts as part of two complexes, mTOR Complex 1 (mTORC1) and mTOR Complex 2 (mTORC2). Both complexes exert their activity by phosphorylating downstream regulators, S6K and Akt in case of mTORC2 and S6K alone in case of mTORC1. In addition to that, phosphorylated Akt may further activate mTORC1 (Mayer and Grummt, 2006). Together, these phosphorylation cascades influence multiple downstream processes including sterol biosynthesis and translational control (Roux *et al.*, 2007; Laplante and Sabatini, 2009). In order to investigate the effect of mTOR signalling on the proliferative mode of keratinocytes, I have decided to target both mTORC1 and mTORC2 activities. This can be achieved by the use of two mTOR inhibitors: Rapamycin and Torin1. Specifically, while Torin1 inhibits both, mTORC1 and mTORC2, Rapamacin acts predominantly on mTORC1, and its effect on the second complex is only observed upon longer treatment (Jankiewicz, Groner and Desrivieres, 2006).

Previously published reports (Nanba *et al.*, 2013) have used Rapamycin to stimulate keratinocyte growth *in vitro.* I therefore decided to use protocols developed by Nanba et al., in my work. Specifically, I supplemented keratinocyte growth medium with 80 nM Rapamycin between day 4 and day 7 post seeding (

Figure 5.7A). At day 7, I imaged the cells and collected protein samples. Capillary electrophoresis immunoassay analysis showed that the protein samples from day 7 cultures treated with Rapamycin contained on average 15% less phosphorylated Akt and 46% less phosphorylated S6K than the control samples, indicating inhibition of mTORC1, and partial inhibition of mTORC2 (

Figure 5.7B and C). The keratinocyte culture imaging performed using IncuCyte has focused on the analysis of well confluence (

Figure 5.7D) and average colony area (

Figure 5.7E). The confluence measurements for control and Rapamycin treated cultures did not show any statistically significant difference (2-tailed Mann Whitney), indicating lack of Rapamycin associated cytotoxicity and suggesting no impact on keratinocyte proliferation. In line with that, the average colony area also did not change in Rapamycin treated cultures when compared with the control ones (2-tailed Mann Whitney) suggesting that the drug may have no effect on keratinocyte colony expansion in the experimental setup proposed by me.

Since I was unable to observe a proliferative phenotype following a treatment with Rapamycin, I decided to use Torin1, which is a more potent inhibitor of both mTOR complexes (Liu *et al.*, 2012). Again, keratinocyte cultures were treated between day 4 and 7 post seeding. A final concentration of 40 nM of Torin1 was used. At the end of the treatment, cultures were imaged using IncuCyte and protein was collected for analysis (Figure 5.8A). A capillary based immunoassay performed on protein lysates collected at the end of the treatment showed an average reduction of 28% in the level of phosphorylated Akt (Figure 5.8B) and 73% reduction in the level of phosphorylated S6K (Figure 5.8C), indicating a more effective inhibition of both mTORC1 and mTORC2. Next, I performed an IncuCyte supported analysis of images acquired at the end of the treatment. Across all 3 replicates of the experiment, there is no significant difference in the percentage confluence of cultures treated with Torin1 and the untreated controls (2-tailed Mann Whitney, Figure 5.8D). There was also no significant difference in the average colony area between the experimental and control cultures (2-tailed Mann Whitney, Figure 5.8E).

Taken together, these observations indicate that inhibition of mTOR signalling is unlikely to have an effect on the establishment of the balanced mode of proliferation. Application of both Rapamycin and Torin1 did result in downregulation of Akt and S6K phosphorylation suggesting successful downregulation of mTOR mediated signalling. However, the lack of observable phenotype in the cell growth and colony behaviour indicates that either the achieved level of inhibition was insufficient to exert an effect or that inhibition of mTOR signalling alone cannot prevent the switch between expanding and balanced modes of keratinocyte proliferation.

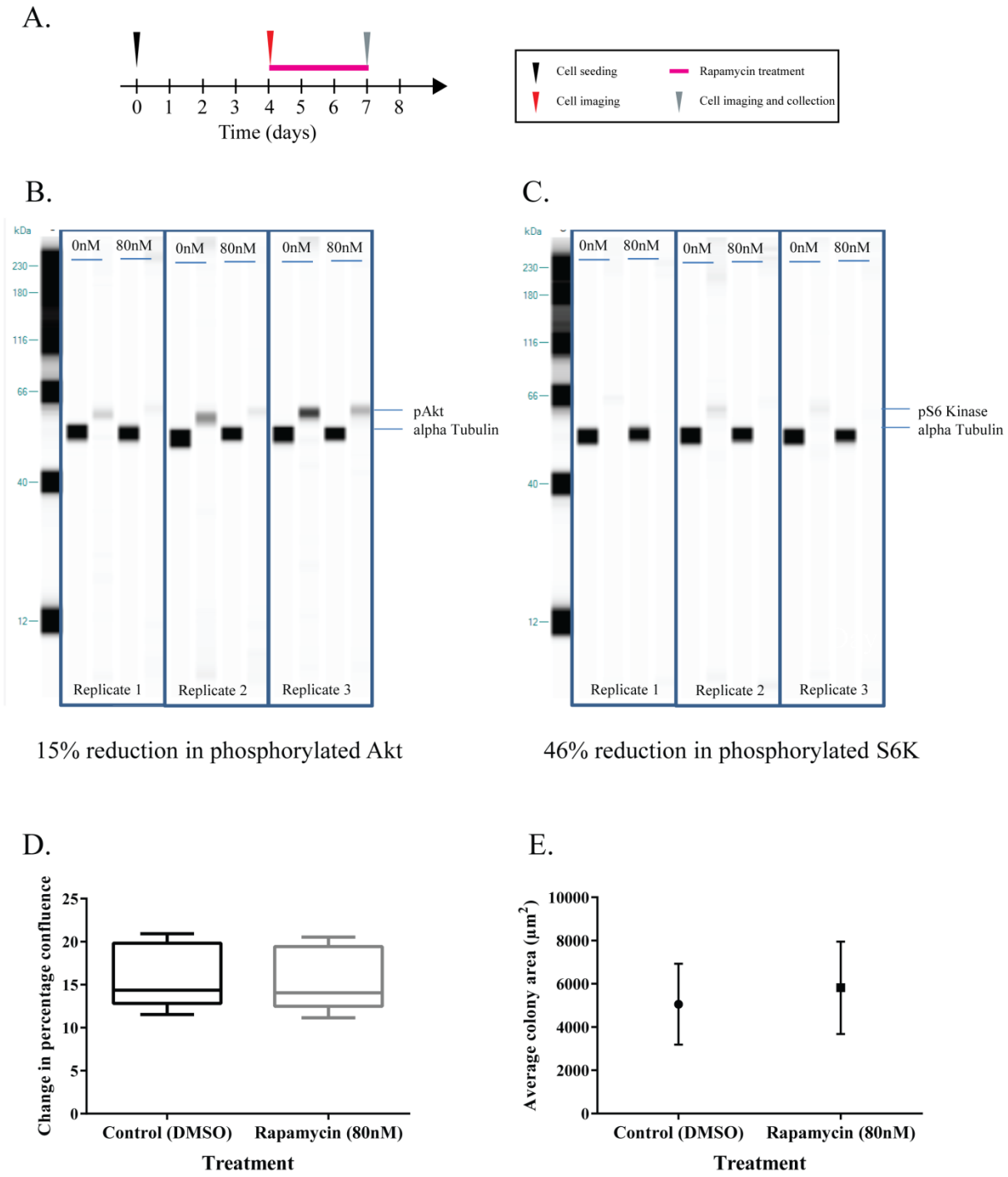

Figure 5.7. Rapamycin treatment.**A**: Experimental outline. **B**: Visual representation of the capillary-based immunoassay results for three replicates of Rapamycim mediated down-regulation of pAkt levels. **C**: Visual representation of the capillary-based immunoassay results for three replicates of Rapamycim mediated down-regulation of pS6K levels. **D**: Percentage confluence of day 7 wells treated with either Rapamycin or the DMSO control. **E:** Average colony area at day 7 for Rapamycin and DMSO treated cells. Experiments were repeated three times.

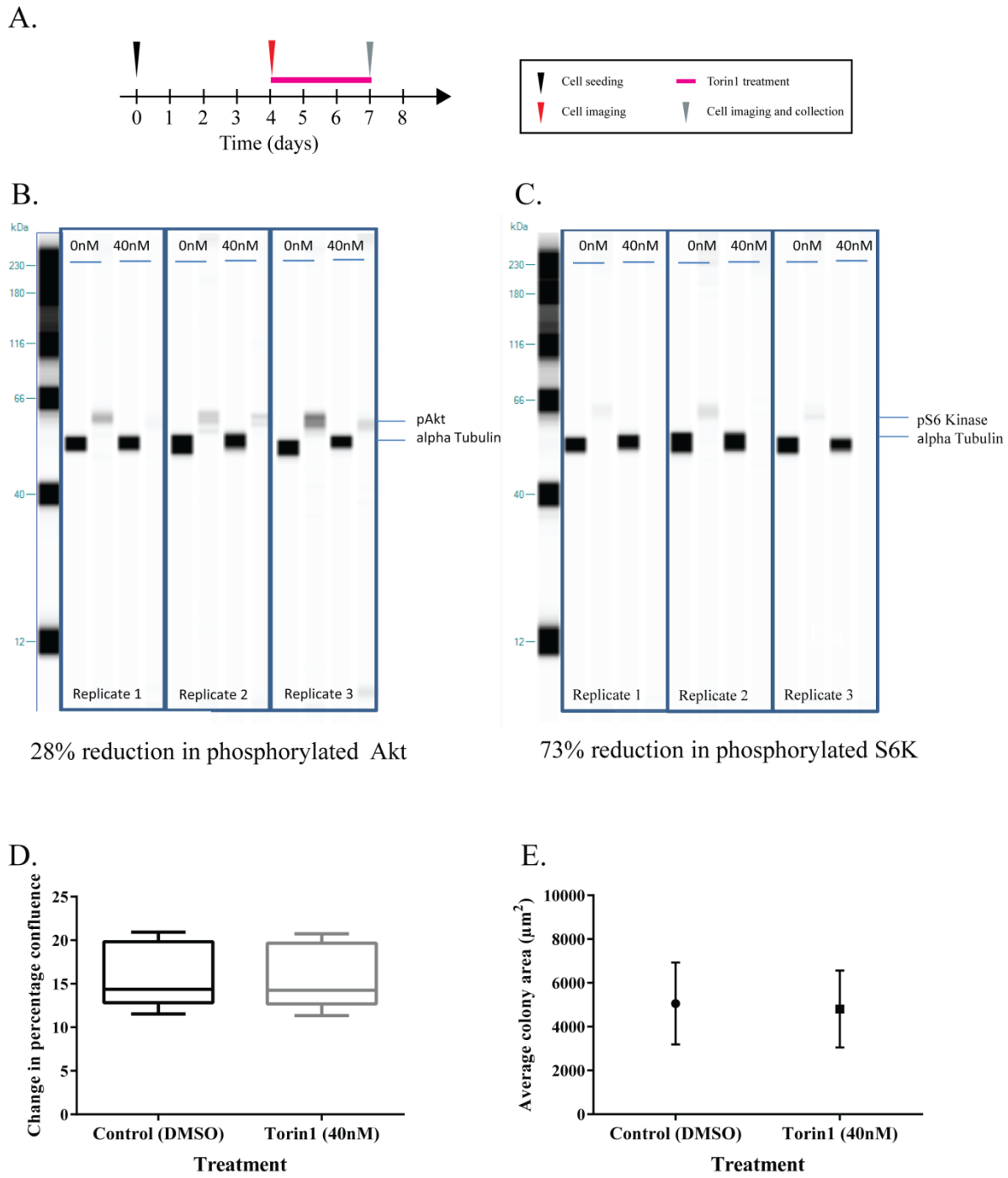

Figure 5.8. Torin1 treatment.**A**: Experimental outline. **B**: Visual representation of the capillary-based immunoassay results for three replicates of Torin1 mediated down-regulation of pAkt levels. **C**: Visual representation of the capillary-based immunoassay results for three replicates of Torin1 mediated down-regulation of pS6K levels. **D**: Percentage confluence of day 7 wells treated with either Torin1 or the DMSO control. **E:** Average colony area at day 7 for Torin1 and DMSO treated cells. Experiments were repeated three times.

5.5. Discussion

The experiments described in this chapter were initially based on the results of the RNA-seq analysis, which showed a clear upregulation of expression of transcripts associated with sterol biosynthesis in day 7 cultures compared to day 5 samples. Based on that, I speculated that this transcriptional change is resulting in an increase in lipid biosynthesis in keratinocyte cultures following the switch towards the balanced mode of proliferation. Indeed, results presented at the start of this chapter do indicate that neutral lipids accumulate to a greater extent in day 7 keratinocyte cultures when compared to day 5 ones.

My work is not the first to observe this increase in lipid accumulation in developing keratinocyte cultures. Early reports indicated that ichtyosis, a rare condition where patients develop thickened, scaly skin, is strongly linked to disruption of neutral lipid storage (Rozenszajn *et al.*, 1966). In line with that, accumulation of neutral lipids was also demonstrated to be a hallmark of keratinocyte differentiation *in vitro* (Williams *et al.*, 1988). More recent work has identified that mutations in comparative gene identification-58 (CGI-58) are common in patients with ichtyosis (Lefevre *et al.*, 2001). Interestingly, expression of CGI-58 lipase is significantly upregulated in developing keratinocytes and it was speculated that the enzyme might be involved in processing of some of the lipids accumulating in differentiating keratinocytes to nuclear hormone receptors (Akiyama *et al.*, 2008). This signalling may be important for transcriptional reprograming needed for keratinocyte differentiation.

Such hypothesis is not necessarily inconsistent with the maintenance of keratinocyte colony growth kinetics observed by me upon Lovastatin treatment and SREBP1 knock-down. It is plausible that other factors, including global upregulation in translation, may be required for the change in the proliferative mode of keratinocytes towards balanced state, while cholesterol biosynthesis may be a downstream process involved in the control of keratinocyte differentiation. Thus, results presented in this chapter may indicate that the process in which keratinocytes change their proliferative mode may be somewhat independent from keratinocyte differentiation. To evaluate this hypothesis further work may be needed to investigate differentiation of keratinocyte cultures upon inhibition of sterol biosynthesis, including repeating the experiments performed by me in delipidised serum media. The approaches developed as part of this chapter are likely to form an excellent platform to undertake such research.

In addition to evaluating the impact of specific inhibition of sterol biosynthesis, this chapter has also focused on the effect of mTOR signalling disruption on the growth of keratinocyte cultures. Again, the decision to target mTOR signalling was made based on the results of the RNA-seq analysis, since the pathway was observed to be upregulated in the day 7 cultures. In line with previous reports, my results indicate that a long treatment with Rapamycin is able, similarly to Torin1 treatment, to partially inhibit the activity of both mTOR complexes (Sarbassov *et al.*, 2006; Nanba *et al.*, 2013). However, unlike in the case of results presented by Nanba et al., my work has not indicated that Rapamycin treatment has an effect on colony growth. Nevertheless, as the main aim of the work performed by Nanba et al. was to investigate the organisation of actin filaments in Rapamycin treated keratinocytes, no replication of the colony growth experiment is presented by the authors. Moreover, the authors did not show the extent of mTOR signalling inhibition upon Rapamycin treatment, so it is difficult to compare my results with their findings (Nanba *et al.*, 2013).

Taken together, the results presented in this chapter indicate that neither inhibition of sterol biosynthesis nor downregulation of the upstream mTOR signalling pathway are likely to have an effect on the switch of keratinocyte proliferation mode from expanding towards balanced, however there is still more work needed to be able to make these findings fully conclusive. Importantly, it remains very likely that these processes are critical for the differentiation of balanced keratinocytes following the switch in the proliferation mode. This indicates that activation of global translation, mediated by proteins such as eIF4G2, may be needed for the switch in the colony growth dynamics while other processes can govern differentiation following completion of the switch process.

Chapter 6 Conclusions and outlook

6.1. Key lessons

In the experiments presented in this doctoral thesis, I have used a combination of cell imaging, RNA sequencing and RNA interference technologies to unravel some of the processes involved in the progenitor fate determination in cultured human keratinocytes.

I started by analysing the transcriptional profiles of cultured keratinocytes with different proliferative potential which allowed me to identify targets for further investigation. Next, I developed ways to distinguish between balanced and expanding mode colonies at an early stage during colony growth using two specific Eukaryotic translation initiation factors, eIF3E and eIF4G2, and a global transcription marker. I also looked at the levels of the identified markers in epithelial samples from human patients, confirming their differential expression between stratifying suprabasal and dividing basal cells, suggesting that my findings could be applied to real-life health and disease models.

Building on the results of the initial experiments, the use of RNA interference allowed me to knock-down eIF3E and eIF4G2 in cultured keratinocytes, leading to an apparent switch in the colony's proliferative potential following the eIF4G2 knock-down. This suggests that while translation initiation or the resulting levels of translation may actually determine the cell fate of human keratinocytes, this relationship is not straight forward. I also evaluated the impact of inhibition of lipid biosynthesis pathways on keratinocyte growth dynamics, using both drugs and RNA interference, which revealed that while increase in lipid synthesis and incorporation is likely to be a hallmark of differentiation, its inhibition alone is not sufficient to change the proliferative mode of treated keratinocytes.

Overall, while these findings bring us closer to understanding the molecular basis of progenitor fate determination, and may give us insight into how epidermal homeostasis is maintained, there are many questions which remain open.

6.2. Open questions and future experiments

The main question which remains unanswered is a one which often troubles biologists. Is what we observe a cause, or rather a consequence of committing to a certain state? Is an increase in translation actually triggering the balanced mode of division? Maybe increase in translation is needed for keratinocyte differentiation and there are simply more differentiated cells in the balanced mode colonies? Although I am unable to give a definite answer to these questions, there are some clues which suggest that the level of translation is actually involved in cell fate determination. Firstly, several studies discussed in this thesis have highlighted the importance of the level of translation in keratinocyte cell fate determination. My study being no different, with both RNA-seq analysis and immunochemistry experiments revealing significant differences in the levels of translation associated transcripts and proteins in balanced and expanding mode colonies. Secondly, and probably most importantly, a closer look at individual cells revealed that there are significant differences in the levels of both eIF3E and eIF4G2 between dividing cells coming from colonies with different proliferative potential. Finally, knock-down of eIF4G2 actually pushed keratinocyte cultures towards producing larger colonies, which strongly suggests that this translation initiation factor is not only required for keratinocyte differentiation, but most likely also involved in maintaining the balanced mode of division. To try and further investigate what is the real role of translation in progenitor fate determination, there are several experiments I would like to perform building on data presented in this thesis.

6.2.1. Further characterisation of pre and post-switch cultures

The transcriptional profiling of samples collected before and after the middle colony switch provided invaluable insight into the molecular processes which underlie the expanding and balanced modes of division. Nevertheless, it is difficult to draw any conclusions from transcriptional data alone. On top of the immunnostaining experiments presented in this thesis, I wanted to look more broadly at the phosphoproteomes of balanced and expanding mode cells. With the help of Dr Mathew Garnett, I was able to arrange a phosphoproteomic analysis of day 5 and day 7 keratinocyte cultures at the MD Anderson Cancer Center, University of Texas. The analysis of cell lysates submitted by me will be carried out using Reverse Phase Protein Array (RPPA). This antibody-based technique allows for functional proteomic analysis, as it looks not only at the levels of expressed proteins, but also at their phosphorylation state (Akbani *et al.*, 2014).

Hopefully, results of the phosphoproteomic analysis will further validate the findings of my RNA-seq experiment, and possibly reveal new directions for investigation. Using the RNA interference protocols developed as part of my project, it should be possible to perform a larger functional screen of targets highlighted by both RNA-seq data and the RPPA analysis.

6.2.2. Characterisation of cultures following eIF4G2 knock-down

One of the most striking observations made during my doctoral studies was the apparent switch in colony's proliferative mode following siRNA knock-down of the translation initiation factor eIF4G2. To further investigate what changes are actually happening following this knock down, I was hoping to perform Ribosome profiling (Ribo-seq) of the knock-down and control samples. This technique, also called active mRNA translation sequencing (ARTseq), isolates RNA that is being processed by the ribosome in order to monitor the translation process and should allow me to see if the knock-down performed by me affects translation on the global scale or rather inhibits translation of selected proteins (Ingolia *et al.*, 2009; Wan and Qian, 2014; Arribere *et al.*, 2016)

Despite the great promise offered by the Ribo-seq, so far it has been proving very challenging technically. Since providing an effective barrier is the main function of human epidermis, naturally, keratinocytes are very sturdy and consequently difficult to lyse, even in culture. Therefore, it requires a lot of optimisation to be able to extract the cross-linked RNAs from keratinocyte cultures without destroying the ribosomes, which is key to obtaining reliable active mRNA translation sequencing data. If the technical challenges are not resolved, it might be more feasible to look at the transcriptional profiles of post knock-down samples which I have already collected using RNA-seq.

6.2.3. Single cell transcriptomics

Finally, a limitation to the experiments presented in this thesis is that majority of them analyse bulk populations, containing a mix of dividing and differentiating cells. Single cells RNA sequencing has been already attempted by other laboratories and the results of them only highlighted the striking heterogeneity of keratinocytes, both *in vivo* and in culture (Jensen and Watt, 2006; Joost *et al.*, 2016). Specifically, Jensen and Watt, who looked at FACS-sorted cells coming from mammalian epidermis, were able to identify a single marker of proliferating cells. This variability was further highlighted by Joost et al., who used single cell RNA-seq to identify 25 distinct keratinocyte populations amongst cells coming from a murine hair follicle. Following a long period of optimisation, we should soon be able to perform a single cell RNA sequencing experiment on keratinocytes collected at day 5 and day 7 post seeding.

List of references

Akbani, R., Becker, K. F., Carragher, N., Goldstein, T., de Koning, L., Korf, U., Liotta, L., Mills, G. B., Nishizuka, S. S., Pawlak, M., Petricoin, E. F., Pollard, H. B., Serrels, B. and Zhu, J. C. (2014) 'Realizing the Promise of Reverse Phase Protein Arrays for Clinical, Translational, and Basic Research: A Workshop Report', *Molecular & Cellular Proteomics,* 13(7), pp. 1625-1643.

Akiyama, M., Sakai, K., Takayama, C., Yanagi, T., Yamanaka, Y., McMillan, J. R. and Shimizu, H. (2008) 'CGI-58 Is an alpha/beta-Hydrolase within Lipid Transporting Lamellar Granules of Differentiated Keratinocytes', *American Journal of Pathology,* 173(5), pp. 1349-1360.

Allenbach, Y., Drouot, L., Rigolet, A., Charuel, J. L., Jouen, F., Romero, N. B., Maisonobe, T., Dubourg, O., Behin, A., Laforet, P., Stojkovic, T., Eymard, B., Costedoat-Chalumeau, N., Campana-Salort, E., Tournadre, A., Musset, L., Bader-Meunier, B., Kone-Paut, I., Sibilia, J., Servais, L., Fain, O., Larroche, C., Diot, E., Terrier, B., De Paz, R., Dossier, A., Menard, D., Morati, C., Roux, M., Ferrer, X., Martinet, J., Besnard, S., Bellance, R., Cacoub, P., Arnaud, L., Grosbois, B., Herson, S., Boyer, O., Benveniste, O. and French Myositis, N. (2014) 'Anti-HMGCR Autoantibodies in European Patients With Autoimmune Necrotizing Myopathies Inconstant Exposure to Statin', *Medicine,* 93(3), pp. 150-157.

Amen, N., Mathow, D., Rabionet, M., Sandhoff, R., Langbein, L., Gretz, N., Jaeckel, C., Groene, H.-J. and Jennemann, R. (2013) 'Differentiation of epidermal keratinocytes is dependent on glucosylceramide:ceramide processing', *Human Molecular Genetics,* 22(20), pp. 4164-4179.

Armstrong, B. K. and Kricker, A. (2001) 'The epidemiology of UV induced skin cancer', *Journal of Photochemistry and Photobiology B-Biology,* 63(1-3), pp. 8-18.

Arribere, J. A., Cenik, E. S., Jain, N., Hess, G. T., Lee, C. H., Bassik, M. C. and Fire, A. Z. (2016) 'Translation readthrough mitigation', *Nature,* 534(7609), pp. 719-+.

Artavanis-Tsakonas, S., Rand, M. D. and Lake, R. J. (1999) 'Notch signaling: Cell fate control and signal integration in development', *Science,* 284(5415), pp. 770-776.

Barrandon, Y., Grasset, N., Zaffalon, A., Gorostidi, F., Claudinot, S., Droz-Georget, S. L., Nanba, D. and Rochata, A. (2012) 'Capturing epidermal stemness for regenerative medicine', *Seminars in Cell & Developmental Biology,* 23(8), pp. 937-944.

Barrandon, Y. and Green, H. (1987) '3 CLONAL TYPES OF KERATINOCYTE WITH DIFFERENT CAPACITIES FOR MULTIPLICATION', *Proceedings of the National Academy of Sciences of the United States of America,* 84(8), pp. 2302-2306.

Beekman, C., Janson, A. A., Baghat, A., van Deutekom, J. C. and Datson, N. A. (2018) 'Use of capillary Western immunoassay (Wes) for quantification of dystrophin levels in skeletal muscle of healthy controls and individuals with Becker and Duchenne muscular dystrophy', *Plos One,* 13(4).

Bell, S. P. and Dutta, A. (2002) 'DNA replication in eukaryotic cells', *Annual Review of Biochemistry,* 71, pp. 333-374.

Bessou, P., Perl, E. R. and Schmittr.La (1969) 'RESPONSE OF CUTANEOUS SENSORY UNITS WITH UNMYELINATED FIBERS TO NOXIOUS STIMULI', *Journal of Neurophysiology,* 32(6), pp. 1025-&.

Bikle, D. D., Teichert, A., Arnold, L. A., Uchida, Y., Elias, P. M. and Oda, Y. (2010) 'Differential regulation of epidermal function by VDR coactivators', *Journal of Steroid Biochemistry and Molecular Biology*, 121(1-2), pp. 308-313.
Blanpain, C. and Fuchs, E. (2009) 'Epidermal homeostasis: a balancing act of stem cells in the skin', *Nature Reviews Molecular Cell Biology*, 10(3), pp. 207-U67.
Borowiec, A. S., Delcourt, P., Dewailly, E. and Bidaux, G. (2013) 'Optimal Differentiation of In Vitro Keratinocytes Requires Multifactorial External Control', *Plos One*, 8(10).
Brash, D. E. (2015) 'UV Signature Mutations', *Photochemistry and Photobiology*, 91(1), pp. 15-26.
Brenner, M. and Hearing, V. J. (2008) 'The protective role of melanin against UV damage in human skin', *Photochemistry and Photobiology*, 84(3), pp. 539-549.
Broome, A. M., Ryan, D. and Eckert, R. L. (2003) 'S100 protein subcellular localization during epidermal differentiation and psoriasis', *Journal of Histochemistry & Cytochemistry*, 51(5), pp. 675-685.
Brown, M. S. and Goldstein, J. L. (1997) 'The SREBP pathway: Regulation of cholesterol metabolism by proteolysis of a membrane-bound transcription factor', *Cell*, 89(3), pp. 331-340.
Buck, S. B., Bradford, J., Gee, K. R., Agnew, B. J., Clarke, S. T. and Salic, A. (2008) 'Detection of S-phase cell cycle progression using 5-ethynyl-2 '-deoxyuridine incorporation with click chemistry an alternative to using 5-bromo-2 '-deoxyuridine antibodies', *Biotechniques*, 44(7), pp. 927-929.
Cakir, B. O., Adamson, P. and Cingi, C. (2012) 'Epidemiology and Economic Burden of Non melanoma Skin Cancer', *Facial Plastic Surgery Clinics of North America*, 20(4), pp. 419-+.
Carrel, A. and Montrose, T. B. (1910) 'The culture of adult tissues outside of the organism (First note)', *Comptes Rendus Des Seances De La Societe De Biologie Et De Ses Filiales*, 69, pp. 293-294.
Chon, S.-H., Tannahill, R., Yao, X., Southall, M. D. and Pappas, A. (2015) 'Keratinocyte differentiation and upregulation of ceramide synthesis induced by an oat lipid extract via the activation of PPAR pathways', *Experimental Dermatology*, 24(4), pp. 290-295.
Clayton, E., Doupe, D. P., Klein, A. M., Winton, D. J., Simons, B. D. and Jones, P. H. (2007) 'A single type of progenitor cell maintains normal epidermis', *Nature*, 446(7132), pp. 185-189.
Connelly, J. T., Gautrot, J. E., Trappmann, B., Tan, D. W.-M., Donati, G., Huck, W. T. S. and Watt, F. M. (2010) 'Actin and serum response factor transduce physical cues from the microenvironment to regulate epidermal stem cell fate decisions', *Nature Cell Biology*, 12(7), pp. 711-U177.
Cooke, M. S., Osborne, J. E., Singh, R., Mistry, V., Farmer, P. B., Evans, M. D. and Hutchinson, P. E. (2007) 'Evidence that oxidative stress is a risk factor for the development of squamous cell carcinoma in renal transplant patients', *Free Radical Biology and Medicine*, 43(9), pp. 1328-1334.
Coolen, N. A., Verkerk, M., Relinen, L., Vlig, M., van den Bogaerdt, A. J., Breetveld, M., Gibbs, S., Middelkoop, E. and Ulrich, M. M. W. (2007) 'Culture of keratinocytes for transplantation without the need of feeder layer cells', *Cell Transplantation*, 16(6), pp. 649-661.
Cross, D. A. E., Alessi, D. R., Cohen, P., Andjelkovich, M. and Hemmings, B. A. (1995) 'INHIBITION OF GLYCOGEN-SYNTHASE KINASE-3 BY INSULIN-MEDIATED BY PROTEIN-KINASE-B', *Nature*, 378(6559), pp. 785-789.
Czarnecki, D. (2018) 'Immigration is the most likely reason for the generational change in melanoma incidence in Queensland, Australia', *International Journal of Cancer*, 143(3), pp. 720-721.

D'Orazio, J., Jarrett, S., Amaro-Ortiz, A. and Scott, T. (2013) 'UV Radiation and the Skin', *International Journal of Molecular Sciences*, 14(6), pp. 12222-12248.
Denecker, G., Ovaere, P., Vandenabeele, P. and Declercq, W. (2008) 'Caspase-14 reveals its secrets', *Journal of Cell Biology*, 180(3), pp. 451-458.
DePianto, D. and Coulombe, P. A. (2004) 'Intermediate filaments and tissue repair', *Experimental Cell Research*, 301(1), pp. 68-76.
Diociaiuti, A., Castiglia, D., Naim, M., Condorelli, A. G., Zambruno, G. and El Hachem, M. (2018) 'Autosomal recessive epidermolysis bullosa simplex due to KRT14 mutation: two large Palestinian families and literature review', *Journal of the European Academy of Dermatology and Venereology*, 32(4), pp. E149-E151.
Doupe, D. P., Alcolea, M. P., Roshan, A., Zhang, G., Klein, A. M., Simons, B. D. and Jones, P. H. (2012) 'A Single Progenitor Population Switches Behavior to Maintain and Repair Esophageal Epithelium', *Science*, 337(6098), pp. 1091-1093.
Doupe, D. P. and Jones, P. H. (2012) 'Interfollicular epidermal homeostasis: dicing with differentiation', *Experimental Dermatology*, 21(4), pp. 249-253.
Doupe, D. P., Klein, A. M., Simons, B. D. and Jones, P. H. (2010) 'The Ordered Architecture of Murine Ear Epidermis is Maintained by Progenitor Cells with Random Fate', *Developmental Cell*, 18(2), pp. 317-323.
Dover, R. and Potten, C. S. (1988) 'HETEROGENEITY AND CELL-CYCLE ANALYSES FROM TIME-LAPSE STUDIES OF HUMAN KERATINOCYTES INVITRO', *Journal of Cell Science*, 89, pp. 359-364.
Eckert, R. L., Crish, J. F. and Robinson, N. A. (1997) 'The epidermal keratinocyte as a model for the study of gene regulation and cell differentiation', *Physiological Reviews*, 77(2), pp. 397-424.
Eckert, R. L., Efimova, T., Dashti, S. R., Balasubramanian, S., Deucher, A., Crish, J. F., Sturniolo, M. and Bone, F. (2002) 'Keratinocyte survival, differentiation, and death: Many roads lead to mitogen-activated protein kinase', *Journal of Investigative Dermatology Symposium Proceedings*, 7(1), pp. 36-40.
Eckert, R. L. and Rorke, E. A. (1989) 'MOLECULAR-BIOLOGY OF KERATINOCYTE DIFFERENTIATION', *Environmental Health Perspectives*, 80, pp. 109-116.
Enver, T., Pera, M., Peterson, C. and Andrews, P. W. (2009) 'Stem Cell States, Fates, and the Rules of Attraction', *Cell Stem Cell*, 4(5), pp. 387-397.
Feingold, K. R. (2009) 'The outer frontier: the importance of lipid metabolism in the skin', *Journal of Lipid Research*, 50, pp. S417-S422.
Fischer, H., Buchberger, M., Napirei, M., Tschachler, E. and Eckhart, L. (2017) 'Inactivation of DNase1L2 and DNase2 in keratinocytes suppresses DNA degradation during epidermal cornification and results in constitutive parakeratosis', *Scientific Reports*, 7.
Freinkel, R. K. and Traczyk, T. N. (1985) 'LIPID-COMPOSITION AND ACID HYDROLASE CONTENT OF LAMELLAR GRANULES OF FETAL-RAT EPIDERMIS', *Journal of Investigative Dermatology*, 85(4), pp. 295-298.
Fuchs, E. (2007) 'Scratching the surface of skin development', *Nature*, 445(7130), pp. 834-842.
Furlong, E. E. (2010) 'The Importance of Being Specified: Cell Fate Decisions and Their Role in Cell Biology', *Molecular Biology of the Cell*, 21(22), pp. 3797-3798.
Gandarillas, A. (2000) 'Epidermal differentiation, apoptosis, and senescence: common pathways?', *Experimental Gerontology*, 35(1), pp. 53-62.
Gloster, H. M., Jr. and Neal, K. (2006) 'Skin cancer in skin of color', *Journal of the American Academy of Dermatology*, 55(5), pp. 741-760.
Grant, W. B. (2008) 'Solar ultraviolet irradiance and cancer incidence and mortality', *Sunlight, Vitamin D and Skin Cancer*, 624, pp. 16-30.

Grice, E. A., Kong, H. H., Conlan, S., Deming, C. B., Davis, J., Young, A. C., Bouffard, G. G., Blakesley, R. W., Murray, P. R., Green, E. D., Turner, M. L., Segre, J. A. and Progra, N. C. S. (2009) 'Topographical and Temporal Diversity of the Human Skin Microbiome', *Science*, 324(5931), pp. 1190-1192.
Grice, E. A. and Segre, J. A. (2011) 'The skin microbiome', *Nature Reviews Microbiology*, 9(4), pp. 244-253.
Griffiths, C. E. M. and Barker, J. (2007) 'Psoriasis 1 - Pathogenesis and clinical features of psoriasis', *Lancet*, 370(9583), pp. 263-271.
Guydosh, N. R. and Green, R. (2014) 'Dom34 Rescues Ribosomes in 3 ' Untranslated Regions', *Cell*, 156(5), pp. 950-962.
Hauben, D. J., Baruchin, A. and Mahler, D. (1982) 'ON THE HISTORY OF THE FREE SKIN-GRAFT', *Annals of Plastic Surgery*, 9(3), pp. 242-246.
Hausmann, C., Zoschke, C., Wolff, C., Darvin, M. E., Sochorova, M., Kovacik, A., Wanjiku, B., Schumacher, F., Tigges, J., Kleuser, B., Lademann, J., Fritsche, E., Vavrova, K., Ma, N. and Schafer-Korting, M. (2019) 'Fibroblast origin shapes tissue homeostasis, epidermal differentiation, and drug uptake', *Scientific Reports*, 9.
Hawker, N. P., Pennypacker, S. D., Chang, S. M. and Bikle, D. D. (2007) 'Regulation of human epidermal keratinocyte differentiation by the vitamin D receptor and its coactivators DRIP205, SRC2, and SRC3', *Journal of Investigative Dermatology*, 127(4), pp. 874-880.
Hirsch, T., Rothoeft, T., Teig, N., Bauer, J. W., Pellegrini, G., De Rosa, L., Scaglione, D., Reichelt, J., Klausegger, A., Kneisz, D., Romano, O., Seconetti, A. S., Contin, R., Enzo, E., Jurman, I., Carulli, S., Jacobsen, F., Luecke, T., Lehnhardt, M., Fischer, M., Kueckelhaus, M., Quaglino, D., Morgante, M., Bicciato, S., Bondanza, S. and De Luca, M. (2017) 'Regeneration of the entire human epidermis using transgenic stem cells', *Nature*, 551(7680), pp. 327-+.
Hunziker, T. and Limat, A. (1999) 'Cultured keratinocyte grafts', *Current problems in dermatology*, 27, pp. 57-64.
Huttenhower, C. and Gevers, D. and Knight, R. and Abubucker, S. and Badger, J. H. and Chinwalla, A. T. and Creasy, H. H. and Earl, A. M. and FitzGerald, M. G. and Fulton, R. S. and Giglio, M. G. and Hallsworth-Pepin, K. and Lobos, E. A. and Madupu, R. and Magrini, V. and Martin, J. C. and Mitreva, M. and Muzny, D. M. and Sodergren, E. J. and Versalovic, J. and Wollam, A. M. and Worley, K. C. and Wortman, J. R. and Young, S. K. and Zeng, Q. D. and Aagaard, K. M. and Abolude, O. O. and Allen-Vercoe, E. and Alm, E. J. and Alvarado, L. and Andersen, G. L. and Anderson, S. and Appelbaum, E. and Arachchi, H. M. and Armitage, G. and Arze, C. A. and Ayvaz, T. and Baker, C. C. and Begg, L. and Belachew, T. and Bhonagiri, V. and Bihan, M. and Blaser, M. J. and Bloom, T. and Bonazzi, V. and Brooks, J. P. and Buck, G. A. and Buhay, C. J. and Busam, D. A. and Campbell, J. L. and Canon, S. R. and Cantarel, B. L. and Chain, P. S. G. and Chen, I. M. A. and Chen, L. and Chhibba, S. and Chu, K. and Ciulla, D. M. and Clemente, J. C. and Clifton, S. W. and Conlan, S. and Crabtree, J. and Cutting, M. A. and Davidovics, N. J. and Davis, C. C. and DeSantis, T. Z. and Deal, C. and Delehaunty, K. D. and Dewhirst, F. E. and Deych, E. and Ding, Y. and Dooling, D. J. and Dugan, S. P. and Dunne, W. M. and Durkin, A. S. and Edgar, R. C. and Erlich, R. L. and Farmer, C. N. and Farrell, R. M. and Faust, K. and Feldgarden, M. and Felix, V. M. and Fisher, S. and Fodor, A. A. and Forney, L. J. and Foster, L. and Di Francesco, V. and Friedman, J. and Friedrich, D. C. and Fronick, C. C. and Fulton, L. L. and Gao, H. Y. and Garcia, N. and Giannoukos, G. and Giblin, C. and Giovanni, M. Y. and Goldberg, J. M. and Goll, J. and Gonzalez, A. and Griggs, A. and Gujja, S. and Haake, S. K. and Haas, B. J. and Hamilton, H. A. and Harris, E. L. and Hepburn, T. A. and Herter, B. and Hoffmann, D. E. and Holder, M. E. and Howarth, C. and Huang, K. H. and Huse, S. M. and Izard, J. and Jansson, J. K. and Jiang, H. Y. and Jordan, C. and Joshi, V. and Katancik, J. A.

and Keitel, W. A. and Kelley, S. T. and Kells, C. and King, N. B. and Knights, D. and Kong, H. D. H. and Koren, O. and Koren, S. and Kota, K. C. and Kovar, C. L. and Kyrpides, N. C. and La Rosa, P. S. and Lee, S. L. and Lemon, K. P. and Lennon, N. and Lewis, C. M. and Lewis, L. and Ley, R. E. and Li, K. and Liolios, K. and Liu, B. and Liu, Y. and Lo, C. C. and Lozupone, C. A. and Lunsford, R. D. and Madden, T. and Mahurkar, A. A. and Mannon, P. J. and Mardis, E. R. and Markowitz, V. M. and Mavromatis, K. and McCorrison, J. M. and McDonald, D. and McEwen, J. and McGuire, A. L. and McInnes, P. and Mehta, T. and Mihindukulasuriya, K. A. and Miller, J. R. and Minx, P. J. and Newsham, I. and Nusbaum, C. and O'Laughlin, M. and Orvis, J. and Pagani, I. and Palaniappan, K. and Patel, S. M. and Pearson, M. and Peterson, J. and Podar, M. and Pohl, C. and Pollard, K. S. and Pop, M. and Priest, M. E. and Proctor, L. M. and Qin, X. and Raes, J. and Ravel, J. and Reid, J. G. and Rho, M. and Rhodes, R. and Riehle, K. P. and Rivera, M. C. and Rodriguez-Mueller, B. and Rogers, Y. H. and Ross, M. C. and Russ, C. and Sanka, R. K. and Sankar, P. and Sathirapongsasuti, J. F. and Schloss, J. A. and Schloss, P. D. and Schmidt, T. M. and Scholz, M. and Schriml, L. and Schubert, A. M. and Segata, N. and Segre, J. A. and Shannon, W. D. and Sharp, R. R. and Sharpton, T. J. and Shenoy, N. and Sheth, N. U. and Simone, G. A. and Singh, I. and Smillie, C. S. and Sobel, J. D. and Sommer, D. D. and Spicer, P. and Sutton, G. G. and Sykes, S. M. and Tabbaa, D. G. and Thiagarajan, M. and Tomlinson, C. M. and Torralba, M. and Treangen, T. J. and Truty, R. M. and Vishnivetskaya, T. A. and Walker, J. and Wang, L. and Wang, Z. Y. and Ward, D. V. and Warren, W. and Watson, M. A. and Wellington, C. and Wetterstrand, K. A. and White, J. R. and Wilczek-Boney, K. and Wu, Y. Q. and Wylie, K. M. and Wylie, T. and Yandava, C. and Ye, L. and Ye, Y. Z. and Yooseph, S. and Youmans, B. P. and Zhang, L. and Zhou, Y. J. and Zhu, Y. M. and Zoloth, L. and Zucker, J. D. and Birren, B. W. and Gibbs, R. A. and Highlander, S. K. and Methe, B. A. and Nelson, K. E. and Petrosino, J. F. and Weinstock, G. M. and Wilson, R. K. and White, O. and Human Microbiome Project, C. (2012) 'Structure, function and diversity of the healthy human microbiome', *Nature,* 486(7402), pp. 207-214.

Ingolia, N. T., Ghaemmaghami, S., Newman, J. R. S. and Weissman, J. S. (2009) 'Genome-Wide Analysis in Vivo of Translation with Nucleotide Resolution Using Ribosome Profiling', *Science,* 324(5924), pp. 218-223.

Jablonski, N. G. and Chaplin, G. (2000) 'The evolution of human skin coloration', *Journal of Human Evolution,* 39(1), pp. 57-106.

Jankiewicz, M., Groner, B. and Desrivieres, S. (2006) 'Mammalian target of rapamycin regulates the growth of mammary epithelial cells through the inhibitor of deoxyribonucleic acid binding Id1 and their functional differentiation through Id2', *Molecular Endocrinology,* 20(10), pp. 2369-2381.

Jemal, A., Bray, F., Center, M. M., Ferlay, J., Ward, E. and Forman, D. (2011) 'Global Cancer Statistics', *Ca-a Cancer Journal for Clinicians,* 61(2), pp. 69-90.

Jensen, K. B. and Watt, F. M. (2006) 'Single-cell expression profiling of human epidermal stem and transit-amplifying cells: Lrig1 is a regulator of stem cell quiescence', *Proceedings of the National Academy of Sciences of the United States of America,* 103(32), pp. 11958-11963.

Jones, P., Kafonek, S., Laurora, I., Hunninghake, D. and Investigators, C. (1998) 'Comparative dose efficacy study of Atorvastatin versus Simvastatin, Pravastatin, Lovastatin, and Fluvastatin in patients with hypercholesterolemia (The CURVES study)', *American Journal of Cardiology,* 81(5), pp. 582-587.

Joost, S., Zeisel, A., Jacob, T., Sun, X. Y., La Manno, G., Lonnerberg, P., Linnarsson, S. and Kasper, M. (2016) 'Single-Cell Transcriptomics Reveals that Differentiation and Spatial Signatures Shape Epidermal and Hair Follicle Heterogeneity', *Cell Systems,* 3(3), pp. 221-+.

Jou, P. C., Feldman, R. J. and Tomecki, K. J. (2012) 'UV protection and sunscreens: What to tell patients', *Cleveland Clinic Journal of Medicine*, 79(6), pp. 427-436.
Kanda, T., Sullivan, K. F. and Wahl, G. M. (1998) 'Histone-GFP fusion protein enables sensitive analysis of chromosome dynamics in living mammalian cells', *Current Biology*, 8(7), pp. 377-385.
Kazantseva, A., Goltsov, A., Zinchenko, R., Grigorenko, A. P., Abrukova, A. V., Moliaka, Y. K., Kirillov, A. G., Guo, Z., Lyle, S. and Ginter, E. K. (2006) 'Human hair growth deficiency is linked to a genetic defect in the phospholipase gene LIPH', *Science*, 314(5801), pp. 982-985.
Kim, E. N., Harris, A. G., Bingham, L. J., Yan, W. F., Su, J. C. and Murrell, D. F. (2017) 'A Review of 52 Pedigrees with Epidermolysis Bullosa Simplex Identifying Ten Novel Mutations in KRT5 and KRT14 in Australia', *Acta Dermato-Venereologica*, 97(9), pp. 1114-1119.
Kim, S., Wong, P. and Coulombe, P. A. (2006) 'A keratin cytoskeletal protein regulates protein synthesis and epithelial cell growth', *Nature*, 441(7091), pp. 362-365.
Kim, T. G., Byamba, D., Wu, W. H. and Lee, M. G. (2011) 'Statins inhibit chemotactic interaction between CCL20 and CCR6 in vitro: possible relevance to psoriasis treatment', *Experimental Dermatology*, 20(10), pp. 855-857.
Kirkwood, T. B. L. 1979. Geometric means and measures of dispersion. Biometrics.
Kitano, Y., Nagase, N., Okada, N. and Okano, M. (1983) 'Cinemicrographic study of cell proliferation pattern and interdivision times of human keratinocytes in primary culture', *Current problems in dermatology*, 11, pp. 97-108.
Klann, E. and Dever, T. E. (2004) 'Biochemical mechanisms for translational regulation in synaptic plasticity', *Nature Reviews Neuroscience*, 5(12), pp. 931-942.
Klein, A. M., Brash, D. E., Jones, P. H. and Simons, B. D. (2010) 'Stochastic fate of p53-mutant epidermal progenitor cells is tilted toward proliferation by UV B during preneoplasia', *Proceedings of the National Academy of Sciences of the United States of America*, 107(1), pp. 270-275.
Klein, A. M., Nikolaidou-Neokosmidou, V., Doupe, D. P., Jones, P. H. and Simons, B. D. (2011) 'Patterning as a signature of human epidermal stem cell regulation', *Journal of the Royal Society Interface*, 8(65), pp. 1815-1824.
Kocher, T., Peking, P., Klausegger, A., Murauer, E. M., Hofbauer, J. P., Wally, V., Lettner, T., Hainzl, S., Ablinger, M., Bauer, J. W., Reichelt, J. and Koller, U. (2017) 'Highly efficient and safe CRISPR/Cas9n double nicking-mediated KRT14 repair in epidermolysis bullosa simplex keratinocytes', *Human Gene Therapy*, 28(12), pp. A57-A57.
Kreibich, K. (1914) 'A culture of adult dermis on a solid medium', *Archiv Fur Dermatologie Und Syphilis*, 120, pp. 168-176.
Krude, T. and Keller, C. (2001) 'Chromatin assembly during S phase: contributions from histone deposition, DNA replication and the cell division cycle', *Cellular and Molecular Life Sciences*, 58(5-6), pp. 665-672.
Langsenlehner, U., Renner, W., Yazdani-Biuki, B., Eder, T., Wascher, T. C., Paulweber, B., Clar, H., Hofmann, G., Samonigg, H. and Krippl, P. (2006) 'Integrin alpha-2 and beta-3 gene polymorphisms and breast cancer risk', *Breast Cancer Research and Treatment*, 97(1), pp. 67-72.
Laplante, M. and Sabatini, D. M. (2009) 'An Emerging Role of mTOR in Lipid Biosynthesis', *Current Biology*, 19(22), pp. R1046-R1052.
Lebwohl, M. (2003) 'Psoriasis', *Lancet*, 361(9364), pp. 1197-1204.
Lefevre, C., Jobard, F., Caux, F., Bouadjar, B., Karaduman, A., Heilig, R., Lakhdar, H., Wollenberg, A., Verret, J. L., Weissenbach, J., Ozguc, M., Lathrop, M., Prud'homme, J. F. and Fischer, J. (2001) 'Mutations in CGI-58, the gene encoding a new protein of the

esterase/lipase/thioesterase subfamily, in Chanarin-Dorfman syndrome', *American Journal of Human Genetics*, 69(5), pp. 1002-1012.
Lewis, C. J., Mardaryev, A. N., Poterlowicz, K., Sharova, T. Y., Aziz, A., Sharpe, D. T., Botchkareva, N. V. and Sharov, A. A. (2014) 'Bone Morphogenetic Protein Signaling Suppresses Wound-Induced Skin Repair by Inhibiting Keratinocyte Proliferation and Migration', *Journal of Investigative Dermatology*, 134(3), pp. 827-837.
Li, S., Teegarden, A., Bauer, E. M., Choi, J., Messaddeq, N., Hendrix, D. A., Ganguli-Indra, G., Leid, M. and Indra, A. K. (2017) 'Transcription Factor CTIP1/BCL11A Regulates Epidermal Differentiation and Lipid Metabolism During Skin Development', *Scientific Reports*, 7.
Liakath-Ali, K., Mills, E. W., Sequeira, I., Lichtenberger, B. M., Pisco, A. O., Sipila, K. H., Mishra, A., Yoshikawa, H., Wu, C. C. C., Ly, T., Lamond, A. I., Adham, I. M., Green, R. and Watt, F. M. (2018) 'An evolutionarily conserved ribosome-rescue pathway maintains epidermal homeostasis', *Nature*, 556(7701), pp. 376-+.
Liu, J., Kim, D., Brown, L. D., Madsen, T. and Bouchard, G. F. (2009) 'Comparison of Human, Porcine, and Rodent Wound Healing With New Miniature Swine Study Data', *Journal of the American Association for Laboratory Animal Science*, 48(5), pp. 581-581.
Liu, J., Sato, C., Cerletti, M. and Wagers, A. (2010) 'NOTCH SIGNALING IN THE REGULATION OF STEM CELL SELF-RENEWAL AND DIFFERENTIATION', in Kopan, R. (ed.) *Notch Signaling Current Topics in Developmental Biology*, pp. 367-409.
Liu, Q. S., Kang, S. A., Thoreen, C. C., Hur, W., Wang, J. H., Chang, J. W., Markhard, A., Zhang, J. M., Sim, T., Sabatini, D. M. and Gray, N. S. (2012) 'Development of ATP-Competitive mTOR Inhibitors', *Mtor: Methods and Protocols*, 821, pp. 447-460.
Ljunggren , C. A. 1898. Von Der Fähigkeit Des Hautepithels , Ausserhalb Des Organismus Sein Leben Zu Behalten, Mit Berücksichtigung Der Transplantation.: Berücksichtigung Der Transplantation.
Lomas, A., Leonardi-Bee, J. and Bath-Hextall, F. (2012) 'A systematic review of worldwide incidence of nonmelanoma skin cancer', *British Journal of Dermatology*, 166(5), pp. 1069-1080.
Lowes, M. A., Bowcock, A. M. and Krueger, J. G. (2007) 'Pathogenesis and therapy of psoriasis', *Nature*, 445(7130), pp. 866-873.
Lowes, M. A., Suarez-Farinas, M. and Krueger, J. G. (2014) 'Immunology of Psoriasis', *Annual Review of Immunology, Vol 32*, 32, pp. 227-255.
Lu, W., Li, J., Ren, M., Zeng, Y. J., Zhu, P., Lin, L., Lin, D. Z., Hao, S. Y., Gao, Q., Liang, J. Q., Yan, L. and Yang, C. (2015) 'Role of the mevalonate pathway in specific CpG site demethylation on AGEs-induced MMP9 expression and activation in keratinocytes', *Molecular and Cellular Endocrinology*, 411(C), pp. 121-129.
Luo, W. J. and Brouwer, C. (2013) 'Pathview: an R/Bioconductor package for pathway-based data integration and visualization', *Bioinformatics*, 29(14), pp. 1830-1831.
Ma, A. S. P. and Ozers, L. J. (1996) 'Annexins I and II show differences in subcellular localization and differentiation-related changes in human epidermal keratinocytes', *Archives of Dermatological Research*, 288(10), pp. 596-603.
Madison, K. C. (2003) 'Barrier function of the skin: "La Raison d'Etre" of the epidermis', *Journal of Investigative Dermatology*, 121(2), pp. 231-241.
Manils, J., Fischer, H., Climent, J., Casas, E., Garcia-Martinez, C., Bas, J., Sukseree, S., Vavouri, T., Ciruela, F., de Anta, J. M., Tschachler, E., Eckhart, L. and Soler, C. (2017) 'Double deficiency of Trex2 and DNase1L2 nucleases leads to accumulation of DNA in lingual cornifying keratinocytes without activating inflammatory responses', *Scientific Reports*, 7.

Marks, J. G. and Miller, J. (2006) *Lookingbill and Marks' Principles of Dermatology.* 4th edn.: Elsevier Inc.
Martin, P. (1997) 'Wound healing - Aiming for perfect skin regeneration', *Science,* 276(5309), pp. 75-81.
Martincorena, I., Roshan, A., Gerstung, M., Ellis, P., Van Loo, P., McLaren, S., Wedge, D. C., Fullam, A., Alexandrov, L. B., Tubio, J. M., Stebbings, L., Menzies, A., Widaa, S., Stratton, M. R., Jones, P. H. and Campbell, P. J. (2015) 'High burden and pervasive positive selection of somatic mutations in normal human skin', *Science,* 348(6237), pp. 880-886.
Martini, F. H. and Nath, J. (2009) *Fundamentals of Anatomy and Physiology.* 8th edn.: Pearson Education, p. 158.
Mascre, G., Dekoninck, S., Drogat, B., Youssef, K. K., Brohee, S., Sotiropoulou, P. A., Simons, B. D. and Blanpain, C. (2012) 'Distinct contribution of stem and progenitor cells to epidermal maintenance', *Nature,* 489(7415), pp. 257-+.
Mayer, C. and Grummt, I. (2006) 'Ribosome biogenesis and cell growth: mTOR coordinates transcription by all three classes of nuclear RNA polymerases', *Oncogene,* 25(48), pp. 6384-6391.
McGrath, J. A., Eady, R. A. and Pope, F. M. (2004) *Rook's Textbook of Dermatology.* 7th edn.: Blackwell Publishing, p. 31–36.
Medawar, P. B. (1948) 'THE CULTIVATION OF ADULT MAMMALIAN SKIN EPITHELIUM INVITRO', *Quarterly Journal of Microscopical Science,* 89(2), pp. 187-196.
Menter, A., Gottlieb, A., Feldman, S. R., Van Voorhees, A. S., Leonardi, C. L., Gordon, K. B., Lebwohl, M., Koo, J. Y. M., Elmets, C. A., Korman, N. J., Beutner, K. R. and Bhushan, R. (2008) 'Guidelines of care for the management of psoriasis and psoriatic arthritis - Section 1. Overview of psoriasis and guidelines of care for the treatment of psoriasis with biologics', *Journal of the American Academy of Dermatology,* 58(5), pp. 826-850.
Mi, H. Y., Muruganujan, A., Casagrande, J. T. and Thomas, P. D. (2013) 'Large-scale gene function analysis with the PANTHER classification system', *Nature Protocols,* 8(8), pp. 1551-1566.
Moll, R., Franke, W. W., Schiller, D. L., Geiger, B. and Krepler, R. (1982) 'THE CATALOG OF HUMAN CYTOKERATINS - PATTERNS OF EXPRESSION IN NORMAL EPITHELIA, TUMORS AND CULTURED-CELLS', *Cell,* 31(1), pp. 11-24.
Moqrich, A., Hwang, S. W., Earley, T. J., Petrus, M. J., Murray, A. N., Spencer, K. S. R., Andahazy, M., Story, G. M. and Patapoutian, A. (2005) 'Impaired thermosensation in mice lacking TRPV3, a heat and camphor sensor in the skin', *Science,* 307(5714), pp. 1468-1472.
Muehlenbein, M. (2010) *Human Evolutionary Biology . .* Cambridge University Press, p. 192–213.
Murray, A. W. (2004) 'Recycling the cell cycle: Cyclins revisited', *Cell,* 116(2), pp. 221-234.
Murugesan, P., Muthusamy, T., Balasubramanian, K. and Arunakaran, J. (2005) 'Studies on the protective role of vitamin C and E against polychlorinated biphenyl (Aroclor 1254) - induced oxidative damage in Leydig cells', *Free Radical Research,* 39(11), pp. 1259-1272.
Naeem, A. S., Zhu, Y., Di, W. L., Marmiroli, S. and O'Shaughnessy, R. F. L. (2015) 'AKT1-mediated Lamin A/C degradation is required for nuclear degradation and normal epidermal terminal differentiation', *Cell Death and Differentiation,* 22(12), pp. 2123-2132.
Nanba, D., Toki, F., Matsushita, N., Matsushita, S., Higashiyama, S. and Barrandon, Y. (2013) 'Actin filament dynamics impacts keratinocyte stem cell maintenance', *Embo Molecular Medicine,* 5(4), pp. 640-653.
Nurse, P. and Thuriaux, P. (1980) 'REGULATORY GENES-CONTROLLING MITOSIS IN THE FISSION YEAST SCHIZOSACCHAROMYCES-POMBE', *Genetics,* 96(3), pp. 627-637.

Parshley, M. S. and Simms, H. S. (1950) 'CULTIVATION OF ADULT SKIN EPITHELIAL CELLS (CHICKEN AND HUMAN) INVITRO', *American Journal of Anatomy*, 86(2), pp. 163-189.
Pellegrini, G., Golisano, O., Paterna, P., Lambiase, A., Bonini, S., Rama, P. and De Luca, M. (1999) 'Location and clonal analysis of stem cells and their differentiated progeny in the human ocular surface', *Journal of Cell Biology*, 145(4), pp. 769-782.
Pfeifer, G. P. and Besaratinia, A. (2012) 'UV wavelength-dependent DNA damage and human non-melanoma and melanoma skin cancer', *Photochemical & Photobiological Sciences*, 11(1), pp. 90-97.
Pinkus, H. (1932) 'About tissue cultures in the human epidermis. An article on anatomy of the skin', *Archiv Fur Dermatologie Und Syphilis*, 165(1), pp. 53-85.
Ponec, M., Kempenaar, J., Weerheim, A. and Boonstra, J. (1987) 'DIFFERENTIATION OF HUMAN KERATINOCYTES - CHANGES IN LIPID-SYNTHESIS, PLASMA-MEMBRANE LIPID-COMPOSITION, AND I-125 EGF BINDING UPON ADMINISTRATION OF 25-HYDROXYCHOLESTEROL AND MEVINOLIN', *Journal of Cellular Physiology*, 133(2), pp. 358-364.
Ponec, M., Weerheim, A., Kempenaar, J., Mommaas, A. M. and Nugteren, D. H. (1988) 'LIPID-COMPOSITION OF CULTURED HUMAN KERATINOCYTES IN RELATION TO THEIR DIFFERENTIATION', *Journal of Lipid Research*, 29(7), pp. 949-961.
Proksch, E., Brandner, J. M. and Jensen, J.-M. (2008) 'The skin: an indispensable barrier', *Experimental Dermatology*, 17(12), pp. 1063-1072.
Qiu, B. and Simon, M. C. (2016) 'BODIPY 493/503 Staining of Neutral Lipid Droplets for Microscopy and Quantification by Flow Cytometry', *Bio-protocol*, 6(17).
Radner, F. P., Grond, S., Haemmerle, G., Lass, A. and Zechner, R. (2011) 'Fat in the skin: Triacylglycerol metabolism in keratinocytes and its role in the development of neutral lipid storage disease', *Dermato-endocrinology*, 3(2), pp. 77-83.
Radtke, C., Reimers, K., Allmeling, C. and Vogt, P. M. (2009) 'Efficient Production of Transfected Human Keratinocytes under Serum-Free and Feeder Layer-Free Conditions', *Handchirurgie Mikrochirurgie Plastische Chirurgie*, 41(6), pp. 333-340.
Rheinwald, J. G. and Green, H. (1975) 'SERIAL CULTIVATION OF STRAINS OF HUMAN EPIDERMAL KERATINOCYTES - FORMATION OF KERATINIZING COLONIES FROM SINGLE CELLS', *Cell*, 6(3), pp. 331-344.
Rheinwald, J. G. and Green, H. (1977) 'EPIDERMAL GROWTH-FACTOR AND MULTIPLICATION OF CULTURED HUMAN EPIDERMAL KERATINOCYTES', *Nature*, 265(5593), pp. 421-424.
Roberson, E. D. O. and Bowcock, A. M. (2010) 'Psoriasis genetics: breaking the barrier', *Trends in Genetics*, 26(9), pp. 415-423.
Rogerson, C., Bergamaschi, D. and O'Shaughnessy, R. F. L. (2018) 'Uncovering mechanisms of nuclear degradation in keratinocytes: A paradigm for nuclear degradation in other tissues', *Nucleus*, 9(1), pp. 56-64.
Rompolas, P., Deschene, E. R., Zito, G., Gonzalez, D. G., Saotome, I., Haberman, A. M. and Greco, V. (2012) 'Live imaging of stem cell and progeny behaviour in physiological hair-follicle regeneration', *Nature*, 487(7408), pp. 496-U1600.
Roshan, A., Murai, K., Fowler, J., Simons, B. D., Nikolaidou-Neokosidou, V. and Jones, P. H. (2016) 'Human keratinocytes have two interconvertible modes of proliferation', *Nature Cell Biology*, 18(2), pp. 145-+.
Roux, P. P., Shahbazian, D., Vu, H., Holz, M. K., Cohen, M. S., Taunton, J., Sonenberg, N. and Blenis, J. (2007) 'RAS/ERK signaling promotes site-specific ribosomal protein S6 phosphorylation via RSK and stimulates cap-dependent translation', *Journal of Biological Chemistry*, 282(19), pp. 14056-14064.

Rozenszajn, L., Klajman, A., Yaffe, D. and Efrati, P. (1966) 'JORDANS ANOMALY IN WHITE BLOOD CELLS - REPORT OF CASE', *Blood-the Journal of Hematology,* 28(2), pp. 258-+.
Saladi, R. N. and Persaud, A. N. (2005) 'The causes of skin cancer: A comprehensive review', *Drugs of Today,* 41(1), pp. 37-53.
Sampath, P., Pritchard, D. K., Pabon, L., Reinecke, H., Schwartz, S. M., Morris, D. R. and Murry, C. E. (2008) 'A hierarchical network controls protein translation during murine embryonic stem cell self-renewal and differentiation', *Cell Stem Cell,* 2(5), pp. 448-460.
Sarbassov, D. D., Ali, S. M., Sengupta, S., Sheen, J. H., Hsu, P. P., Bagley, A. F., Markhard, A. L. and Sabatini, D. M. (2006) 'Prolonged rapamycin treatment inhibits mTORC2 assembly and Akt/PKB', *Molecular Cell,* 22(2), pp. 159-168.
Sata, A. (1900) 'The appearance of fat in the skin and in glands, in the so-called protein glands', *Beitrage Zur Pathologischen Anatomie Und Zur Allgemeinen Pathologie,* 27(3), pp. 555-574.
Schmitz, G. and Muller, G. (1991) 'STRUCTURE AND FUNCTION OF LAMELLAR BODIES, LIPID-PROTEIN COMPLEXES INVOLVED IN STORAGE AND SECRETION OF CELLULAR LIPIDS', *Journal of Lipid Research,* 32(10), pp. 1539-1570.
Schurer, N., Kohne, A., Schliep, V., Barlag, K. and Goerz, G. (1993) 'Lipid composition and synthesis of HaCaT cells, an immortalized human keratinocyte line, in comparison with normal human adult keratinocytes', *Experimental dermatology,* 2(4), pp. 179-85.
Schweiger, M., Lass, A., Zimmermann, R., Eichmann, T. O. and Zechner, R. (2009) 'Neutral lipid storage disease: genetic disorders caused by mutations in adipose triglyceride lipase/PNPLA2 or CGI-58/ABHD5', *American Journal of Physiology-Endocrinology and Metabolism,* 297(2), pp. E289-E296.
Seery, J. P. and Watt, F. M. (2000) 'Asymmetric stem-cell divisions define the architecture of human oesophageal epithelium', *Current Biology,* 10(22), pp. 1447-1450.
Shao, J. Y., Evers, B. M. and Sheng, H. M. (2004) 'Roles of phosphatidylinositol 3 '-kinase and mammalian target of rapamycin/p70 ribosomal protein S6 kinase in K-Ras-mediated transformation of intestinal epithelial cells', *Cancer Research,* 64(1), pp. 229-235.
Shier, D., Butler, J. and Lewis, R. (1999) *Hole's Human Anatomy and Physiology.* 8th ed: McGraw Hill, pp. 160–183.
Simons, B. D. and Clevers, H. (2011) 'Strategies for Homeostatic Stem Cell Self-Renewal in Adult Tissues', *Cell,* 145(6), pp. 851-862.
Singer, A. J. and Clark, R. A. F. (1999) 'Mechanisms of disease - Cutaneous wound healing', *New England Journal of Medicine,* 341(10), pp. 738-746.
Smirnov, S. V., Kiseley, I. V., Rogovaya, O. S., Vasil'ev, A. V. and Terskikh, V. V. (2003) 'Skin repair by transplantation of cultured keratinocytes', *Bulletin of Experimental Biology and Medicine,* 135(6), pp. 608-609.
Sotiropoulou, P. A. and Blanpain, C. (2012) 'Development and Homeostasis of the Skin Epidermis', *Cold Spring Harbor Perspectives in Biology,* 4(7).
Stucker, M., Struk, A., Altmeyer, P., Herde, M., Baumgartl, H. and Lubbers, D. W. (2002) 'The cutaneous uptake of atmospheric oxygen contributes significantly to the oxygen supply of human dermis and epidermis', *Journal of Physiology-London,* 538(3), pp. 985-994.
Sullivan, T. P., Eaglstein, W. H., Davis, S. C. and Mertz, P. (2001) 'The pig as a model for human wound healing', *Wound Repair and Regeneration,* 9(2), pp. 66-76.
Tabor, A., Pergolizzi, J. V., Jr., Marti, G., Harmon, J., Cohen, B. and Lequang, J. A. (2017) 'Raising Awareness Among Healthcare Providers about Epidermolysis Bullosa and Advancing Toward a Cure', *The Journal of clinical and aesthetic dermatology,* 10(5), pp. 36-48.

Takazawa, Y., Ogawa, E., Saito, R., Uchiyama, R., Ikawa, S., Uhara, H. and Okuyama, R. (2015) 'Notch down-regulation in regenerated epidermis contributes to enhanced expression of interleukin-36 alpha and suppression of keratinocyte differentiation during wound healing', *Journal of Dermatological Science*, 79(1), pp. 10-19.
Tan, J. Z., Yang, H. T., Fan, J. C., Fan, Y. L. and Xiao, F. (2018) 'Patients with neutral lipid storage disease with myopathy (NLSDM) in Southwestern China', *Clinical Neurology and Neurosurgery*, 168, pp. 102-107.
Taylor, G., Lehrer, M. S., Jensen, P. J., Sun, T. T. and Lavker, R. M. (2000) 'Involvement of follicular stem cells in forming not only the follicle but also the epidermis', *Cell*, 102(4), pp. 451-461.
Thierry-Mieg, D. and Thierry-Mieg, J. (2006) 'AceView: a comprehensive cDNA-supported gene and transcripts annotation', *Genome Biology*, 7.
Tohya, S., Mochizuki, A., Imayama, S. and Iwasa, Y. (1998) 'On rugged shape of skin tumor (basal cell carcinoma)', *Journal of Theoretical Biology*, 194(1), pp. 65-78.
Walko, G., Woodhouse, S., Pisco, A. O., Rognoni, E., Liakath-Ali, K., Lichtenberger, B. M., Mishra, A., Telerman, S. B., Viswanathan, P., Logtenberg, M., Renz, L. M., Donati, G., Quist, S. R. and Watt, F. M. (2017) 'A genome-wide screen identifies YAP/WBP2 interplay conferring growth advantage on human epidermal stem cells', *Nature Communications*, 8, pp. 16.
Wan, J. and Qian, S. B. (2014) 'TISdb: a database for alternative translation initiation in mammalian cells', *Nucleic Acids Research*, 42(D1), pp. D845-D850.
Weathers, W. M., Bhadkamkar, M., Wolfswinkel, E. M. and Thornton, J. F. (2013) 'Full-Thickness Skin Grafting in Nasal Reconstruction', *Seminars in Plastic Surgery*, 27(2), pp. 90-95.
Webb, A. R. (2006) 'Who, what, where and when - influences on cutaneous vitamin D synthesis', *Progress in Biophysics & Molecular Biology*, 92(1), pp. 17-25.
Wertz, P. W. (1992) 'EPIDERMAL LIPIDS', *Seminars in Dermatology*, 11(2), pp. 106-113.
Wertz, P. W., Downing, D. T., Freinkel, R. K. and Traczyk, T. N. (1984) 'SPHINGOLIPIDS OF THE STRATUM-CORNEUM AND LAMELLAR GRANULES OF FETAL-RAT EPIDERMIS', *Journal of Investigative Dermatology*, 83(3), pp. 193-195.
Williams, M. L., Rutherford, S. L., Ponec, M., Hincenbergs, M., Placzek, D. R. and Elias, P. M. (1988) 'DENSITY-DEPENDENT VARIATIONS IN THE LIPID-CONTENT AND METABOLISM OF CULTURED HUMAN KERATINOCYTES', *Journal of Investigative Dermatology*, 91(1), pp. 86-91.
Winter, H., Langbein, L., Krawczak, M., Cooper, D. N., Jave-Suarez, L. F., Rogers, M. A., Praetzel, S., Heidt, P. J. and Schweizer, J. (2001) 'Human type I keratin pseudogene phi hHaA has functional orthologs in the chimpanzee and gorilla: evidence for recent inactivation of the human gene after the Pan-Homo divergence', *Human Genetics*, 108(1), pp. 37-42.
Wu, X. W., Nguyen, B. C., Dziunycz, P., Chang, S., Brooks, Y., Lefort, K., Hofbauer, G. F. L. and Dotto, G. P. (2010) 'Opposing roles for calcineurin and ATF3 in squamous skin cancer', *Nature*, 465(7296), pp. 368-U130.
Zhao, X., Psarianos, P., Ghoraie, L. S., Yip, K., Goldstein, D., Gilbert, R., Witterick, I., Pang, H., Hussain, A., Lee, J. H., Williams, J., Bratman, S. V., Ailles, L., Haibe-Kains, B. and Liu, F.-F. (2019) 'Metabolic regulation of dermal fibroblasts contributes to skin extracellular matrix homeostasis and fibrosis', *Nature Metabolism*, 1, pp. 147–157.